Université Mohamed Khider – Biskra
Faculté des Sciences et de la technologie
Département : Génie Civil et Hydraulique
Ref :………………

جامعة محمد خيضر بسكرة
كلية العلوم و التكنولوجيا
: الهندسة المدنية و الري
: ....

Thèse présentée en vue de l'obtention
Du diplôme de

Doctorat en Génie Civil

Spécialité : Modélisation des Matériaux et Structures

Contribution to the Modeling of Structures with Complex Geometries with and without Stiffeners

"Contribution à la modélisation des structures de formes géométriques complexes avec et sans raidisseurs"

Présentée par :
Oussama TEMAMI

Soutenue publiquement le : 17/05/2017

Devant le jury composé de :

Dr. MELLAS Mekki	Professeur	Président	Université de Biskra
Dr. HAMADI Djamal	Professeur	Rapporteur	Université de Biskra
Dr. ASHRAF Ayoub	Professeur	Co-Rapporteur	City University London
Dr. CHEBILI Rachid	Professeur	Examinateur	Université de Biskra
Dr. NOUAOURIA M. Salah	Professeur	Examinateur	Université de Guelma

AKNOWLEDGEMENT

DEDICATION

First of all I dedicate my dissertation work to our almighty god;

Father and Mother, whose affection ,love ,encouragement and prays of day and night make me able to get such success and honor.

My brothers and my sister have never left my side and are very special.

Abstract

In practice, the complex structures such as thin shells, where the structure covers a large area with a very complex geometry and sometimes supporting heavy loads, can cause very large displacements. This fact often requires the addition of stiffeners to increase the rigidity and to minimize the deformation. These complex structures can be analyzed through modeling by the finite element method. In general, joints or connections between the stiffeners and shell structures are difficult to model. The proposed tasks to resolve this problem is through proper modeling of the stiffened shell structures along with validation using experimentally tested representative specimens.

In this thesis, several experimental and numerical investigations regarding the behavior of a cylindrical shell model are conducted. The behavior of cylindrical shell models under a concentrated load, with and without stiffeners and edge beam are studied. Numerical modeling using a flat shell element developed recently and two ABAQUS elements are used. The results obtained experimentally and numerically are compared and commented upon.

Keywords:

Complex Structures, Cylindrical Shell Model, Numerical Modeling, Stiffeners, Experimental work.

من الناحية العملية، وبالنسبة للمنشآت ذات التركيب الهندسي المعقد مثل القشريات، حيث أن هذا النوع من المنشآت يستعمل عموما لتغطية مساحات شاسعة وقد تكون في بعض الحالات خاضعة لأحمال معتبرة، مما يتسبب في حدوث انتقالات وتشوهات كبيرة جدا.

هذه المنشآت تتطلب استعمال دعائم لتقوية صلادة الهيكل والتقليل من التشوهات. يمكن إجراء الدراسة التحليلية لهذه الهياكل المعقدة من خلال النمذجة باستخدام طريقة العناصر   . إن الروابط بين الدعامة   هياكل القشرية ليست من السهولة نمذجتها.

المقترحة لحل هذه   ة، تتمثل في إجراء النمذجة العددية للهياكل إلى جانب العمل التجريبي النموذجي، وذلك من أجل اختبار نتائج التحليل العددي لمثل

.

في هذه   يبية وعددي   من قشريات أسطوانية
. حيث   ها   تأثير   بدون دعامة تقوية في حالات،
تقوية وحز   . أجريت النمذجة العددية باستخدام عنصر
م عنصرين ABAQUS.   م الحصول عليها
تجريبيا وعدديا ت   تها والتعليق عليها.

المفتاحية:

الهياكل المركبة، نموذج اسطوانة قشرية ، النمذجة العددية، دعامة، عمل تجريبي.

Contents

Chapter 1

General Introduction

Chapter 2

Shell Structures: Design And Analysis

Chapter 3

Description Of The Experimental Work and The Numerical Analysis

Chapter 4

Experimental And Numerical Investigation Of The Behavior Of A Cylindrical Shell Model

Chapter 5

Experimental And Numerical Investigation Of The Behavior Of The Cylindrical Shell Model With Stiffeners

Chapter 6

Effect Of Boundary Conditions And The Stiffeners On The Cylindrical Shells

Figure Captions

Chapter 1

General Introduction

Chapter 2

Shell Structures: Design And Analysis

Chapter 3

Description Of The Experimental Work and The Numerical Analysis

Chapter 4

Experimental And Numerical Investigation Of The Behavior Of A Cylindrical Shell Model

Chapter 5

Experimental And Numerical Investigation Of The Behavior Of The Cylindrical Shell Model With Stiffeners

Chapter 6

Effect of Boundary Conditions and The Stiffeners On The Cylindrical Shells

Table Captions

Chapter 4

Experimental And Numerical Investigation Of The Behavior Of A Cylindrical Shell Model

Chapter 5

Experimental And Numerical Investigation Of The Behavior Of The Cylindrical Shell Model With Stiffeners

Chapter 6

Effect Of Boundary Conditions And The Stiffeners On The Cylindrical Shells

Notation

n_{xx}, n_{yy}	The membrane forces
n_{yx}	The shear membrane force
m_{xx}, m_{yy} and m_{xy}	The bending moments
v_x, v_y	The shear forces
u, v	The in-plane displacements along the x and y axes
$[K^p]$	The stiffness matrix
$\{f^P\}$	The nodal forces
$\{q^P\}$	The displacement element
FEM	Finite Element Method
E	The elasticity modulus
υ	Poisson ratio
L	Length
R	radius
t	Thickness
CNDNS2	Cylindrical shell with no end diaphragms and no stiffeners, t = 2 mm
CNDNS	Cylindrical shell with no end diaphragms and no Stiffeners, t =1.2 mm
CDNS	Cylindrical shell with two end rigid Diaphragms and no Stiffeners, t=1.2mm
CNDS	Cylindrical shell with no end Diaphragms and two Stiffeners, t=1.2 mm
CDS	Cylindrical shell with two end Diaphragms and two Stiffeners, t=1.2mm
CDSS	Cylindrical shell with two end Diaphragms and two Stiffeners resting on longitudinal beams "Stringers", t=1.2mm
$[D]$	The constitutive matrix
$[A]$	The transformation matrix
$[Q]$	The strain matrix
$[K_e]$	The elementary stiffness matrix
W_1	The vertical displacement at point 1
W_2	The vertical displacement at point 2
W_3	The vertical displacement at point 3

Chapter 1

General Introduction

Chapter 1

General Introduction

1.1 Introduction

For many years, the analysis of structures is the subject of further studies by researchers and engineers from varied industries. Thus, the civil engineering structures, the transportation, the ships and aircraft are to a large extent, faced with the need to predict their behavior. Different types and levels of complexity are found: complexity due to geometry shapes, structural elements, materials used (composite, glass). Most complex structures are constituted by structural elements of relatively simple shapes as beams, plates and shells of various geometries.

In practice, the analysis of complex structures such as thin shells, where the structures covers a large area with a very complex geometry and sometimes supporting heavy loads, can cause very large displacements. This fact often requires the addition of stiffeners to increase the rigidity and to minimize deformation. Depending on the geometric shape of these structures, these stiffeners may be straight (beam member) or curved in an arc shape. These complex structures can be analyzed through modeling by finite element. In general, joints or connections between the stiffeners and shell structures are difficult to model.

The resistance of cylindrical shells in bending, buckling and any other possible deformation is often improved by the use of circumferential stiffening and / or longitudinal ones. The size, spacing and position of the stiffeners on the outer or inner surfaces of the cylinder wall are factors that influence the behavior instability of the shell. Thus stiffened shells are prominent in the field of engineering such as in aerospace structures, mechanical as well as in marine structures. Most of these structures are subjected to different loads that can lookout the shell characteristics. Therefore, several methods were developed to study the behavior of stiffened shells. Thus, researchers have tried to analyze the behavior of stiffened shell structures for different shapes. Indeed, the different forms of shells that were studied have either simple gaits such as cylindrical and conical shells or more complex shapes such as

assembly of simple shapes. The coupling shells with stiffeners take several aspects [Sin1967, Ven1982, Haz1989, Man2000]

Indeed, we find shells coupled with circumferential or longitudinal stiffeners or with both [Man2000]. Also the position of the stiffeners at the shell provides a good number of researches. The stiffeners may be either equally spaced or located at well defined places. They can be eccentric to the shell or the average line located the shell. All these forms and positions of stiffeners greatly influence the structures of stiffened shells [Haz1989].

The most used approach for modeling of these structures now is the Finite Element Method "FEM". The results of this approach are very reliable and efficient from the moment we took care to define a mesh with good fit from the standpoint of basic formulations used and finesse. The second point remains the main limitation of this method insofar as one can quickly reach the limits for computing resources.

In general, each structure is divided into simpler components analyzed independently of each other. This is often uncertain. So we do sometimes tries to analyze the whole structure, as complex as it is, through modeling using the finite element method. The latter cut the structure into elementary components which together are calculated at once. Generally, joints or connections between two structures are parts that are difficult to model. Despite several efforts made to eliminate the numerical locking problems for such structures, some serious improvements still perpetuate. The compatibility of components with each other often poses a difficult problem for the discretization of the complicated structure, because of nodal unknowns that are not the same; this compatibility is necessary to ensure convergence.

In this thesis, we try to offer a contribution to the modeling of such structures, taking into account the parameters cited above (element type, geometry for both structures).

The importance of this work lies mainly in the vast fields of application in the field of engineering, and more particularly that of civil engineering structures.

1.2 Advantages of the Finite Element Method

The finite element method is a well established procedure in the numerical and applied mathematics fields , and has been largely developed to be capable of solving with approximate accuracy the problems encountered in engineering structural analysis domain, with different formulations (displacement, stress, mixed and hybrid models) [Ham2006, Ham2014]. Among many advantages of the finite element, the capacity to handle a big

amount of load conditions and boundary conditions through computer simulations, in addition, the finite element method enables the designer to detect stress, vibration, and thermal problems during the design process and to evaluate design changes before the construction of a possible prototype. Thus confidence in the acceptability of the prototype is enhanced. Moreover, if used properly, the method can reduce the number of prototypes that need to be built [Log2007]. Even though the finite element method was initially used for structural analysis, it has since been adapted to many other disciplines in engineering and mathematical physics, such as fluid flow, heat transfer, electromagnetic potentials, soil mechanics, and acoustics [Zie1965, Wil1966, Gir1968, Mar1969, You1975, Sil1983].

1.3 Modeling the structure

The model should be chosen to represent the real structure as closely as possible with regard to the geometrical shape, loading and boundary conditions. The geometrical form of the structure is the major factor to be considered when deciding the type of elements to be used [Ham2006]. Another factor in the idealisation process is the size of the elements used. This, however, depends on many other factors, such as the efficiency of the elements and the importance of local features in the structure, e.g. stress concentrations. In many cases, only one type of elements is used for a given problem, but sometimes it is more convenient to adopt a mixed subdivision in which more than one type of elements is used, e.g. a beam element is connected to a shell element as a stiffener (Fig.1.1 (a) and (b)).
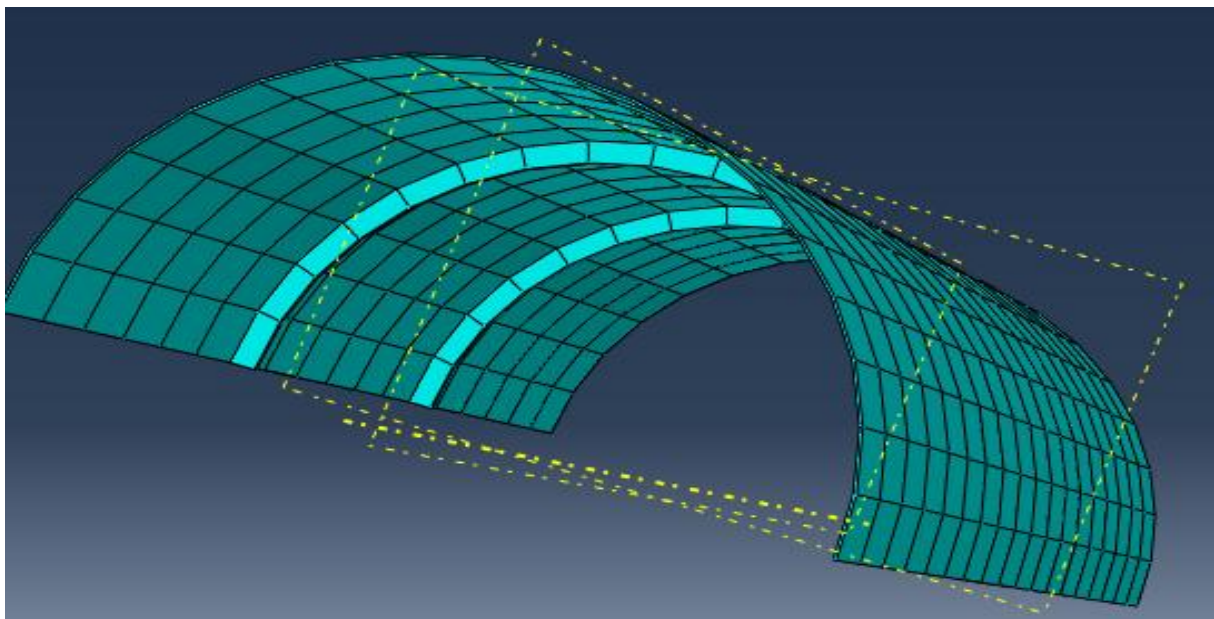
(a)
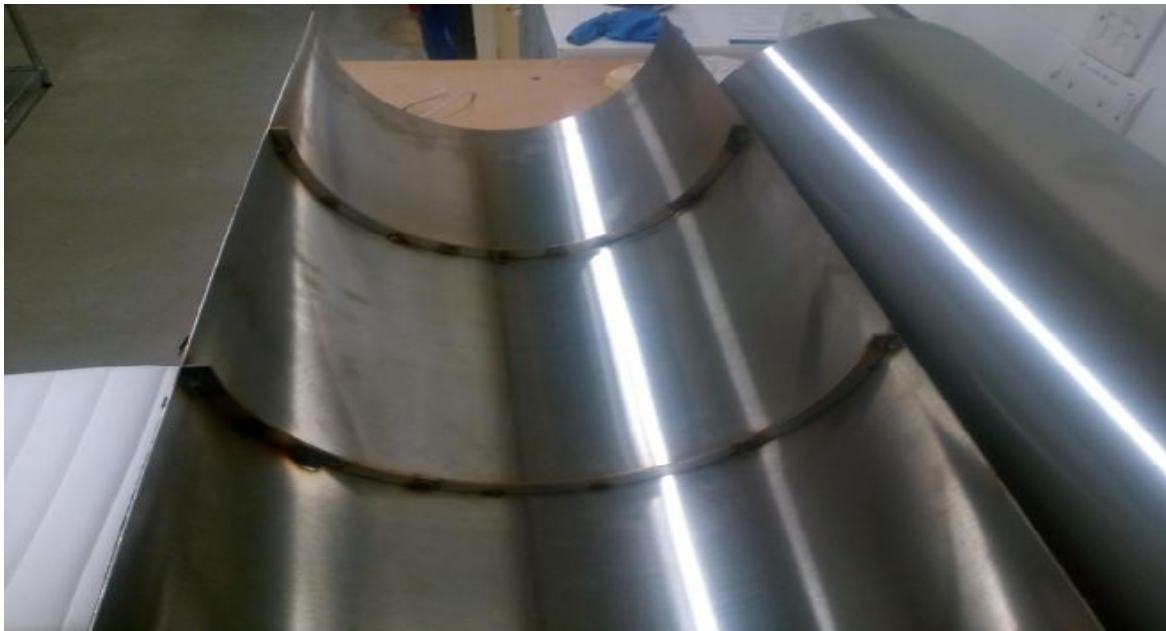
(b)

Fig. 1.1 Shell Structure with stiffeners

1.4 Discretisation

The first step in the procedure of solving a problem using the finite element method is the discretization of a continuum domain as an example in structural mechanics into a finite number of elements .This is equivalent to replacing the domain having an infinite number of differential elements in mathematical calculus into a set of elements with a finite known number of degrees of freedom. The type, shape, size, number and configuration of elements have to be chosen carefully so that the original body or domain is simulated as accuratley as possible without increasing the computational effort needed for the solution[Zie2005a, Zie2005b, Hug2000]. The various considerations to be taken in the discretization process are:

   • Type of elements
   • Size of elements
   • Location of nodes
   • Number of elements
   • Simplifications afforded by the physical configuration of the body
   • Finite representation of infinite bodies
   • Node numbering scheme
   • Automatic node generation

After meshing of the body it is necessary to add the material properties, external loads, and apply the boundary conditions. Before starting the solution procedures of the problem, some parameters of the calculation regime should be added to the input file.

1.5 Objective of the thesis

The main objective of this thesis is to provide a contribution to the modeling of complex structures with and without stiffeners. This research is conducted through many experimental and numerical investigations regarding the behavior of a cylindrical shell model. For the first case, the cylindrical shell model is studied without stiffeners, and for the second one the study of the behavior of cylindrical shell is conducted with stiffeners and edge beams. The effect of the stiffeners positions and the boundary condition on the cylindrical shell is presented and commented upon.

The work of this thesis is divided into six chapters:

The first chapter presents a general introduction describing behavior of complex structures such as thin shells with and without stiffeners, different approaches used for modeling structures by finite element method, the necessary steps used and the objectives of the thesis.

In the second chapter, the presentation of the state of the art regarding the analysis of shell structures, stiffened shells and their applications are described. Description of different theories, followed by a review about various studies of stiffened shells are detailed.

Chapter three contains the methodology of experimental work and apparatus used, and it divided in two parts, experimental part and numerical part. For the numerical part; the ACM-RSBE5 element used to analyze thin shell structures is presented, in addition to the ABAQUS elements S4R and C3D8IH. A brief description of the ABAQUS software for the analysis of complex structures such as cylindrical shells with stiffeners, different thickness and boundary conditions is given. For the experimental part, a series of test has been done for a cylindrical shell model, with and without stiffeners, undergoing a concentrated static load, with different values of thickness and varying boundary conditions.

The fourth chapter is devoted for the experimental and numerical investigation of the behavior of a cylindrical shell model. The numerical results obtained with the quadrilateral flat shell element with four nodes and six degrees of freedom per node "ACM-RSBE5" and

the ABAQUS element S4R are presented and compared with those obtained with the experimental tests.

The fifth chapter study and evaluate the structural performance of cylindrical shells under ultimate load conditions with stiffeners and edge beams. A laboratory experiments on representative specimens is conducted and numerical simulations of several structural models of cylindrical shells are performed, taking into account the different geometric and material parameters. The behavior of the stiffened cylindrical shells with different boundary conditions experimentally and numerically obtained are compared and commented upon.

In the last chapter, the effectiveness of boundary conditions on cylindrical shells and the stiffeners positions are studied and discussed.

The thesis is closed by a general conclusion and recommendations for further future works.

Chapter 2

Shell Structures: Design and Analysis

Chapter 2

Shell Structures: Design and Analysis

2.1 Introduction

Structural design refers to the iterative process of designing an efficient structural system which support and transfers different applied loads to foundation systems through safe and economic optimum choice. For shell structures, the structural design and the geometrical form converge in the three-dimensional curved shell surface. The shell needs the spatial curvature to develop the profound membrane behavior and the geometrical shape has major influence on how the shell behaves and how the shell fails. Obviously, the expression 'form active structural surface' finds its origin here. To design an efficient shell structure, it is of crucial importance to evaluate the interrelation between the variations of geometrical parameters and mechanical behavior thoroughly, the optimality of the design is relative to the pattern of the structural response which leads to the best possible structural morphology. An optimal shell design provides an advantageous geometrical and structural interaction which results in a prevalent membrane stress field [Pee2008].

Thin shells are characterized by a very good bearing capacity. Their qualities have been well proven in nature and mainly reside their form which derives logically the efforts they have to bear. Their rapid expansion in the last century in the field of civil engineering and architecture (concrete shells) is associated with designers [Pee2008].

The development of shell elements is directly related to the theoretical approach and variational formulation adopted (displacement, mixed, hybrid). Include three different theoretical approaches:

(i)   - Three-dimensional elements degenerate or not approach;

(ii) - Flat shell elements approach;

(iii) - Curved shell elements approach.

2.2 Shells Theory

2.2.1 Membrane Behavior

In shell structures the membrane behavior refers to a state of stress where a shell element is subjected only to in-plane normal and shear stress resultants that transfers loads to the supports, as illustrated in Figure 2.1. In thin shells, the stress component normal to the shell surface is neglected in comparison to the other internal stress components and this can only be satisfied by taking into account a compatible state of boundary conditions as to make the classical thin shell theories in agreement with their corresponding hypothesis. The curvature of the shell surface gives the ability to the shell to carry even loads perpendicular to the surface by in-plane stresses only [Hoe2003].

The carrying mode of loads only by in-plane extensional stresses is similar to the way in which membranes carry their loads. A membrane under external load mainly produces in-plane stresses. In case of shells, the external load also causes stretching or contraction of the shell as a membrane, without producing significant bending or local curvature changes. Hence, this is referred to as the membrane behavior of shells, described by the membrane theory. Carrying the load by in-plane membranes stresses is far more efficient in compression only materials such as concrete than the mechanism of bending, which is often observed in other structural elements such as beams. Consequently, it is possible to construct very thin shell structures. Also, thin shell structures are unable to resist significant bending moments because the flexural rigidity is much smaller than the extensional rigidity, and, therefore, their design must allow and aim for a predominant membrane state. Bending stresses eventually arise when the membrane stress field is insufficient to satisfy specific equilibrium or deformation requirements.
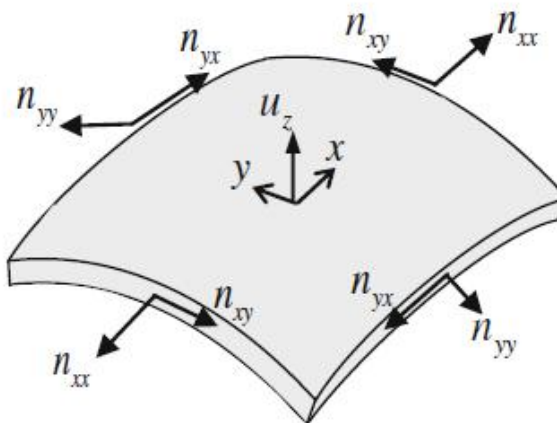
Fig. 2.1 Forces on a cylindrical shell element [Hoe2014]

2.2.2 Bending Behavior

In regions where the membrane solution is not sufficient for describing the equilibrium and/or deformations requirements, bending moments arise to compensate for the shortcoming of the membrane behavior. For example at the supports, by local concentrated load thin shell structures are exceptionally suited to carrying distributed loads, however, they are unsuited to carrying concentrated loads or a sudden change in geometry and the membrane state is disturbed causing bending action, see Figure 2.2. Bending moments only compensate the membrane solution and do not carry loads. Hence, this is often referred to compatibility moments. Due to their compensating character, bending moments are confined to a small region; the major part of the shell still behaves as a true membrane. It is this most important feature of shells that is responsible for the most profound and efficient structural performance.
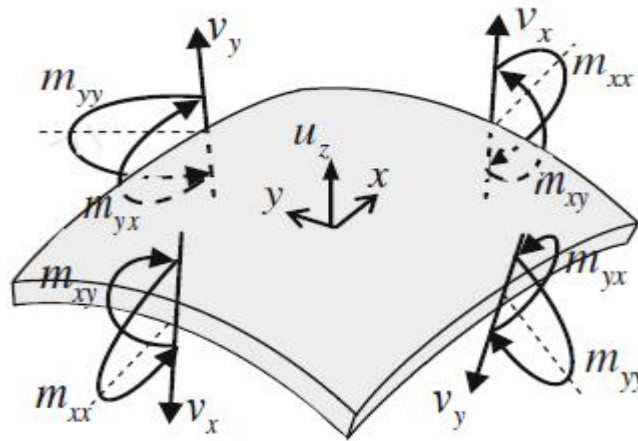
Fig. 2.2 Bending moments on a cylindrical shell element [Hoe2014]

The membrane action is preferred structural response motivated by the thinness of the shell. In thicker shells the preference is not so notorious and eventually it may be reversed. According to Farshad [Far1992], shells can be categorized into membrane dominated; bending dominated and mixed shell problems. The categorization can be made more distinctive by considering the asymptotic behavior of shells.

2.3   Review of the Assumptions and Numerical Modeling of Shell structures

From the historical point of view, the first shell models (like many other structural models) have been developed on the basis of engineering evaluation of experiments and heuristic assumptions. The first consistent theory of thin shells goes back to August E.H. Love in 1888 [Lov1888]. As Love's publication is based on Kirchhoff's work, this shell model became known as the Kirchhoff-Love model, Kirchhoff is credited to be the founder of modern plate theory with his publication in 1850 [Kir1850].

Several theories have been proposed and each has its application areas and limitations. In general, there are two groups of basic assumptions on which the theories of the shells are based. The first group includes the assumptions for the theories of thin shells such as Koiter theory [Koi1960]. Other hypotheses like the theory of plate Kirchhoff; there is still a thin hypothesis:

- The thickness of the shell is low concerning the minimum bend radius of the average surface.

All previous assumptions applied in thin shells are commonly named assumptions KIRCHHOFF-LOVE.

The second group relates to theories of moderate thick shells. It contains all assumptions of the theory of plate-MINDLIN REISSNER.

The principal assumption is that a mid-surface plane can be used to represent the three-dimensional plate in two dimensional forms. This model has no (independent) rotational degrees of freedom and assumes the cross section to remain straight, unstretched and normal to the mid-surface after deformation. As the strains in thickness direction are assumed to be zero, an appropriate modification of general three-dimensional material laws is required before usage.

Budiansky and Sanders [Bud1963] and Koiter's [Koi1960] works are some of the examples. A simple set of nonlinear equations for cylindrical shells were presented by Donnell [Don1933]. Vlasov [Vla1958] extended Love's theory to shallow shells of general geometry in a form commonly known as Donnel-Mushatan-Vlasov (DMV) equations for quasi-shallow shells. Cheng and Ho presented the general linear theoretical solutions to anisotropic cylinders [Che1963, Jon1967, Jon1969]. Nonlinear equations for shells of general shapes were presented by Novozhilov [Nov1953]. Several theoretical analyses limited to

orthotropic shell configurations were performed by Schnell and Bush [Sch1989], Thielmann et al. [Thi1960], and Hess [Hes1988].

Several papers compared the efficiency and accuracy of Flugge's [Flu1932] linear shell theory, which was employed by Cheng and Ho [Che1963], and other shell theories such as the work of Tasi et al. [Tas1965], Martin and Drew [Mar1989], whose theory was based on Donnell's equations, and the work done by Chao [Cha1960] whose analysis was based on Timoshenko's buckling equations. The theories discussed above are derived from the classical shell theory in which the Love-Kirchhoff assumptions are used. The Love-Kirchhoff assumptions treat the shells as infinitely rigid in the transverse direction by neglecting transverse shear strains. The theory has some shortcomings like underestimating the deflections and stresses and the overestimation of natural frequencies and buckling loads. However the transverse shear moduli of composite materials are usually very small compared to the in-plane moduli, the transverse shear strains must be accounted for, in order to have a more actual representation of the structural response in laminated plates and shells. Numerous plate and shell theories which account for transverse shear deformations are extensively discussed in the literature.

Nagdhi presented the corresponding concise theory for shells in 1972 [Nag1972]. Introducing a polynomial description of the displacements in thickness direction, he opened the door for shell models that match the three-dimensional theory with arbitrary exactness. Nevertheless, these shear-deformable shell models are commonly called shells with Reissner-Mindlin kinematics due to the origin of the assumption of shear-deformable cross-sections. Following the naming of Bischoff [Bis1999], the pure displacement-based shell formulations with shear deformation are called five-parameter formulation. This name relates to the use of five kinematic degrees of freedom (3 displacements and 2 rotational degrees of freedom).

The fundamental idea of shell models is based on the dimensional reduction of the 3D continuum: Taking advantage of the disparity in length scale, the semi-discretization of the continuum is performed to end up in a two-dimensional problem description. This discretization in thickness direction is completely independent from the (later) discretization within the shell mid-surface. Starting from the mechanical model, two general approaches can be chosen:

_ The Cosserat models are derived from the weak form of the shell equilibrium differential equation of the Cosserat surface. This method to derive shell models is usually called direct approach.

_ Continuum-based shell models start from the formulation of three-dimensional continua under consideration of shell-specific assumptions.

In principle, the two approaches can lead to the same system of differential equations. However, the Cosserat models are based on a two-dimensional shell model which defines the equilibrium equations directly via stress resultants, without considering the related stresses of a three-dimensional model [Cos1965, Gre1965]. Here, the shell is described as a directed continuum which means that every point is defined via position vector and director vector. These shell models are often called geometrically exact since Simo and Fox in 1989 [Sim1989a, Sim1989b], as the two-dimensional Cosserat surface is exactly described in this formulation. However, this does not imply any approximation to the quality of the shell deformation or any comparison to continuum-based shell models. A general drawback of the direct method is the difficult application of 3D continuum relations like three-dimensional material laws.

A more detailed investigation and review of the influences of different model assumptions and the related consequences can be found in the literature, e.g. at Bischoff et al. [Bis2004]. In 2016 Touzout and Chebili [Tou1016] proposed an approach for the optimization of concrete domes and vaults, Their results shows a high accuracy compared to finite element based optimization. A generalized laminate theory called Layerwise Laminate theory has been developed by Reddy [Red1984] that provides a framework upon which any of the displacement-based, two-dimensional laminate theories can be derived. Based on this work, a layerwise shell theory that is capable of modeling three-dimensional kinematics in shells has been developed by Reddy. The Layerwise Shell Theory of Reddy gives an accurate description of the displacement field. The three-dimensional displacement field is expanded as a function of a surface-wise two-dimensional displacement field and a one-dimensional interpolation function through the thickness. The use of higher order polynomial interpolation functions or more sub-divisions through the thickness improves the degree of accuracy in expanding the three-dimensional displacement field [Red1992]. The resulting transverse strains are discontinuous at the layer interfaces if a piece-wise continuous polynomial interpolation of the displacements through the thickness is used. As a result, continuous transverse stresses can be obtained at the ply interfaces.

2.3.1 Modeling Approach used for Shell Structures by Flat Shell Finite Elements

Flat shell elements are widely used to model the curved geometry of a structure. Shell elements based on classical shell theories are very difficult to develop. Many simplifying approximations are involved in the development, which leads to less accurate results.

These types of elements are very efficient in modeling the curved geometry of the structure. However, because of the complexities involved, the alternative approach of modeling the structure with a series of flat elements, which is simpler and easier to implement, became more popular for the analysis of shell structures.

In 1961, Green *et al.* first developed the concept of using triangular flat shell elements to model arbitrary shaped shell structures [Zie1971]. Shells with cylindrical shapes or regular curved surfaces can be modeled using rectangular or quadrilateral flat shell elements. Zienkiewicz [Zie1971] recommended modeling curved surfaces by a series of flat shell elements, rather than using the more complex curved shell elements. He suggested developing a built up element by combining membrane and plate bending elements to develop a flat shell elements.

The development of a flat shell element consist of combining a membrane behavior that contains two in-plane translational degrees and a bending behavior that imitates a plate bending element that contains two rotational degrees of freedom and one out of plane translational degree of freedom. Because of the non-inclusion of the in-plane rotational degrees of freedom, the membrane stiffness matrix will consist of zero values corresponding to those eliminated degrees of freedom which are generally called drilling degrees of freedom (drilling rotation), this state will introduce a singularity in the global stiffness matrix of the structure if all the elements are co-planar. Chen [Che1992] suggested that problems occur in solving in-fill frames, folded plate structures and other complex structural systems when the in-plane rotational stiffness is not included in the stiffness matrix of the shell element.

In the objective of removing the appearance of singularity in the stiffness matrix, several authors have suggested different methods to avoid this problem. The normal methodology that can deal with the stiffness of the drilling degrees of freedom is the approximation of its corresponding stiffness. Knight [Kni1997] suggested that a very small value be specified for the stiffness of the drilling degrees of freedom so that the contribution to the strain energy equation from this term will be zero. The matrix for the stiffness of the

drilling degrees of freedom was developed by Zienkiewicz [Zie1971] for the triangular flat shell elements. Bathe and Ho [Boe1981] approximated the stiffness for drilling degrees of freedom by using a small approximate value.

Batoz and Dhatt [Bat1972], using the discrete Kirchhoff formulation for plate bending element formulated two elements, the first one is a triangular shell element named KLI element containing 15 degrees of freedom, the second is a quadrilateral shell element named KQT element which contains 20 degrees of freedom. The KQT element has been developed via the combination of four triangular elements with the mid-nodes on the sides. Dawe [Daw1972] formulated a simple triangular flat element for the analysis of shells using the displacement method.

McNeal [McN1978] developed a quadrilateral shell element baptized QUAD4, by considering two in-plane displacements, one out-of-plane displacement and two rotations. He introduced some modifications using a reduced order integration scheme for shear terms. In order to take into account the bending strain energy he included curvature and transverse shear flexibility to avoid the deficiency in it.

Bathe and Ho [Bat1981] using Mindlin theory of plates for developing another flat shell element based on the combination of membrane element with plate bending element, he studied two approaches for the development of shell elements. The first approach uses the higher order isoparametric elements, which are formulated on the basis of three dimensional stress conditions and using the higher order shape functions and integration scheme. The second approach uses lower order shell elements, which are developed by superimposing previously available membrane and plate bending elements and hence obtaining the membrane and bending properties of the shell element, a fictitious drilling rotation degree of freedom is introduced to construct the element stiffness matrix. It is concluded that the second approach is more cost effective than the first; because of the simplicity of development. The lower order terms used in the formulation require less computation effort and time. It is also concluded that higher order elements give far superior results than the lower order elements, but they are costly to implement on the computer because of the large size of the stiffness matrix.

Sabir and Ramadhani [Sab1985] developed an even simpler curved element for general shell analysis. Sabir [Sab1987] developed a rectangular element contains the essential five external nodal degrees of freedom only at each corner on his four nodes; this element was

tested and applied to the analysis of cylindrical as well as spherical shells. The results obtained found to be of a high accuracy compared to the reference solution with relatively finer meshes.

Dhatt et al. [Dha1986] formulated a new 6-node triangular bending element called DKTP based on a discrete Kirchhoff model and a flat-shell element DLTP having quadratic variation of in-plane displacement.

McNeal and Harder [McN1988] suggested in their study that, the higher order elements take three times more solution effort than the lower order elements. Another inconvenient of higher order elements is the use of high order numerical integration procedures to avoid misleading zero energy modes. Lower order elements require a large number of elements to model the structure but they require less computational effort and hence are still cheaper as compared to the higher order elements. However, the effectiveness of the element and accuracy of results of the lower order elements largely depends on the type of the element selected for the formulation of the shell element.

Batoz and Dhatt [Bat1992] developed many elements, from those elements there is the DKT12 obtained from the superposition of the CST membrane element and DKT6 bending element.

Some other elements for shells have been also developed by Djoudi et al. [Djo1995] and Sabir et al. [Sab1996]. From the validation tests, these elements have been shown to produce results of an acceptable degree of accuracy without the use of large number of elements. Another shell element with 24 DOF was formulated by Poulsen and Damkilde [Pou1996]. Also, Cook [Coo1994] developed a quadrilateral flat shell element having 24 degrees of freedom and good results have been obtained. Furthermore, Djoudi and Bahai [Djo2003] formulated a new strain-based shell element for the linear and nonlinear analysis of cylindrical shells; the effectiveness of this element was demonstrated and good convergence was also observed.

For the analysis of both thin and thick shell problems, a new simple four-node quadrilateral shell element called DKMQ24 with 24-dof has been developed by Irwan et al. [Irw2015], this element takes into account membrane, bending and shear effects.

Recently, Hamadi et al. [Ham2015] developed a flat shell element called ACM-RSBE5; it is a rectangular element obtained by the superposition of the RSBE5 (rectangular strain based element) with the ACM standard plate bending element [Adi1961], [Mel1963].

2.3.2 Flat Shell Finite Element Formulation

In classical formulations of flat shell element, Zienkiewicz and Taylor combined plane stress element with plate bending element [Zie1977, Zie1991], we know that for plane stress actions, the state of strain is uniquely described in terms of the *u* and *v* displacements at each typical node *i*. These modeling assumptions are shown in Figure 2.3.

A right-handed coordinate frame is employed, the variables *u* and *v* for in-plane displacements along the *x* and *y* axes respectively, the variable *w* for displacements perpendicular to the plane of the shell element, and the variables θ_x, θ_y, and θ_z for clockwise rotations about the *z*, *y* and *z* axes.

a). Plane Membrane Actions and Deformations

b). Bending Actions and Deformations
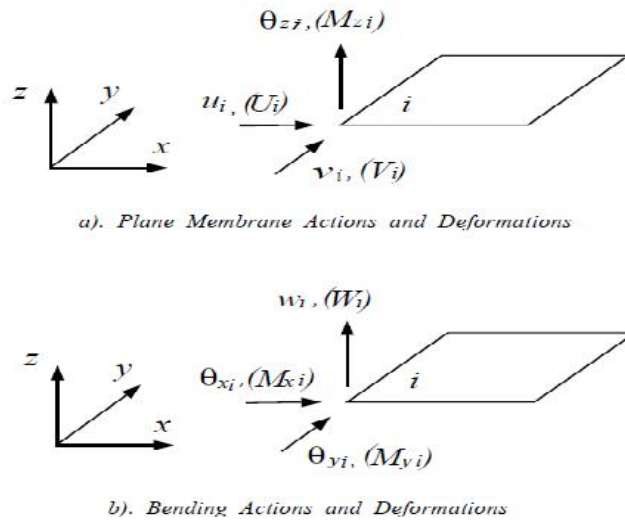
Fig. 2.3 A flat shell element subject to plane membrane and bending action.

By minimizing total potential energy, the classical formulation leads to a stiffness matrix $[K^p]$, nodal forces $\{f^P\}$, and element displacement $\{q^P\}$, where :

$$\{f^P\} = [K^p]\{q^p\} \tag{2.1}$$

with $\{q_i^p\} = \begin{Bmatrix} u_i \\ v_i \end{Bmatrix}$ and $\{f_i^p\} = \begin{Bmatrix} U_i \\ V_i \end{Bmatrix}$ for $i = 1,2,3,4$.

Here the superscript '*p*' to denote in-plane deformation of the shell element. Similarly, when bending action is considered, the state of strain is given uniquely by the nodal

displacements in the z direction, w, and the two rotations θ_x and θ_y. The result is bending stiffness matrices of the type :

$$\{f^b\} = [K^b]\{q^b\} \tag{2.2}$$

Where
$$\{q_i^b\} = \begin{Bmatrix} w_i \\ \theta_{xi} \\ \theta_{yi} \end{Bmatrix} \text{ and } \{f_i^b\} = \begin{Bmatrix} W_i \\ M_{xi} \\ M_{yi} \end{Bmatrix}, \text{ for } i = 1, 2, 3, 4.$$

2.4 Analysis of stiffened shell Structures

2.4.1 General description

The analysis of complex structures poses some challenges to the engineer. Traditionally, each structure is divided into simpler components analyzed independently of each other (decoupled structural functions). This is often questionable. So we do sometimes try to analyze the whole structure, as complex as it is, through the finite element method. The latter cut the structure into elementary components which together are calculated at once. The advantages are many:

- Fewer simplifying assumptions
- Consideration of interactions between components
- Better view of the overall behavior of the structure
- Detection of its potential weaknesses
- Economical design.

However, the compatibility of some elements with others is often a delicate problem of the discretization of a complicated structure. This compatibility is necessary to ensure convergence, although it can be slightly relaxed thanks to the patch test. Such compatibility problems arise when one combines solid and structural elements; may contain membrane elements and beam; the nodal unknowns membranes are two translations U and V (W), incompatible with the nodal unknowns of beams, which further to U and V, include the θz rotation. Similar difficulties occur at the intersection of shells or folded structures, the beams connecting nodes and shells with stiffeners, the junctions of structures with foundation blocks, etc. Figures 2.4 present some examples of stiffened cylindrical shells. The curvature of the system can generate at supports a large horizontal reaction. If the structure rests directly on the ground, this reaction is taken up by the foundation block. Otherwise, it must be reversed either by tie rods, usually placed at the foot arches or by the underlying structural elements (pillars, walls, etc.) **[Man2000].**

    (a) General case   (b) Without generators   (c) Without Arcs
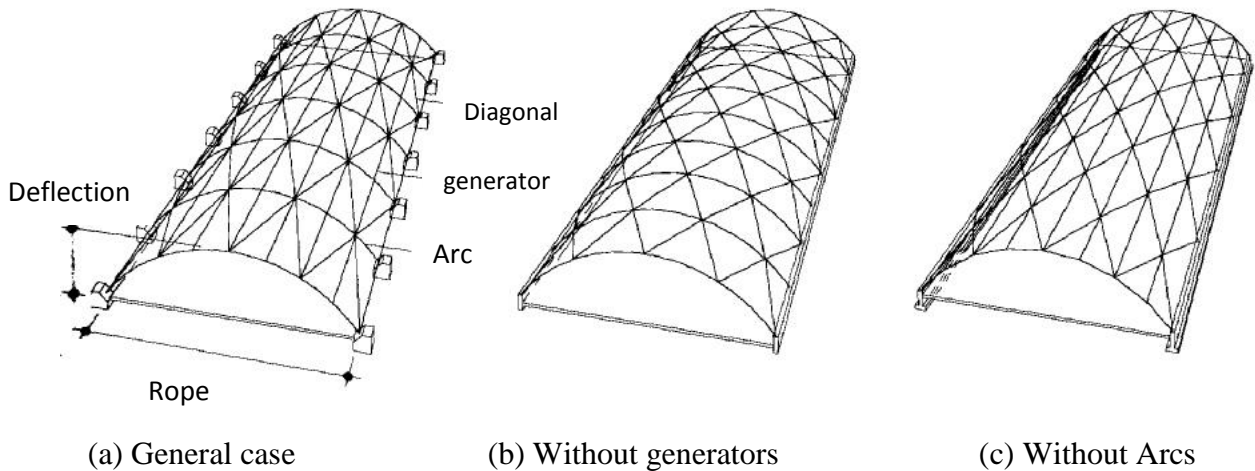
Fig . 2.4 Stiffened cylindrical shells **[Man2000]**

2.4.2 Review of Stiffened Shells and finite element modeling

The finite element method allows solving the problem of shells with stiffeners via the formulation of a beam element with compatible displacement pattern. A 16 degree of freedom isotropic beam finite element was proposed by Kohnke and Schnobrich [Koh1972], its displacements are compatible with the cylindrical shell element from which the beam element is reduced. However, its application is limited to isotropic cylindrical shells.

A doubly curved laminated anisotropic quadrilateral shell element with 48 degrees of freedom was formed by Venkatesh and Rao [Ven1980] for the analysis of laminated anisotropic thin shells of revolution. The results obtained are satisfactory.also , In 1982 Venkatesh and Rao [Ven1982] developed a stiffness matrix of laminated anisotropic curved beam finite element with 16 degrees of freedom for the analysis of curved anisotropic laminated beams. The curved stiffener element and the quadrilateral shell element [Ven1980,Ven1982], by using the principle of superposition, they have been used to solve problems of laminated anisotropic stiffened shells [Ven1983].

Carr and Clough [Car1969] and Schmit [Sch1968] used an alternative approach where axial stiffeners (stringers) and radial stiffeners (rings) were approximated by the same element type as the shell. The main disadvantage of their proposed approach was that a substantial number of extra nodes and nodal displacements are introduced as unknowns. Ferguson and Clark [Fer1979] developed a variable thickness curved beam and shell stiffener element with transverse shear deformation capabilities.

A complex type of hyperbolic paraboloid shell, which is usually referred to as the gable (or hipped) roof, is analyzed By Hazim [Haz1989]. This structure is usually constructed by a combination of four hypar shells together with crown and edge beams. Hazim analyzed only one quadrant of the shell, Due to symmetry of geometry and the uniform loading, is carried out using his strain based element. Kassegne [Kas1992] used a finite element model of the layerwise theory for shells and shell stiffener elements, the accuracy and reliability of the elements is investigated through a wide variety of examples.

Hector [Hec1993] brought a contribution of two solutions "pressurization and stiffening" to strengthen thin shells. This is an experimental approach and is based on parallel numerical modeling. The study is divided into two parts. The first part is devoted to the study of stiffened shells under internal pressure and axial compression, and the second part on non-stiffened shells under internal pressure, axial compression and transverse force.

2.4.3 Various studies on stiffened shells

2.4.3.1 Ring-Stiffened Cylindrical Shells

A ring-stiffened cylindrical shell under axial compression may fail in two forms of instability, local buckling of the sub-shell between the rings or general Instability of the stiffened shell as a whole. One type of general instability - buckling as an Euler column - occurs only in very long shells and may usually be excluded. In both forms of instability axisymmetric or asymmetric modes may occur, depending of the geometry of the shell. Furthermore, there may be a noticeable restraining effect of the rings on the local buckling and there may be interaction between the two forms of instability that may lower the general instability load.

An elementary linear analysis of the buckling of an axially compressed ring-stiffened cylindrical shell considers the sub-shell separately as a simply supported isotropic shell and then examines the general instability of a shell reinforced by the "distributed" or "smeared" stiffness of the rings [Sin1967a].

In order to investigate the effect of discreteness of the rings, the buckling of ring-stiffened cylindrical shells is analyzed by a linear "discrete" theory, instead of being "smeared", the rings are now considered as linear discontinuities represented by the Dirac delta function but otherwise the analysis is similar to that of [Sin1967b]. Other investigators

[Ste1951, Moe1958, Blo1964] may be noted that the delta function representation of rings has been employed, but without consideration of the eccentricity of the rings. The details of the method used in [Sin1967a], that is based on the formulation of Baruch [Bar1965] are given in [Sin1967c], where also extensive parametric studies are discussed.

It should be pointed out that the Dirac delta function representation is satisfactory only as long as the width of the stiffeners is not comparable to the distance between them, hence it could not be applied, for example, to the very closely stiffened shells of Milligan and all [Mil1966], and its reliability becomes doubtful in any shell with very wide stiffeners.

Though for buckling under hydrostatic pressure appreciable load reductions were found in Singer and Haftka [Sin1967c] for discrete rings, the discreteness effect was always found to be very small for ring-stiffened cylinders under axial compression. A similar conclusion was reached in Block [Blo1964] for orthotropic ring-stiffened cylinders by an analysis that did not take ring eccentricity into account. For completeness, however, the "discrete" buckling load, in addition to the "smeared" one is computed for some of the test cylinders. Hence, If the ring-spacing and the rotational restraint due to rings ensure axisymmetric local buckling and if the rings are placed on the outside or have high torsional stiffness to compensate for internal placing, an initially stable axisymmetric general instability should dominate and tests should agree well with predicted buckling loads. Figure 2.5 presents the cylindrical shell and the ring stiffener with details [Sin1967a].
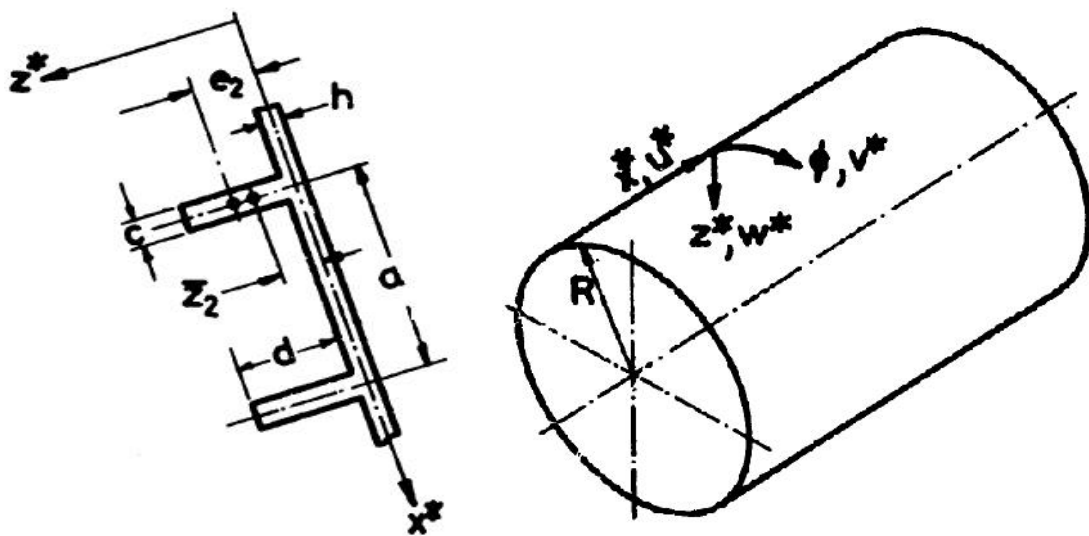
Fig. 2.5 Cylindrical shell and Detail of rings [Sin1967a]

2.4.3.2 Stringer-Stiffened Cylindrical Shells

Singer studied the instability of a cylindrical shell with and without stiffeners. A stringer-stiffened cylindrical shell under axial compression may be the subject of failure in two forms of instability, a general instability of the stiffened shell as a whole or a local buckling of the panel between the stringers.

Axisymmetric buckling modes will occur, in both forms of instability, only for short shells, and hence has to be considered only in the case of stringer stiffened shells reinforced also by strong rings. This discussion is therefore [Sin1967a] limited to asymmetric modes, that include for general instability the n =1 or "longitudinal" buckling modes mentioned in [Mil1966]. There may be an appreciable restraining effect of the stringers on the local buckling and there may be interaction between local and general instability. n: number of half longitudinal waves in cylindrical shell.

The elementary analysis again separates the consideration of buckling of the panels between the stringers and the study of the general instability of the "smeared-stringer" shell. The buckling and initial post buckling behavior of cylindrical panels has been studied by Koiter [Koi1956] for stringers that exert no rotational restraint on the panel. In the absence of restraining effects of the stringers except the radial one, the panel will buckle in the same mode and the same critical stress as the corresponding complete unstiffened cylindrical shell provided the angle between the equally spaced stringers Φ_0 satisfies $\phi_0 \geq \pi/m$.

Figure 2.6 presents the stiffened cylindrical shell with stringers.

Where:

$$m = (1/2)[12(1-\nu^2)]^{1/4}(\tfrac{R}{h})^{1/2} \tag{2.3}$$
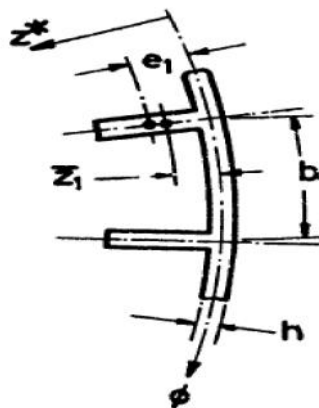
Fig. 2.6 Detail of stringers [Sin1967a]

23

The general instability of the "smeared-stringer" stiffened cylindrical shell under axial compression is discussed in detail in Singer and all [Sin1967b]. Slightly less accurate methods for calculation of the general instability are also given in [Hed1965]. It should be pointed out that in the case of stringer-stiffened shells very appreciable eccentricity effects appear and the boundary conditions affect the buckling loads considerably.

The effect of the discreteness of the stringers can again be investigated by a linear "discrete" theory in which the stringers are considered linear discontinuities represented by the Dirac delta function. The analysis of [Sin1967c] has been extended to stringer-stiffened shells and calculations are in progress. Preliminary results indicate that for thin shells of practical dimensions the discreteness effect is negligible. This is not surprising on account of the large number of stringers required to prevent local buckling.

2.4.3.3 Gabled Hyperbolic Paraboloid Shell

Shell structures have been used historically in large spatial structures [Par2005,Lai2009] and the concept of the form-resistant-structure is continuously adopted in current architectural forms [Kim2011]. The gabled hyperbolic paraboloid shell (referred to as gabled hyper) is one of the most common types of hyperbolic paraboloid shell structures. The basic unit of the gabled hyper consists of four shell panels, which have straight edges and four columns as supports. The support conditions influence on the behavior of a single gabled hyper is large. Usually four corners of a single gabled hyper are confined using tie rods or tie beams in order to restrain excessive lateral movements.

Shell panels have zero curvature along the direction of the perimeter but have convex or concave surfaces along the diagonal direction (Fig.2.7.a). In general, beams are located at the boundaries of shell panels. The beams located along the sloping lines of shell panels are referred to as edge beams, and beams located along the straight lines where the shell panels meet are called ridge or crown beams (Fig.2.7.b) [Rha2015].

The rationale for locating beams at the edges of the shell panels stems from the membrane theory. The membrane theory assumes that the gravitational loads that act on the shell panels are resisted by the in-plane shear stress of the shell, and the shearing forces will be transformed into compressive and tensile forces by concave or convex arch action and then transferred to the perimeter (i.e., edge beams and ridge beams) as axial forces, the effects of

the flexural stress and out-of-plane shearing force of the shell panels cannot be considered [Bil1982].

Numerical analysis using the finite element method is capable of considering the flexural moment, out-of-plane shearing forces, and their interactions with the in-plane shearing forces. The results from the refined finite element analysis show that shell loads are transferred to the supports through a different mechanism, which cannot be explained using the membrane theory. That is, the shell loads are directly transferred to corner supports by the convex arch action along the diagonal direction of the shell panel (from the crown to the corner supports), and the tensile forces created by concave arch action in the perpendicular direction are comparatively insignificant [Sha1976, Sim1989].

In similar cases, stresses on perimeter beams are minimized, however, shell panels, especially those in the vicinity of the supports, are subjected to a very high compressive stress state. Reduced significance of the perimeter beams resulted in the proposal of a new and simple gabled hyper shape, in which the edge beams along the slant edge line were removed [Jad1995].

(a) **(b)**
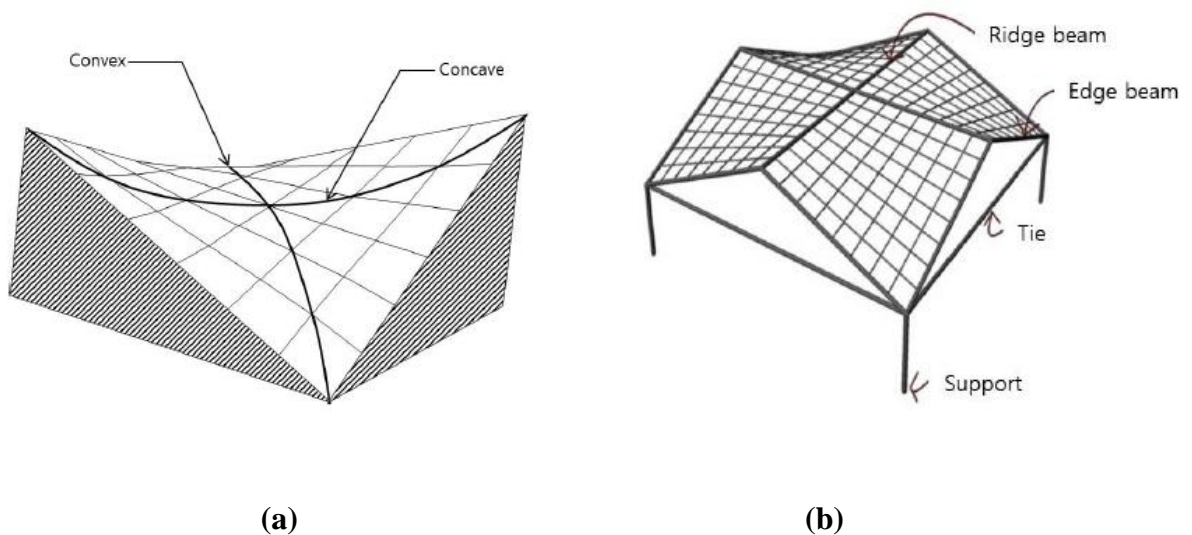
Fig. 2.7 Gabled Hyperbolic Paraboloid Shell [Rha2015]

Figure 2.8 shows a typical configuration of the traditional gabled hyper, which includes ridge beams and edge beams. Shaaban and Ketchum [Sha1976] analyzed the structural behavior of the traditional gabled hyper subjected to gravity load when support movements were restrained. They revealed that the shell loads were transferred mainly by the

compressive force due to the arch action from the crown to corner supports. Tensile forces due to the concave arch action in the perpendicular direction diminished due to the inward displacement of the perimeter beams. Jadik and Billington [Jad1995] removed the edge beams since the tensile action between end points of the ridge became insignificant. Based on the FE analysis results, they asserted that a gabled hyper can be designed without edge beams if there is sufficient shell thickness in the vicinity of the supports in order to resist high compressive stress.

However, the geometry, especially the rise ratio, may affect the global behavior of the gabled hyper, and the effects of lateral movement of supports should be considered. Thus, in this study, the effects of such factors were examined using FE analysis for the cases when the edge beams were and were not used, respectively.

Modeling and analysis were carried out using the finite element analysis software package SAP2000 [CSI2005]. Shell panels were modeled using four-node quadrilateral shell elements with conventional Kirchhoff's thin-plate theory, which neglects the out-of-plane shear effects. Edge beams were modeled as a typical frame element and combined with a shell, as shown in Fig 2.8, were simulated by a layered shell element, which is a built-in element in the SAP2000 element library. This element is useful when the centerline of the shell is not aligned with the centerline of the beams and yields reasonable results [Kim2012].
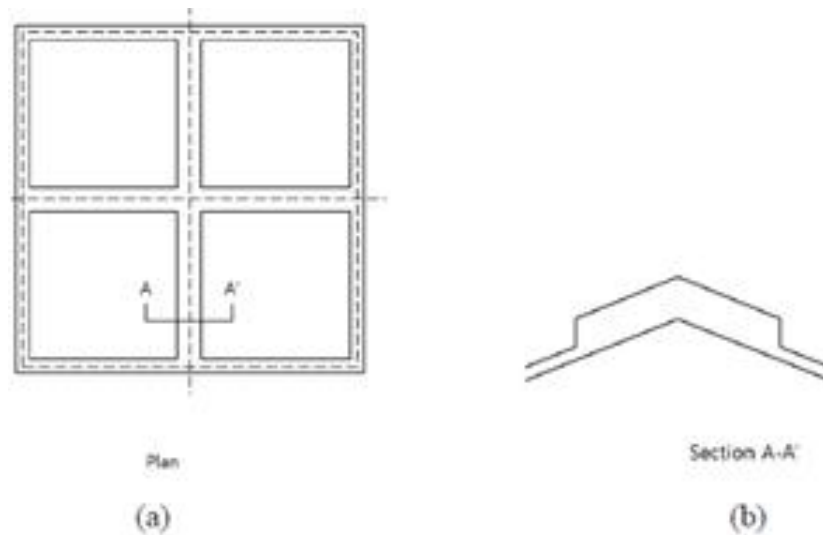
Fig. 2.8 Gabled Hyper Model [Rha2015]

2.5 Conclusion

This chapter is dedicated to the acquisition of some theoretical knowledge about shell structures. Starting with presentation of brief review of their fundamentals theories, and then described some types of stiffened shells.

The literature review presented the structural instability phenomena (Bending or buckling) caused by mechanical stresses, which requires a good understanding of these weaknesses in order to avoid a bad design. Also, a brief summary of assumptions and numerical modeling of shell structures is given.

The bending and the buckling phenomena on thin shells still need some other components like stiffeners, to improve the behavior of thin shell structures, especially in bending and buckling.

Chapter 3

Description of The Experimental

Work and The Numerical Analysis

Chapter 3

Description of The Experimental Work and The Numerical Analysis

3.1 Introduction

The analysis of thin shell structures has generally been purely carried out on a theoretical basis and it is of importance to try to establish the validity of the theories pounded by comparing their correlation with experimental results. It will be appreciated that the numerical analysis exposed in this study has assumed that the material from which the shell was constructed is perfectly elastic. In attempting to verify this theory by experimental test it would be natural to use such a perfectly elastic material. This would obviously provide the closest correlation between experimental and numerical results.

This chapter contains two parts; the experimental tests and the numerical analysis. For the experimental part, a series of tests have been performed for a cylindrical shell model, with and without stiffeners, undergoing a concentrated static load, with different thickness and boundary conditions. For the numerical analysis of cylindrical shell model, a quadrilateral flat shell element baptized "ACM-RSBE5", with four nodes and 6 degrees of freedom per node is used. The ABAQUS elements "S4R" and "C3D8IH" are also used for the analysis of the cylindrical shell model with stiffeners.

The results obtained by the numerical analysis of the cylindrical shell model, using both elements ACM-RSBE5 and S4R are compared to those given by the experimental tests. Also, we provide a contribution to the modeling of complex structures by using a cylindrical shell model with stiffeners and edge beam. Through several experimental tests, the efficiency of the boundary condition and the capability of the C3D8IH element ABAQUS of modeling cylindrical shell model are studied. The results obtained by the numerical analysis are compared to those obtained experimentally.

3.2 Experimental work

The experimental investigations have been conducted at the Civil Engineering Laboratory at the City, University of London (U.K). The important steps of the test's procedures are explained in the next paragraphs.

3.2.1 System set-up

The present study was performed on six cylindrical shell models, each model made of stainless steel 304 and with different thickness; the six models have the same shapes and dimensions. The shape is a semi cylinder with R=160 mm of radius and L= 900 mm of length (Fig. 3.1). The material properties have been assumed to be: The elasticity modulus E=190000 N/mm2, the Poisson ratio υ = 0.265. A concentrated load is applied at the top for all the models. All tests and models with different boundary conditions are explained in details in next paragraphs.
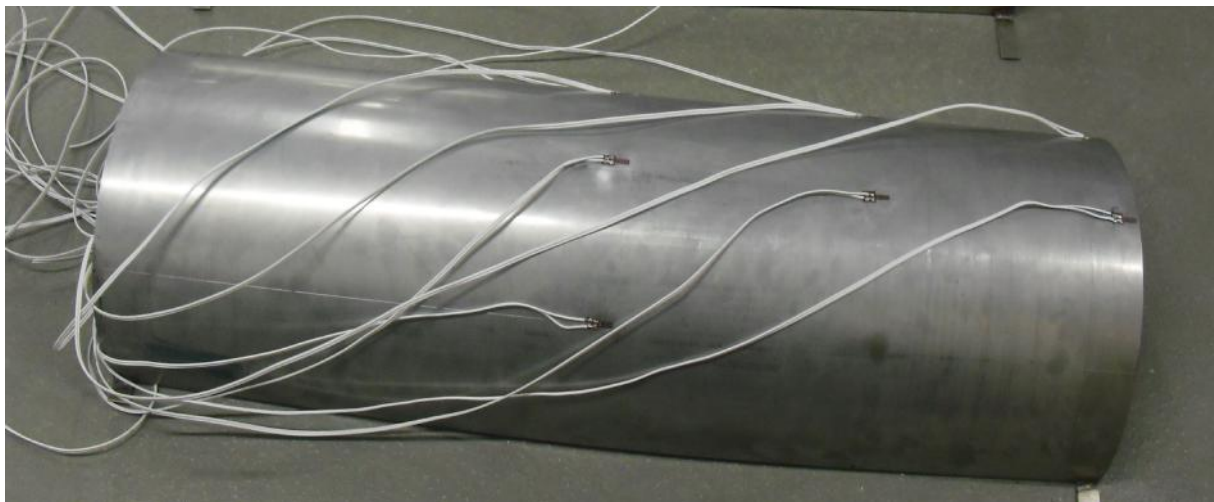
Fig. 3.1 The cylindrical shell model

3.2.1.1 Test 1: *Cylindrical shell with no end diaphragms and no stiffeners (t = 2 mm, CNDNS2)*

For the first test, the thickness of the cylindrical shell is t = 2 mm. In this test, many loads are applied and the vertical displacements at the points 1, 2 and 3 for each load at points 1 to 10 are recorded (fig 3.2). The positioning of the specimen on the UNIFLEX 300 machine are shown in Figure.3.2 below.

Fig. 3.2 The specimen on UNIFLEX 300 machine

3.2.1.2 Test 2: *Cylindrical shell with no end diaphragms and no Stiffeners (t =1.2 mm, CNDNS)*

The same procedure is used here for this test; but the thickness of the cylindrical shell model is different, t = 1.2 mm.

3.2.1.3 Test 3: *Cylindrical shell with two end rigid Diaphragms and no Stiffeners (t=1.2mm, CDNS)*

The thickness of the cylindrical shell model is t=1.2 mm, with end rigid diaphragms. In this test, also many loads are applied and the vertical displacements at the points 3, 5v, 9 and the horizontal displacement at the point 6h are recorded. Figure 3.3 shows the positioning of the specimen on the UNIFLEX 300 machine, the dial gauges and strain gauges.
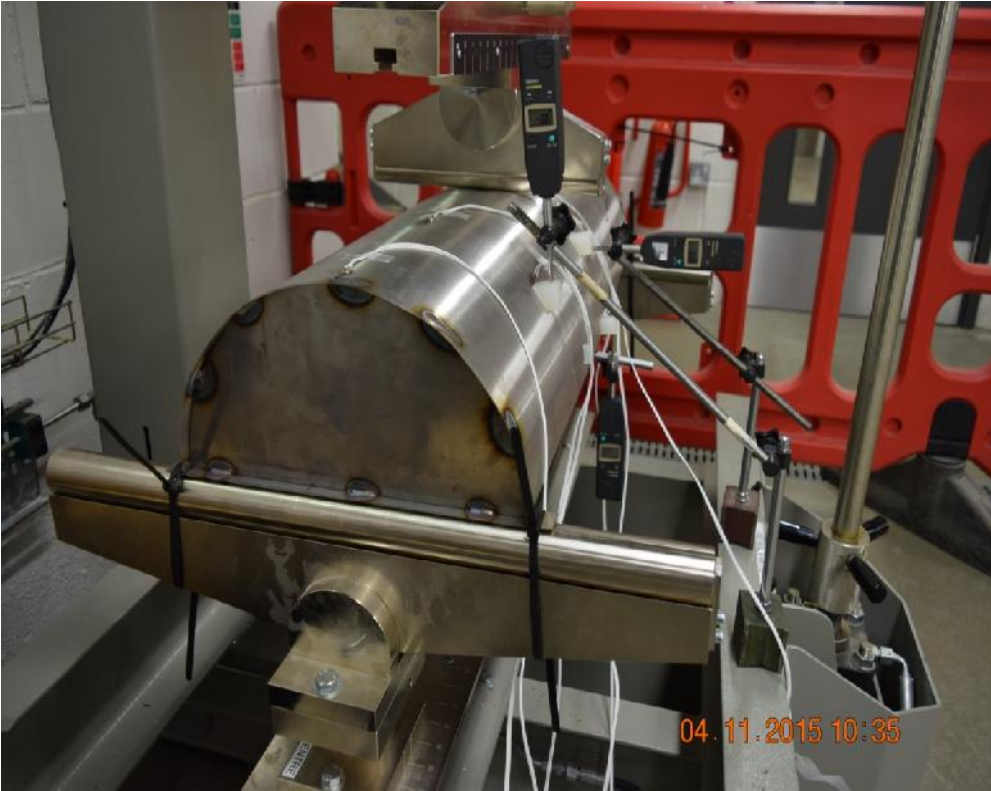
Fig. 3.3 Cylindrical shell model with rigid diaphragms boundary conditions

3.2.1.4 Test 4: *Cylindrical shell with no end Diaphragms and two Stiffeners (t=1.2 mm, CNDS)*

The thickness of the cylindrical shell model used is t =1.2 mm. In this test, two stiffeners are added (Figs. 3.4, a and b). The same procedure is used as the previous test.
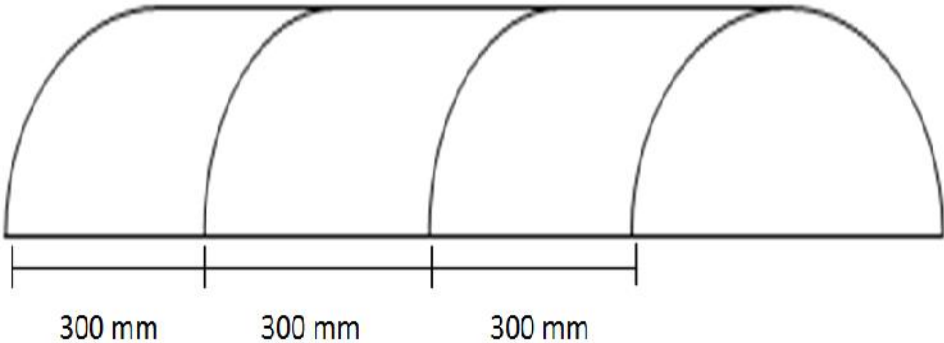
-a-
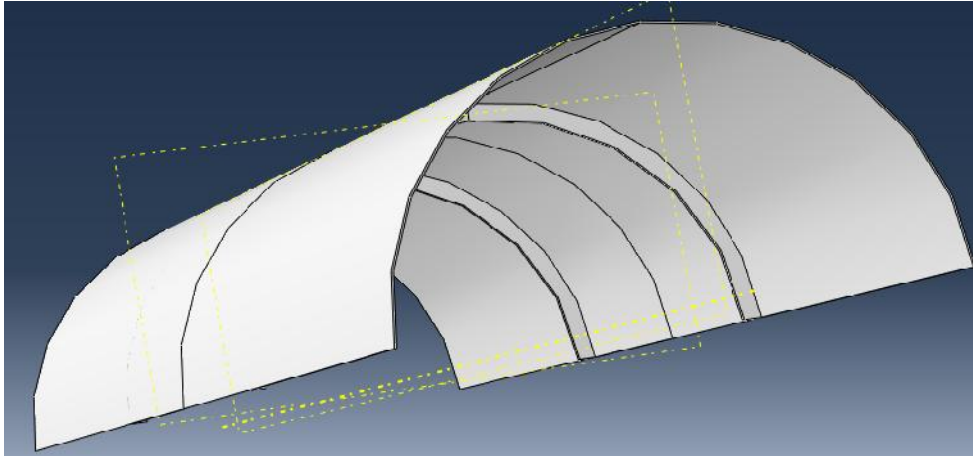
-b-

Fig. 3.4 Positioning of the stiffeners at the cylinder (-a- and -b-)

Fig. 3.5 Cylindrical shell with two stiffeners
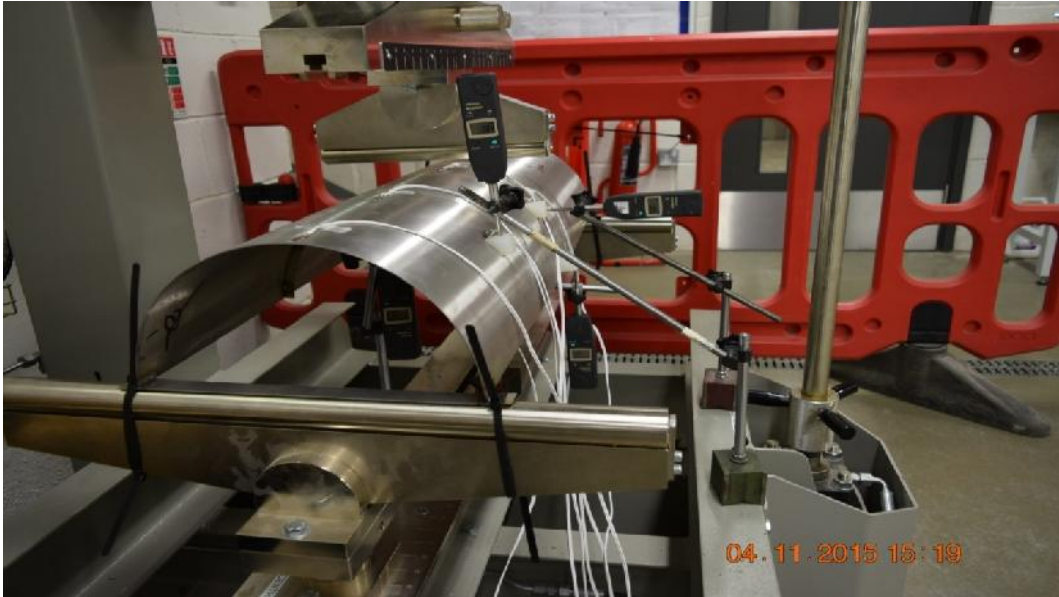
Fig. 3.6 Positioning of the cylindrical shell model with two stiffeners on the UNIFLEX 300

machine

33

3.2.1.5 Test 5 : *Cylindrical shell with two end Diaphragms and two Stiffeners (t=1.2 mm, CDS)*

The thickness of the cylindrical shell is t=1.2 mm, with two stiffeners and end rigid diaphragms. The same procedure is used for the loadings as the previous test and the reading of the displacement the points 3, 5v, and 9 and the horizontal displacement at the point 6h are recorded. The positioning of the two stiffeners are shown in Figure 3.5.

3.2.1.6 Test 6: *Cylindrical shell with two end Diaphragms and two Stiffeners resting on longitudinal beams "Stringers", (t=1.2mm, CDSS)*

In this test, two longitudinal beams "stringers" are added. The thickness of the cylinder is t=1.2mm. The applied loadings are similar to the previous one. The vertical displacements at the points 3, 5v, 9 and the horizontal displacement at the points 6h and 9h are recorded. Figure 3.7 shows the positioning of the two stringers.
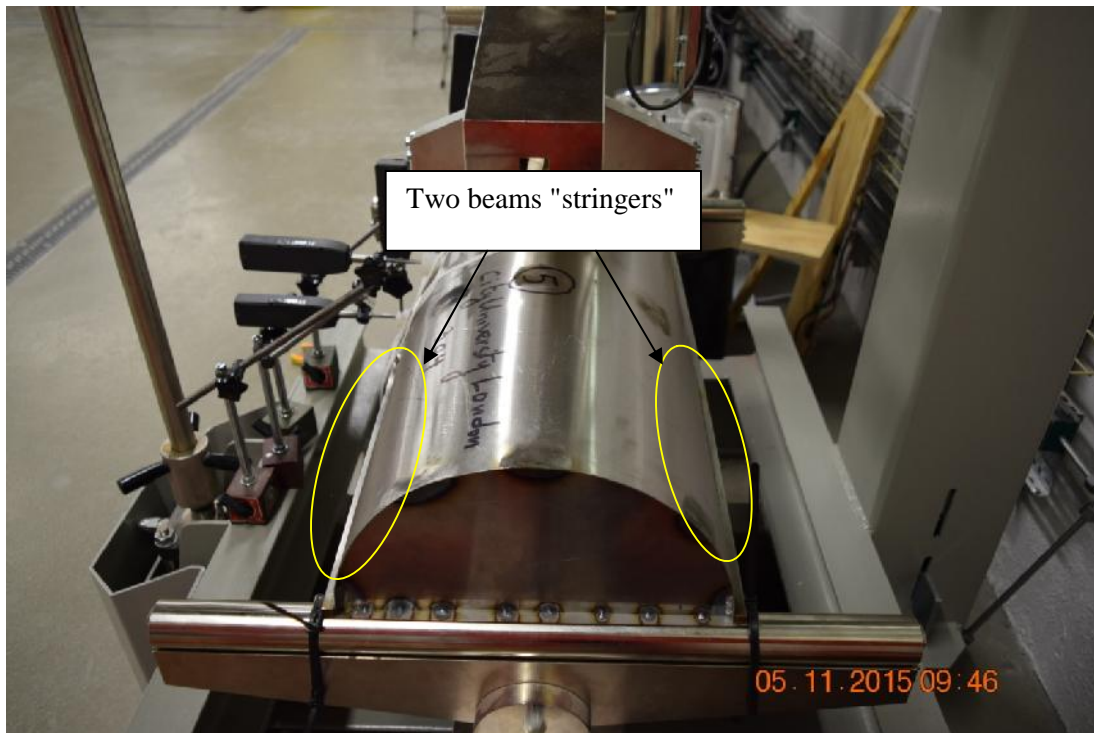
Fig. 3.7 The positioning of the two beams "stringers".

3.2.1.7 Stiffeners characteristics

In this experimental work, two types of stiffeners; ring stiffeners and stringers, both of them have the same material properties; the elasticity modulus E=190000 N/mm² and the

Poisson's ratio υ =0.265. The figures 3.8 show the geometrical properties of the ring stiffeners and the stringers "edge beams".
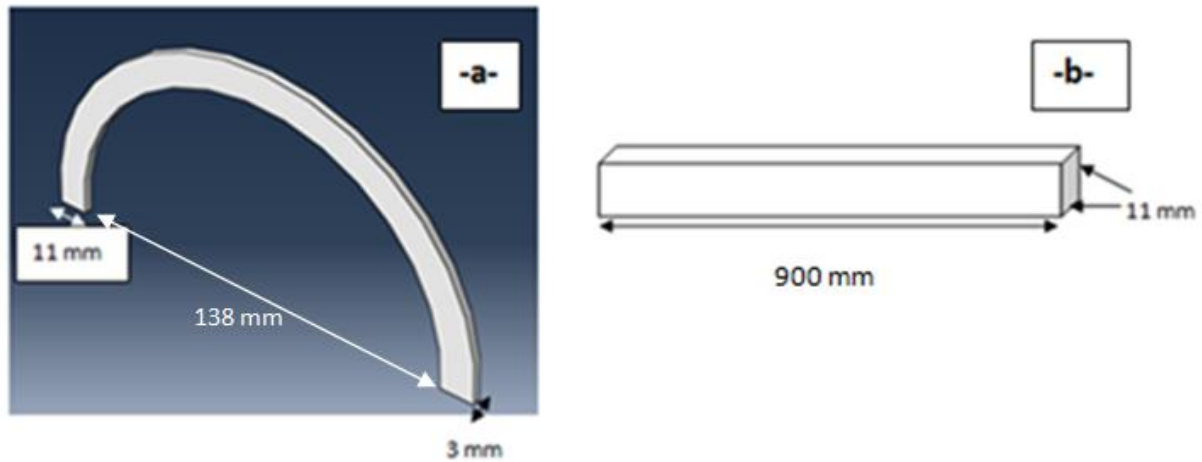
Fig. 3.8 Geometrical dimensions of the stiffeners

-a- Ring stiffeners, **-b-** Stringers "Edge beam"

3.2.1.8 Boundary conditions

The boundary conditions used are described separately for each model as follows:
- For the tests 1, 2 and 4: The model is free along the four edges, fixed at 4 corner points (Fig.3.9-a).
- For the tests 3, 5 and 6: The model is free along the two lateral long sides and fixed with two rigid diaphragms at the curved sides (Fig.3.9-b).

-a- Specimen without Rigid Diaphragms   **-b-** Specimen with Rigid Diaphragms
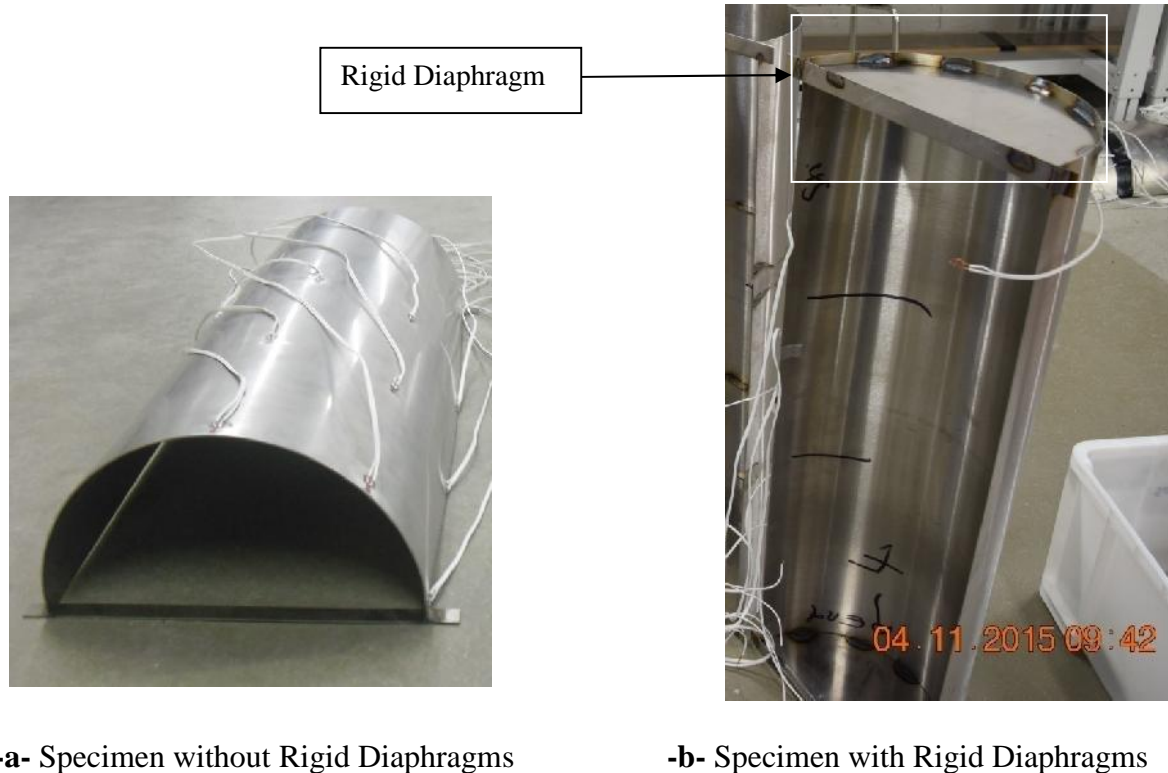
Fig. 3.9 Cylindrical shell model with different boundary conditions

3.2.2 Apparatus used

The machine used is 50-C1601 UNIFLEX 300 (Fig 3.10) and it has a high precision load unit for the load measurement and large testing space for a wide range of accessories for conventional and tests under control of displacement and strain rate. This machine is connected to a suitable control consoles 50-C9842 ADVANTEST 9. The ADVANTEST 9 can be easily performed under specific load, displacement and strain control. It is monitoring and displaying all tests data and parameters, either in graphic or numerical format and it gives the real time variation of the setting including the control method - load, displacement or strain- (Fig 3.11).

The displacements at the top of the cylinder where the load is applied can be measured by the ADVANTEST 9 and it gives readings with 0.001mm of resolution, while at the other points it measured by the dial gauge ABSOLUTE Digimatic Indicator ID-U Series 575 of 0.01 mm of resolution and 25.4 mm of range (Fig 3.12).

Fig. 3.10 UNIFLEX 300 machine

Fig. 3.11 ADVANTEST9   **Fig. 3.12** Digimatic Indicator

3.2.3 Measurements

For all the tests, the same dialing of the points is used. The readings of displacements are then recorded as needed, (more details are given in Appendix A).

Figure 3.13 shows the dial gauge location. It should be mentioned that the deflection at point 3 has been recorded by the ADVANTEST 9.
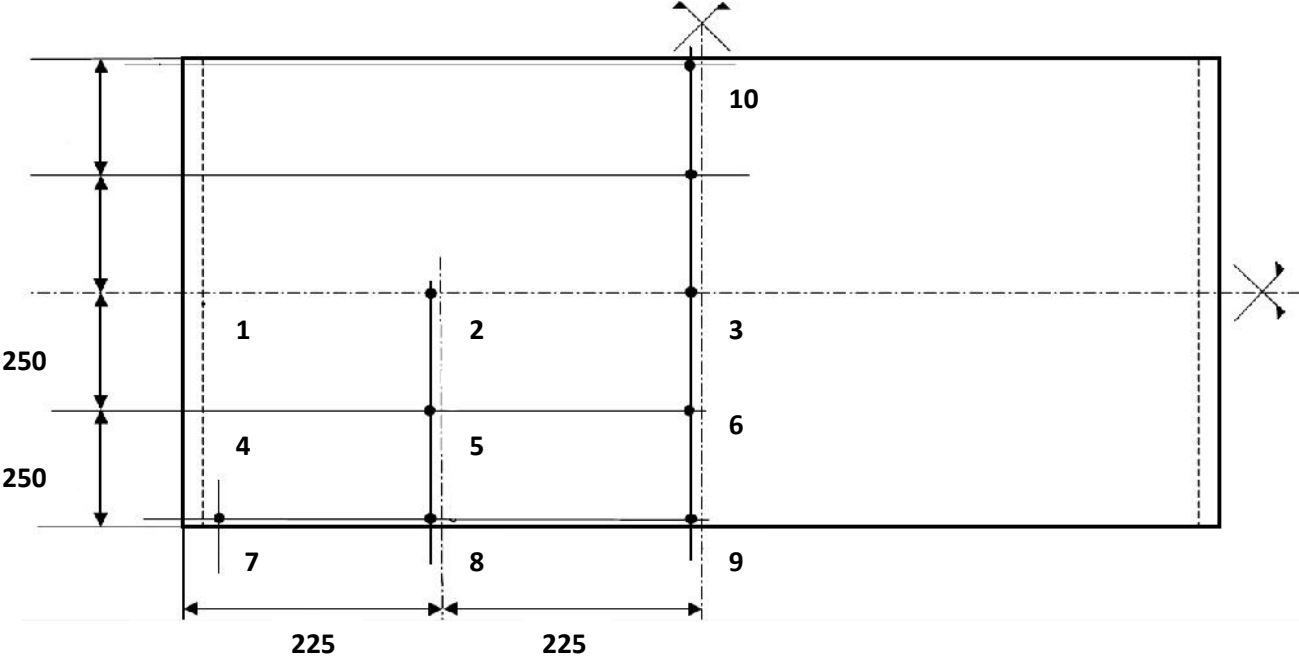
Fig. 3.13 Dial gauges locations; (distance in mm)

Figure 3.14 shows the specimen on the UNIFLEX 300 machine, and the vertical and horizontal dial gauges positioning.

Fig. 3.14 Dial gauges positioning, and applied loading

3.2.4 Applied loads

The applied load is a concentrated static load for all the tests, the structure is closed by a vertical rod hydraulically clamped and controlled assuring high rigidity, fitted with high precision strain gauges load cell for accurate and reliable test results. The frame has to be connected to a control console like we mentioned above. The tests under control of displacement and strain rate can only be performed with the ADVANTEST 9 (Servo hydraulic control console).

3.3 Numerical Analysis

In this work the numerical results are obtained by **S4R** and **C3D8IH** elements of ABAQUS code [ABA2014] and those given by the **ACM-RSBE5** element [Ham2015].

3.3.1 ABAQUS Code

3.3.1.1 Introduction

ABAQUS code is written and maintained by Hibbitt, Karlsson & Sorensen [HKS1995] in 1978 by graduates of the program PILD of brun in Solid Mechanics. It is the leading global provider of software and services for advanced finite element analysis. ABAQUS software suite has an unsurpassed reputation for technology, quality and reliability. It offers a powerful and comprehensive solution for solving linear and nonlinear engineering problems. A wide range of structural analysis, thermal and multi-physics is supported.

The software provides an unparalleled environment, presenting a compelling alternative to implementations involving multiple products and vendors. Thanks to the robustness of its products and the high quality of its engineering services, ABAQUS allows users to benefit from nonlinear multiphysics simulation software that give them the keys to successful modeling of a wide range of engineering problems.

Solvers ABAQUS can treat all types of nonlinearities:

   • Materials non-linearities.

   • Geometric nonlinearities.

   • Boundary conditions Non-linearities (advanced contact modeling).

ABAQUS is designed primarily for shaping the behavior of solids and structures under the externally applied load. It includes the following features:

   - Opportunities for static and dynamic problems;

   - The ability to modeling very large changes in form of solids, in two and three dimensions

- An extensive library of element, including a full set continuum elements, beam elements, shell and flat elements, among others;

- Sophisticated possibilities in contact between the solid model;

- An advanced material library, including the usual elastic and elastic - plastic solids; models for foam, concrete, soil, piezoelectric materials, and many others;

- The possibilities to shape a number of phenomena of interest, including vibrations, coupled interactions, fluid / structure, acoustic, loop problems, and so on.

More details concerning the use of ABAQUS are given in Appendix B.

3.3.2 Type of ABAQUS elements used for analysis in this thesis

ABAQUS provides a wide range of finite elements for different geometries and analysis types. For the present study, two different elements are used: **S4R** (shell element) and **C3D8IH** (Solid element).

3.3.2.1 S4R Element

S4R is a quadrilateral finite-membrane-strain element with a uniformly reduced integration to avoid shear and membrane locking (Figure 3.15).

- The S4R element has several hourglass modes that may propagate over the mesh.

- Flexible Converges to shear theory for thick shells and classical theory for thin shells.

S4R is a robust, general-purpose element that is suitable for a wide range of applications.
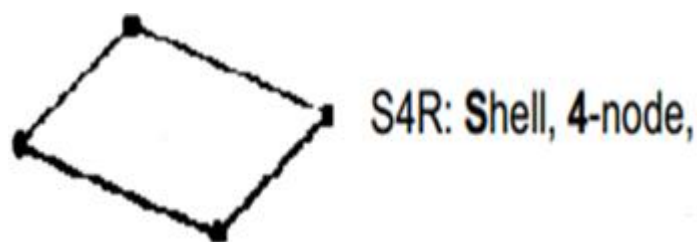
Fig. 3.15 S4R element with 6 DOF at each node

• 4-node doubly curved used for thin and thick shell element

• 6 DOF at each node (3 displacements and 3 rotations)

3.3.2.2 C3D8IH Element

The **C3D8IH** element is a general purpose linear brick element, with full integration points, hybrid formulation and incompatible modes.

The node numbering follows the convention as shown in (Fig 3.16) .
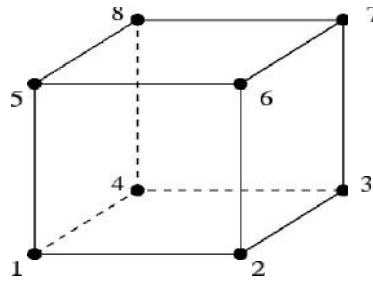
Fig. 3.16 8-node brick element

The incompatible mode eight-node brick element is an improved version of the C3D8 element. In particular, shear locking is removed and volumetric locking is much reduced. This is obtained by supplementing the standard shape functions with so-called bubble functions, which have a zero value at all nodes and nonzero values in between, so the quality of the C3D8I element is far better than the C3D8 element.

3.3.3 The flat shell element ACM-RSBE5 [Ham2015]

The quadrilateral flat shell element used (ACM-RSBE5) is obtained by the superposition of the **RSBE5** membrane strain based finite element with the **ACM** standard plate bending element [Adi1961, Mel1963]. We have obtained a flat shell element called **ACM-RSBE5.**

Figure 3.17 shows the shell element **ACM-RSBE5**.
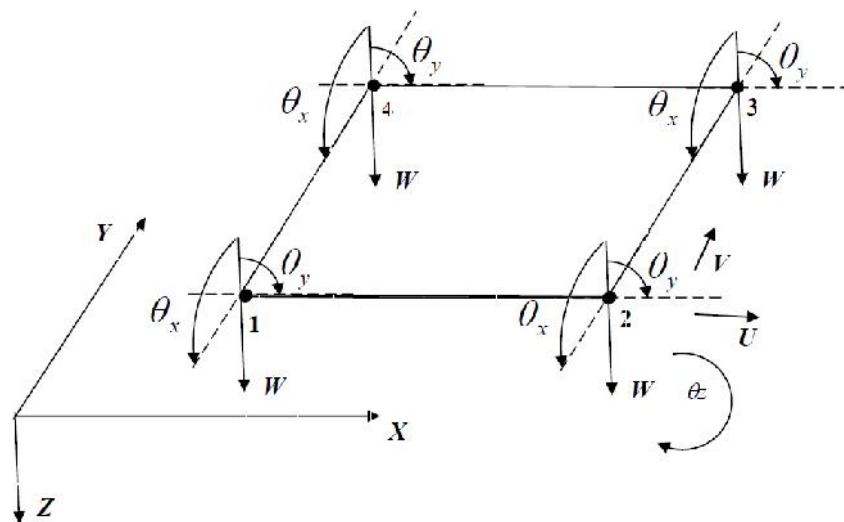
Fig. 3.17 The shell element ACM-RSBE5

The stiffness matrix of the shell element **ACM-RSBE5** is obtained by using the analytical integration of the membrane and bending stiffness matrix. The calculation of the element stiffness matrix is summarized with the following well known expressions Eqs. (3.1, 3.2 and 3.3):

$$[K_e] = [A^{-1}]^T \left[\iint_S [Q]^T [D][Q].dx.dy \right] [A^{-1}] \tag{3.1}$$

$$[K_e] = [A^{-1}]^T [K_0][A^{-1}] \tag{3.2}$$

With: $$[K_0] = \iint_S [Q]^T [D][Q] \, d\,x.d\,y \tag{3.3}$$

To calculate the displacement for all the models by using the flat shell element ACM-RSBE5, a Fortran program elaborated by [Ham2006], the flow chart below shows the main steps;
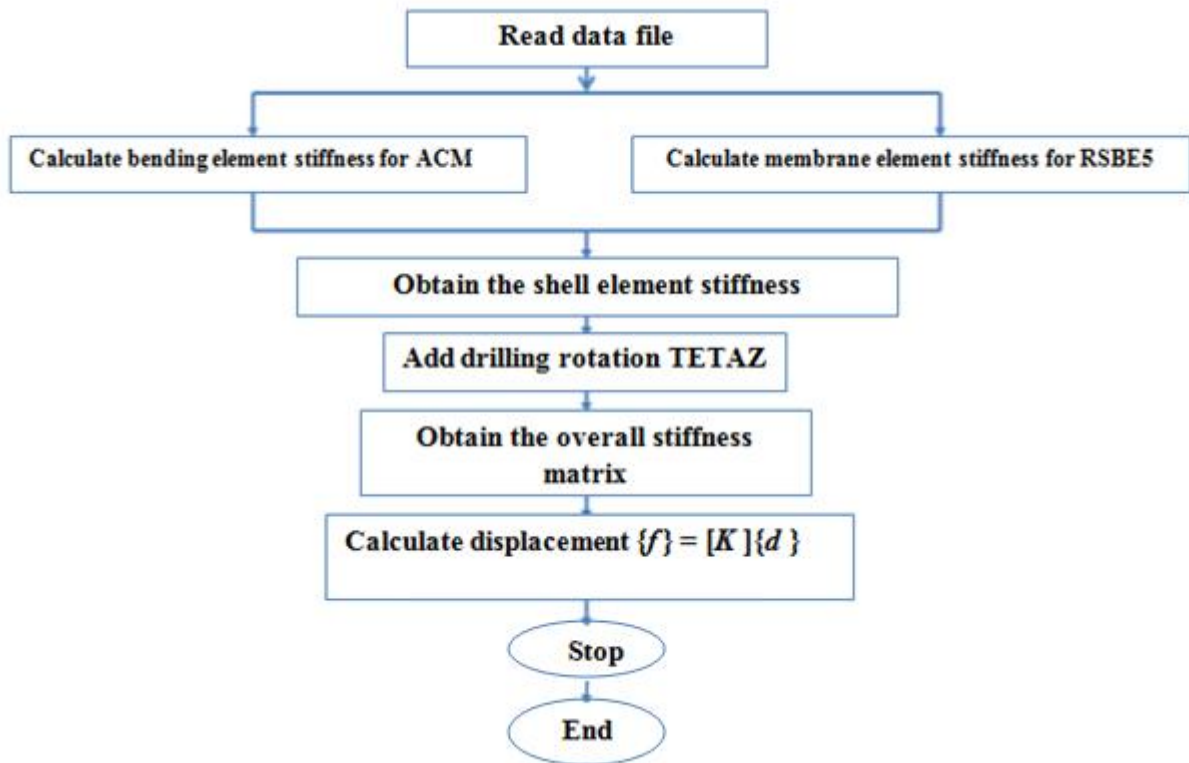
Fig. 18. General flow chart

Chapter 4

Experimental and Numerical Investigation of The Behavior of a Cylindrical Shell Model

Chapter 4

Experimental and Numerical Investigation of The Behavior of a Cylindrical Shell Model

4.1 Introduction

The analysis of thin shell structures has generally been purely carried out on a theoretical basis such as the superposing of the membrane and bending behavior. A new flat shell element called **ACM-RSBE5** [Ham2015] composed of strain based quadrilateral membrane element **RSBE5** and the standard plated bending element **ACM** is used for the numerical analysis in addition to the **S4R** ABAQUS element. It is of great importance to carry out some experimental tests. A series of test has been done for a cylindrical shell models with different types of boundary conditions and different thickness are used and undergoing a concentrated progressive load. The results obtained by the numerical analysis are compared to those given by the experimental test.

This chapter illustrates and presents the experimental and numerical results. We used three tests for a cylindrical shell models with different type of boundary conditions and different thickness. We will recapitulate it in next paragraphs. The obtained results was published [Tem2016].

4.2 Cylindrical shell with no end Diaphragms, t = 2 mm

The following loads are applied [2500N, 2750N, 3000N, 3250N, 3500N and 3750N] and the vertical displacements for points 1, 2 and 3 for each load are recorded. The diagrams presented below show the convergence of displacement. In each diagram the number of elements used is presented with X-axis and the normalized results (W_{num}/W_{exp}) with Y-axis. The results obtained for vertical displacements are given in Figs. 4.1, 4.2 and 4.3 (a, b, c and d case loading) and compared with those obtained by the numerical analysis ACM-RSBE5 element and S4R element of ABAQUS code.

4.2.1 Vertical Displacements at point 1

Table 4.1 The vertical Displacements at point 1 for the Load 2750N

Meshes	Displacement W_1 at point 1		Normalised Results W_{num}/W_{exp}	
	ACM-RSBE5	**S4R element**	**ACM-RSBE5**	**S4R element**
2 x 2	2.140	1.382	0.61230329	0.39542203
4 x 4	3.107	3.126	0.88898426	0.8944206
6 x 6	3.319	3.33	0.94964235	0.9527897
8 x 8	3.400	3.410	0.97281831	0.97567954
10 x 10	3.418	3.459	0.97796853	0.98969957
Experimental solution	**3.495**		1	

Table 4.2 The vertical Displacements at point 1 for the Load 3000N

Meshes	Displacement W_1 at point 1		Normalised Results W_{num}/W_{exp}	
	ACM-RSBE5	**S4R element**	**ACM-RSBE5**	**S4R element**
2 x 2	2.334	1.507	0.59088608	0.38151899
4 x 4	3.390	3.408	0.85822785	0.86278481
6 x 6	3.621	3.630	0.91670886	0.91898734
8 x 8	3.709	3.717	0.93898734	0.94101266
10 x 10	3.728	3.770	0.94379747	0.95443038
Experimental solution	**3.95**		1	

Table 4.3 The vertical Displacements at point 1 for the Load 3250N

Meshes	Displacement W_1 at point 1		Normalised Results W_{num}/W_{exp}	
	ACM-RSBE5	**S4R element**	**ACM-RSBE5**	**S4R element**
2 x 2	2.529	1.632	0.58841322	0.37971149
4 x 4	3.672	3.690	0.85435086	0.85853886
6 x 6	3.923	3.930	0.91275012	0.91437878
8 x 8	4.018	4.024	0.93485342	0.93624942
10 x 10	4.039	4.082	0.93973941	0.94974407
Experimental solution	**4.298**		**1**	

Table 4.4 The vertical Displacements at point 1 for the Load 3500N

Meshes	Displacement W_1 at point 1		Normalised Results W_{num}/W_{exp}	
	ACM-RSBE5	**S4R element**	**ACM-RSBE5**	**S4R element**
2 x 2	2.723	1.756	0.5773961	0.37234945
4 x 4	3.955	3.972	0.83863444	0.84223919
6 x 6	4.224	4.230	0.8956743	0.89694656
8 x 8	4.327	4.331	0.91751484	0.91836302
10 x 10	4.350	4.393	0.92239186	0.93150975
Experimental solution	**4.716**		1	

As an example of application of the ACM-RSBE5 element, the data and results files are given in appendix C for 2x2 meshes for the load 3500N (table 4.4).
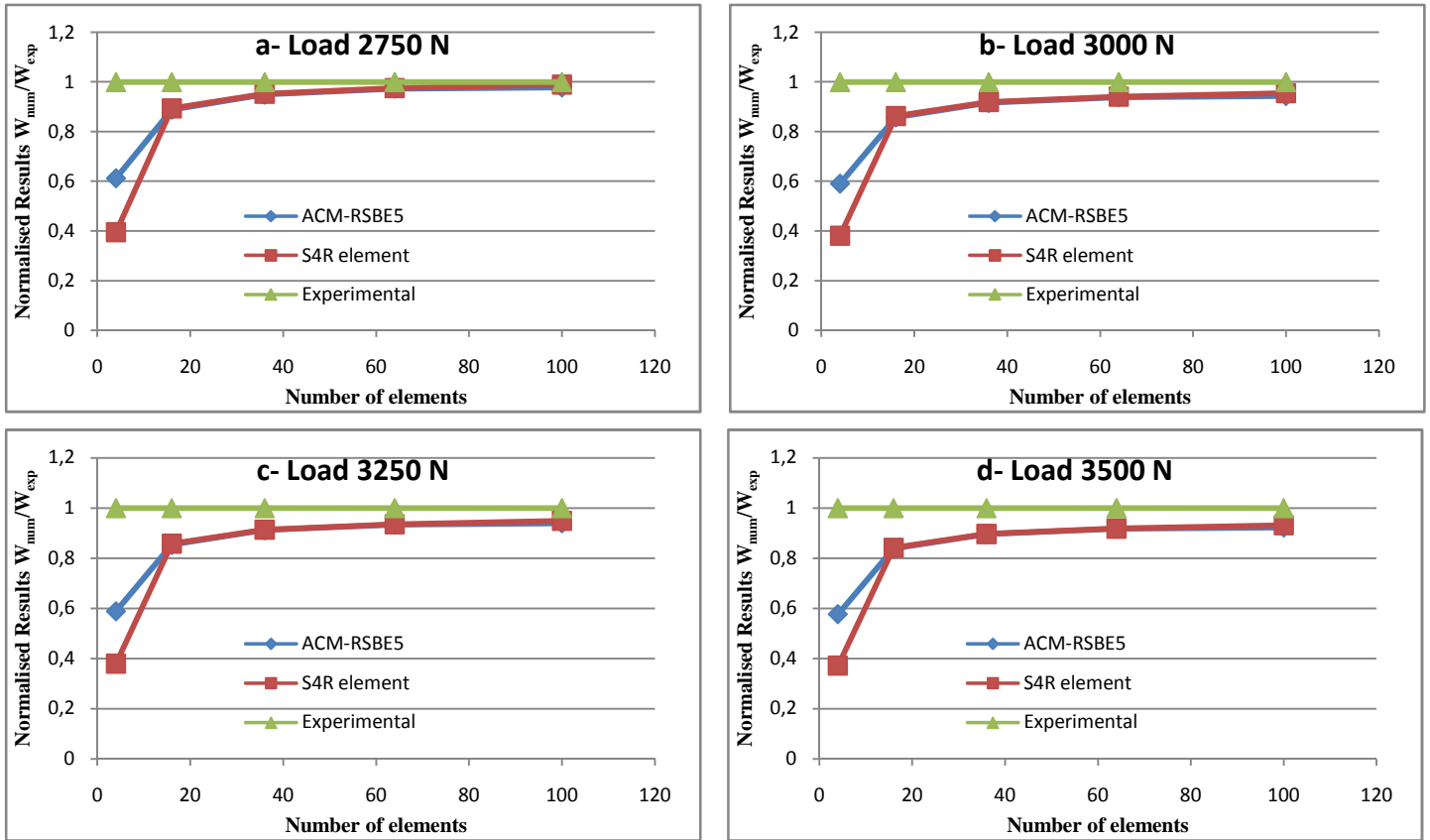
Fig. 4.1 Convergence curve for the deflections W_1 at point 1 under different loads

4.2.2 Vertical Displacements at point 2

Table 4.5 The vertical Displacements at point 2 for the Load 2750N

Meshes	Displacement W_2 at point 2		Normalised Results W_{num}/W_{exp}	
	ACM-RSBE5	**S4R element**	**ACM-RSBE5**	**S4R element**
2 x 2	2.534	1.092	0.69787937	0.3007436
4 x 4	3.304	3.258	0.90994216	0.89727348
6 x 6	3.474	3.462	0.95676122	0.95345635
8 x 8	3.545	3.530	0.97631506	0.97218397
10 x 10	3.562	3.603	0.98099697	0.99228863
Experimental solution	**3.631**		**1**	

Table 4.6 The vertical Displacements at point 2 for the Load 3000N

Meshes	Displacement W_2 at point 2		Normalised Results W_{num}/W_{exp}	
	ACM-RSBE5	S4R element	ACM-RSBE5	S4R element
2 x 2	2.765	1.191	0.67936118	0.29262899
4 x 4	3.604	3.553	0.88550369	0.87297297
6 x 6	3.79	3.775	0.93120393	0.92751843
8 x 8	3.868	3.849	0.95036855	0.94570025
10 x 10	3.885	3.928	0.95454545	0.96511057
Experimental solution	**4.07**		**1**	

Table 4.7 The vertical Displacements at point 2 for the Load 3250N

Meshes	Displacement W_2 at point 2		Normalised Results W_{num}/W_{exp}	
	ACM-RSBE5	S4R element	ACM-RSBE5	S4R element
2 x 2	2.995	1.29	0.67182593	0.28936743
4 x 4	3.905	3.847	0.87595334	0.86294302
6 x 6	4.106	4.087	0.92104083	0.91677882
8 x 8	4.190	4.168	0.93988336	0.93494841
10 x 10	4.209	4.253	0.94414536	0.95401525
Experimental solution	**4.458**		**1**	

Table 4.8 The vertical Displacements at point 2 for the Load 3500N

Meshes	Displacement W_2 at point 2		Normalised Results W_{num}/W_{exp}	
	ACM-RSBE5	**S4R element**	**ACM-RSBE5**	**S4R element**
2 x 2	3.226	1.389	0.66873964	0.28793532
4 x 4	4.205	4.142	0.87168325	0.85862355
6 x 6	4.421	4.400	0.91645937	0.91210614
8 x 8	4.512	4.486	0.93532338	0.92993367
10 x 10	4.533	4.578	0.93967662	0.94900498
Experimental solution	**4.824**		**1**	
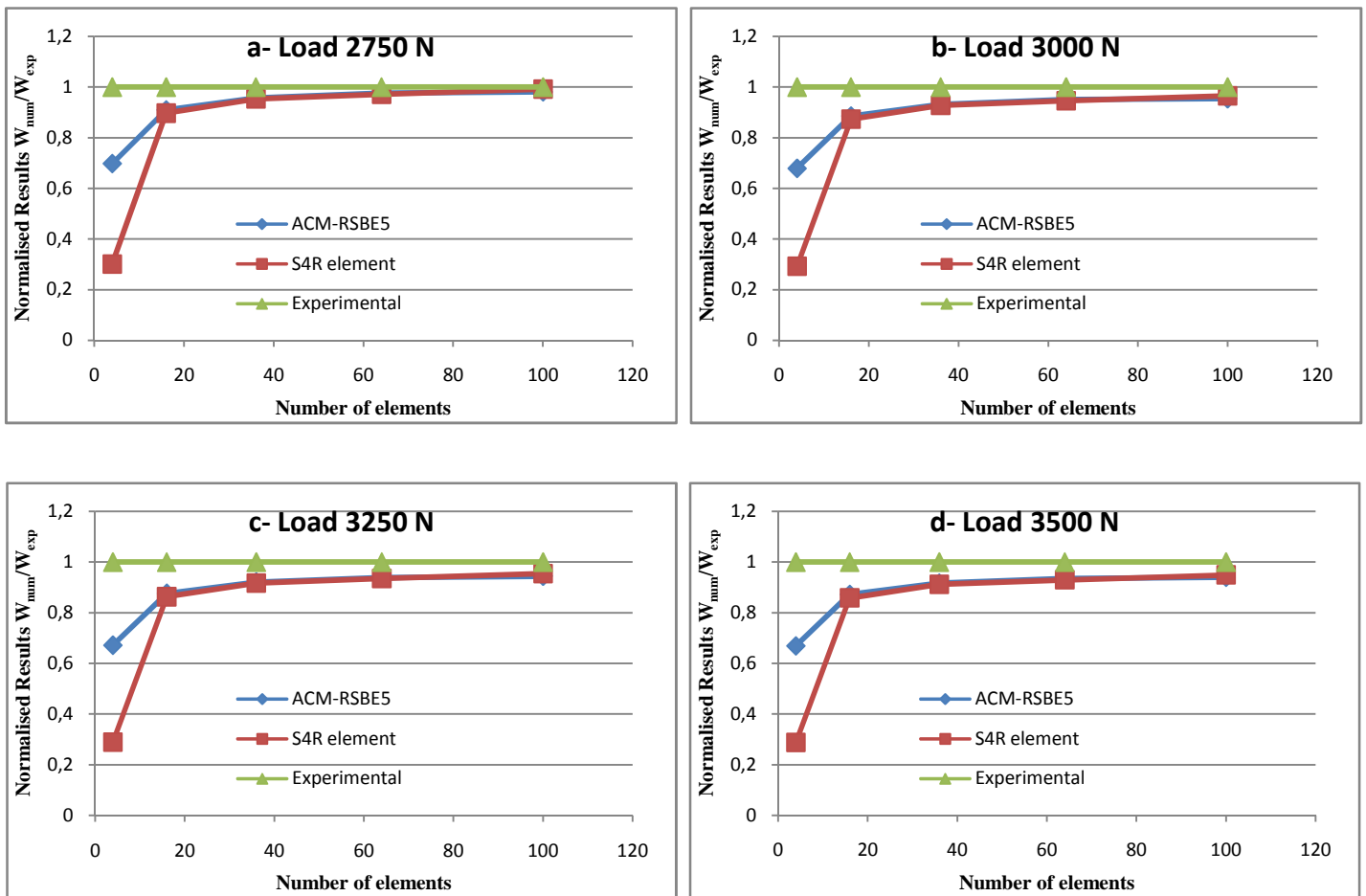
Fig. 4.2 Convergence curve for the deflection W_2 at point 2 under different loads

4.2.3 Vertical Displacements at point 3

Table 4.9 The vertical Displacements at point 3 for the Load 2500N

Meshes	Displacement W_3 at point 3		Normalised Results W_{num}/W_{exp}	
	ACM-RSBE5	**S4R element**	**ACM-RSBE5**	**S4R element**
2 x 2	2.508	3.945	0.65465936	1.02975724
4 x 4	3.515	3.411	0.91751501	0.89036805
6 x 6	3.813	3.761	0.99530149	0.98172801
8 x 8	3.949	3.896	1.03080136	1.01696685
10 x 10	4.007	3.974	1.04594101	1.03732707
Experimental solution	**3.831**		**1**	

Table 4.10 The vertical Displacements at point 3 for the Load 2750N

Meshes	Displacement W_3 at point 3		Normalised Results W_{num}/W_{exp}	
	ACM-RSBE5	**S4R element**	**ACM-RSBE5**	**S4R element**
2 x 2	2.759	4.341	0.6246321	0.98279375
4 x 4	3.866	3.750	0.8752547	0.84899253
6 x 6	4.195	4.135	0.94973964	0.93615576
8 x 8	4.344	4.284	0.98347295	0.96988906
10 x 10	4.407	4.369	0.99773602	0.9891329
Experimental solution	**4.417**		**1**	

Table 4.11 The vertical Displacements at point 3 for the Load 3000N

Meshes	Displacement W_3 at point 3		Normalised Results W_{num}/W_{exp}	
	ACM-RSBE5	**S4R element**	**ACM-RSBE5**	**S4R element**
2 x 2	3.010	4.737	0.60466051	0.95158698
4 x 4	4.218	4.090	0.84732824	0.82161511
6 x 6	4.576	4.509	0.91924468	0.90578546
8 x 8	4.739	4.671	0.95198875	0.93832865
10 x 10	4.808	4.764	0.96584974	0.95701085
Experimental solution	**4.978**		**1**	

Table 4.12 The vertical Displacements at point 3 for the Load 3250N

Meshes	Displacement W_3 at point 3		Normalised Results W_{num}/W_{exp}	
	ACM-RSBE5	**S4R element**	**ACM-RSBE5**	**S4R element**
2 x 2	3.261	5.133	0.59323267	0.93378206
4 x 4	4.569	4.429	0.83118064	0.80571221
6 x 6	4.957	4.883	0.9017646	0.88830271
8 x 8	5.134	5.058	0.93396398	0.92013826
10 x 10	5.208	5.159	0.94742587	0.93851192
Experimental solution	**5.497**		**1**	

Table 4.13 The vertical Displacements at point 3 for the Load 3500N

Meshes	Displacement W_3 at point 3		Normalised Results W_{num}/W_{exp}	
	ACM-RSBE5	**S4R element**	**ACM-RSBE5**	**S4R element**
2 x 2	3.512	5.530	0.58640842	0.92335949
4 x 4	4.921	4.769	0.82167307	0.7962932
6 x 6	5.339	5.257	0.89146769	0.87777592
8 x 8	5.529	5.445	0.92319252	0.90916681
10 x 10	5.609	5.554	0.93655034	0.92736684
Experimental solution	**5.989**		**1**	

Table 4.14 The vertical Displacements at point 3 for the Load 3750N

Meshes	Displacement W_3 at point 3		Normalised Results W_{num}/W_{exp}	
	ACM-RSBE5	**S4R element**	**ACM-RSBE5**	**S4R element**
2 x 2	3.762	5.926	0.5727771	0.90225335
4 x 4	5.272	5.108	0.80267966	0.77771011
6 x 6	5.720	5.631	0.87088916	0.85733861
8 x 8	5.924	5.832	0.90194884	0.88794153
10 x 10	6.010	5.949	0.91504263	0.90575518
Experimental solution	**6.568**		**1**	
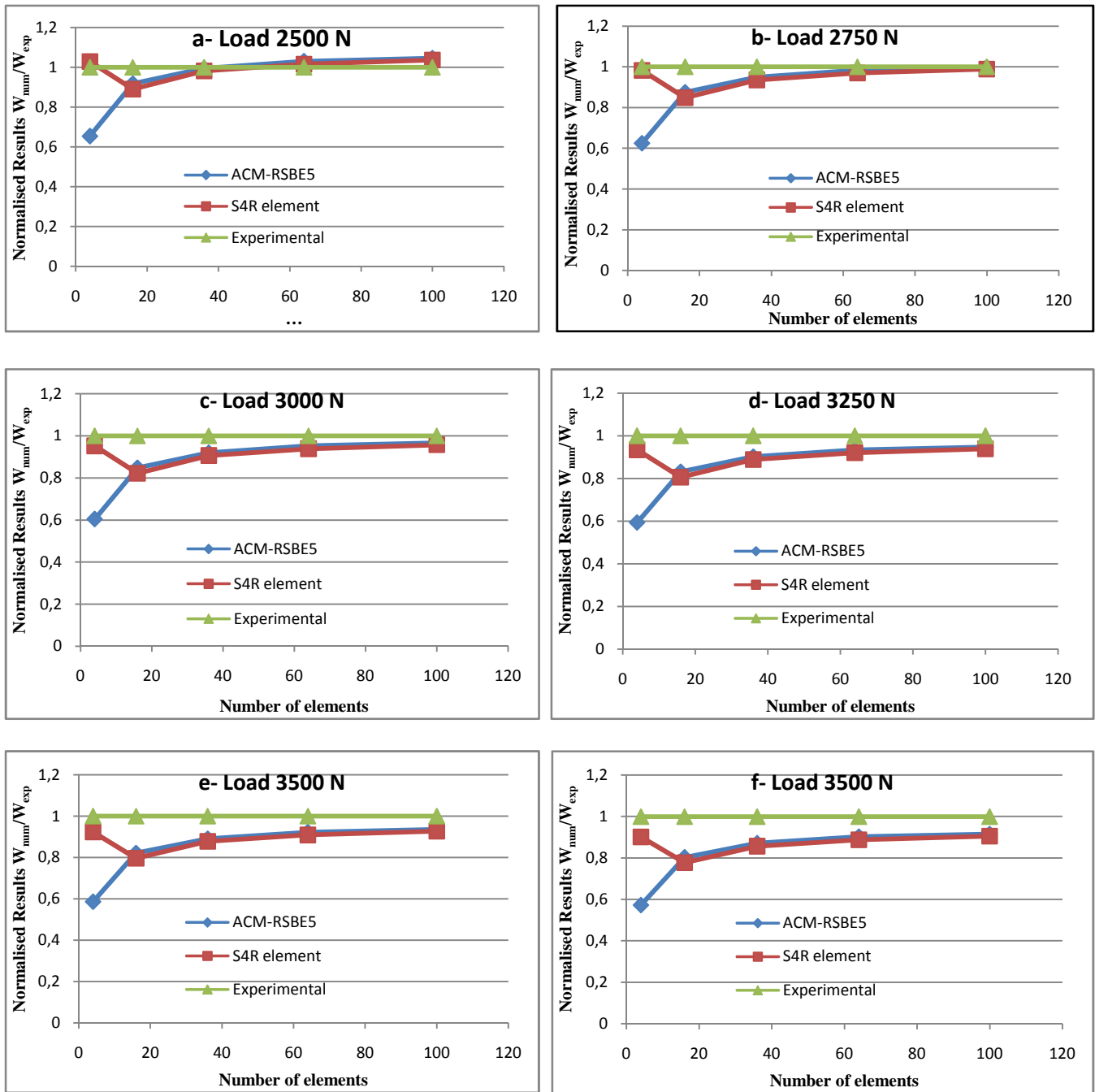
Fig. 4.3 Convergence curve for the deflection W_3 at point 3 under different loads

For the first case (a), we observed that **ACM-RSBE5** element gives very good convergence up to 99% for 10x10 meshes (Figs. 4.1, 4.2 and 4.3), also **ACM-RSBE5** element converge much better than **S4R** element ABAQUS element.

4.2.4 Vertical Displacements W (mm) Under Different Applied Loadings with numerical analysis (10x10) meshes, deflection for points 1,2 and 3

Table 4.15 summarizes the vertical displacements W obtained by the experimental tests and the numerical analysis for the points 1, 2 and 3 under different loads.

Table 4.15 Vertical deflection W (mm) Under Different Applied Loads at points 1, 2 and 3

	Points	*1*	*2*	*3*
	ACM-RSBE5	3.418	3.562	4.407
Case a *Load =2750 N*	*S4R Element*	3.459	3.603	4.369
	Exp. Work	**3.495**	**3.631**	**4.417**
	ACM-RSBE5	3.728	3.885	4.808
Case b *Load =3000 N*	*S4R Element*	3.770	3.928	4.764
	Exp. Work	**3.95**	**4.07**	**4.978**
	ACM-RSBE5	4.039	4.209	5.208
Case c *Load =3250 N*	*S4R Element*	4.082	4.253	5.159
	Exp. Work	**4.298**	**4.458**	**5.497**
	ACM-RSBE5	4.350	4.533	5.609
Case d *Load =3500 N*	*S4R Element*	4.393	4.578	5.554
	Exp. Work	**4.716**	**4.824**	**5.989**
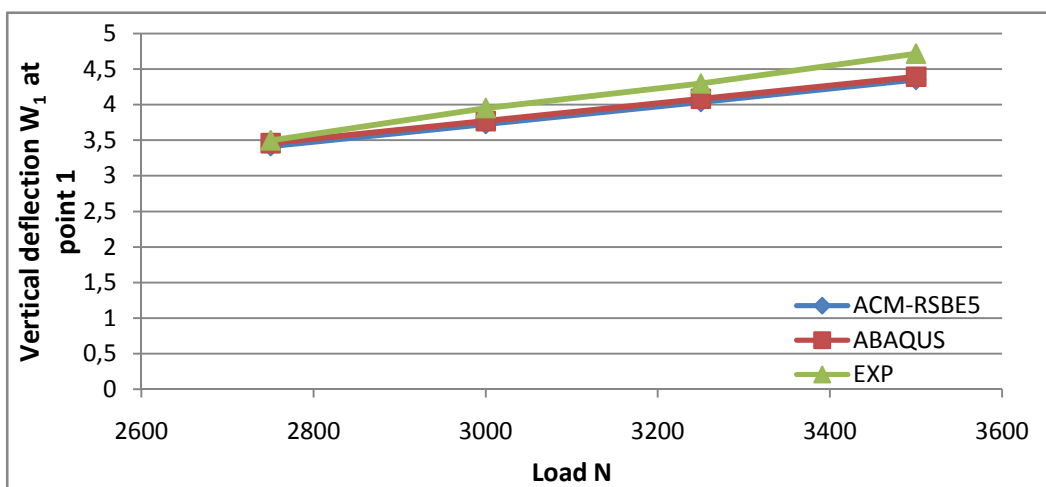
Fig. 4.4 Vertical displacement at point 1
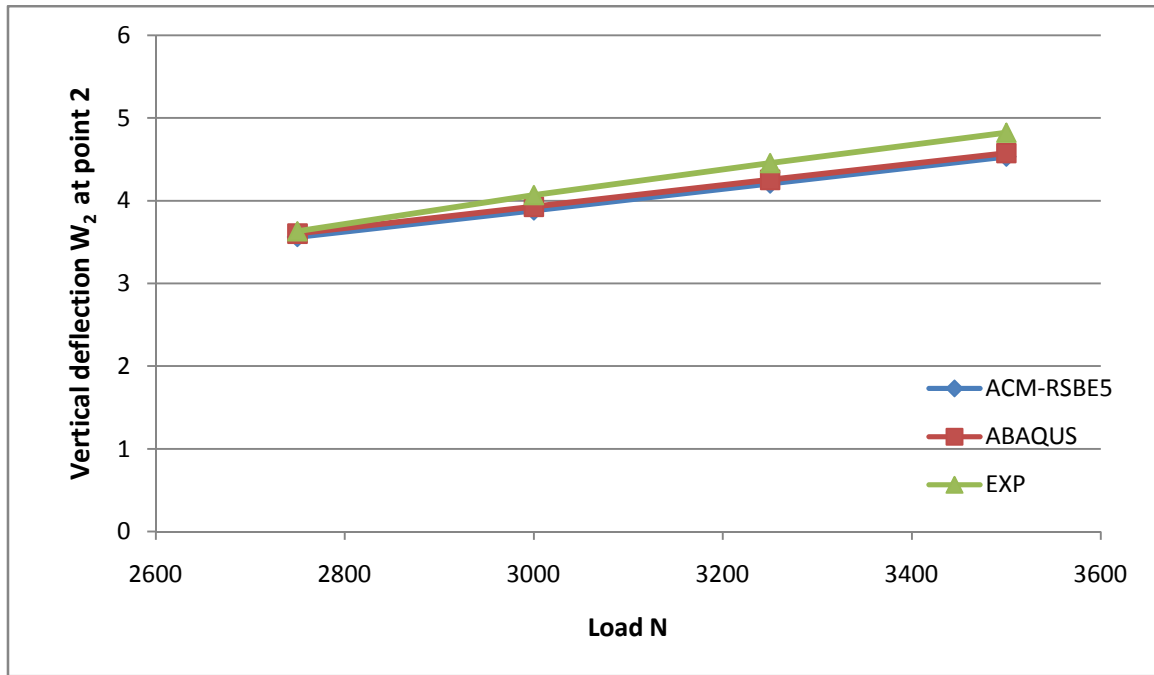
Fig. 4.5 Vertical displacement at point 2
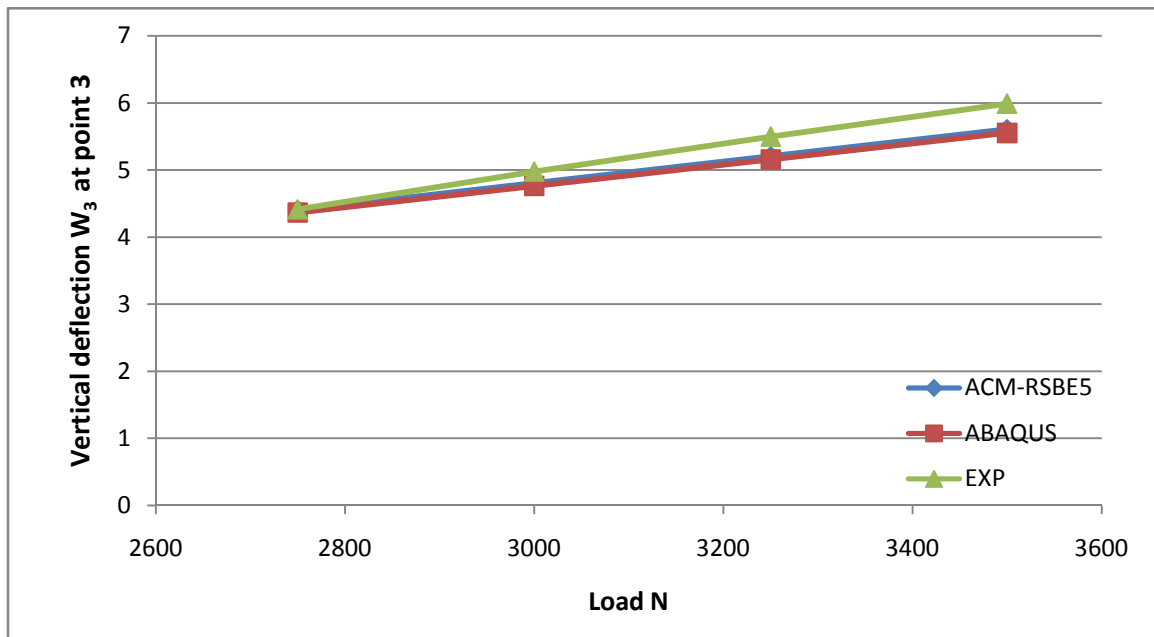
Fig. 4.6 Vertical displacement at point 3

Table 4.15 summarizes the vertical deflections under different applied loads at points 1, 2 and 3. Figures 4.4, 4.5 and 4.6 show that the results obtained with ACM-RSBE5 element and ABAQUS are very close to the experimental results, but when the load reach 4000N the deflection start to diverge, which may be explained by the beginning of the nonlinear stage,

55

and the shell goes to the plastic behavior, while the present element is formulated with linear behavior theory, so we have to develop this element with nonlinear behavior in future work.

Figure 4.7 shows the shell model undergoing loading and the figure 4.8 shows the deformed shape of the shell.

Fig. 4.7 Cylindrical shell model undergoing the loading
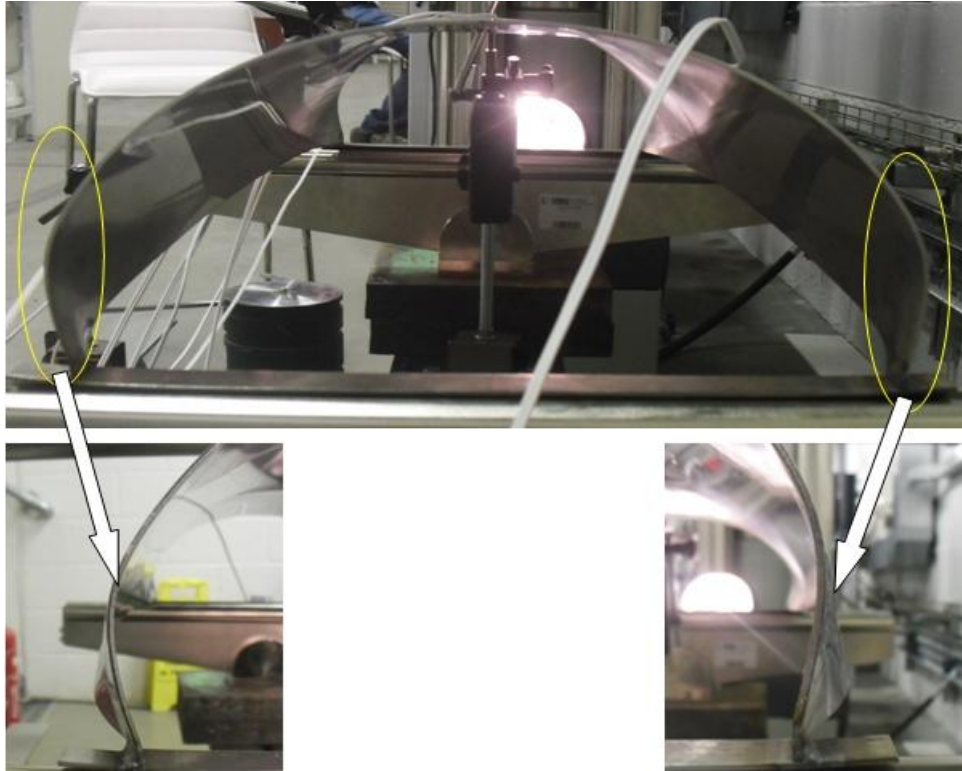
Fig. 4.8 The deformed shape of the cylindrical shell model, at node of supporting

4.3 Cylindrical shell with no end Diaphragms, (t = 1.2mm)

4.3.1 Vertical Displacements at point 3

In this test many loads are applied (800,825,850 and 875 N) and the Vertical displacements are recorded just at point 3. The same the procedure is used here like the first test.

Table 4.16 The vertical Displacements at point 3 for the Load 800N

Meshes	Displacement W_3 at point 3		Normalised Results W_{num}/W_{exp}	
	ACM-RSBE5	**S4R element**	**ACM-RSBE5**	**S4R element**
2 x 2	3.449	4.473	0.67653982	0.8774029
4 x 4	4.740	4.530	0.92977638	0.88858376
6 x 6	5.050	4.980	0.99058454	0.97685367
8 x 8	5.190	5.145	1.01804629	1.0092193
10 x 10	5.224	5.241	1.02471557	1.02805022
Experimental solution	**5.098**		**1**	

Table 4.17 The vertical Displacements at point 3 for the Load 825N

Meshes	Displacement W_3 at point 3		Normalised Results W_{num}/W_{exp}	
	ACM-RSBE5	S4R element	ACM-RSBE5	S4R element
2 x 2	3.326	5.235	0.5932929	0.93382091
4 x 4	4.660	4.517	0.83125223	0.80574385
6 x 6	5.055	4.980	0.90171245	0.88833393
8 x 8	5.236	5.158	0.93399929	0.92008562
10 x 10	5.311	5.261	0.94737781	0.93845879
Experimental solution	**5.606**		**1**	

Table 4.18 The vertical Displacements at point 3 for the Load 850N

Meshes	Displacement W_3 at point 3		Normalised Results W_{num}/W_{exp}	
	ACM-RSBE5	S4R element	ACM-RSBE5	S4R element
2 x 2	3.664	4.756	0.60462046	0.78481848
4 x 4	5.036	4.811	0.8310231	0.79389439
6 x 6	5.366	5.288	0.88547855	0.87260726
8 x 8	5.515	5.463	0.91006601	0.90148515
10 x 10	5.551	5.564	0.9160066	0.91815182
Experimental solution	**6.060**		**1**	

Table 4.19 The vertical Displacements at point 3 for the Load 875N

Meshes	Displacement W_3 at point 3		Normalised Results W_{num}/W_{exp}	
	ACM-RSBE5	**S4R element**	**ACM-RSBE5**	**S4R element**
2 x 2	3.772	4.897	0.58735596	0.76253504
4 x 4	5.184	4.951	0.80722516	0.77094363
6 x 6	5.523	5.442	0.86001246	0.84739956
8 x 8	5.677	5.621	0.88399253	0.8752725
10 x 10	5.714	5.726	0.88975397	0.89162255
Experimental solution	**6.422**		**1**	
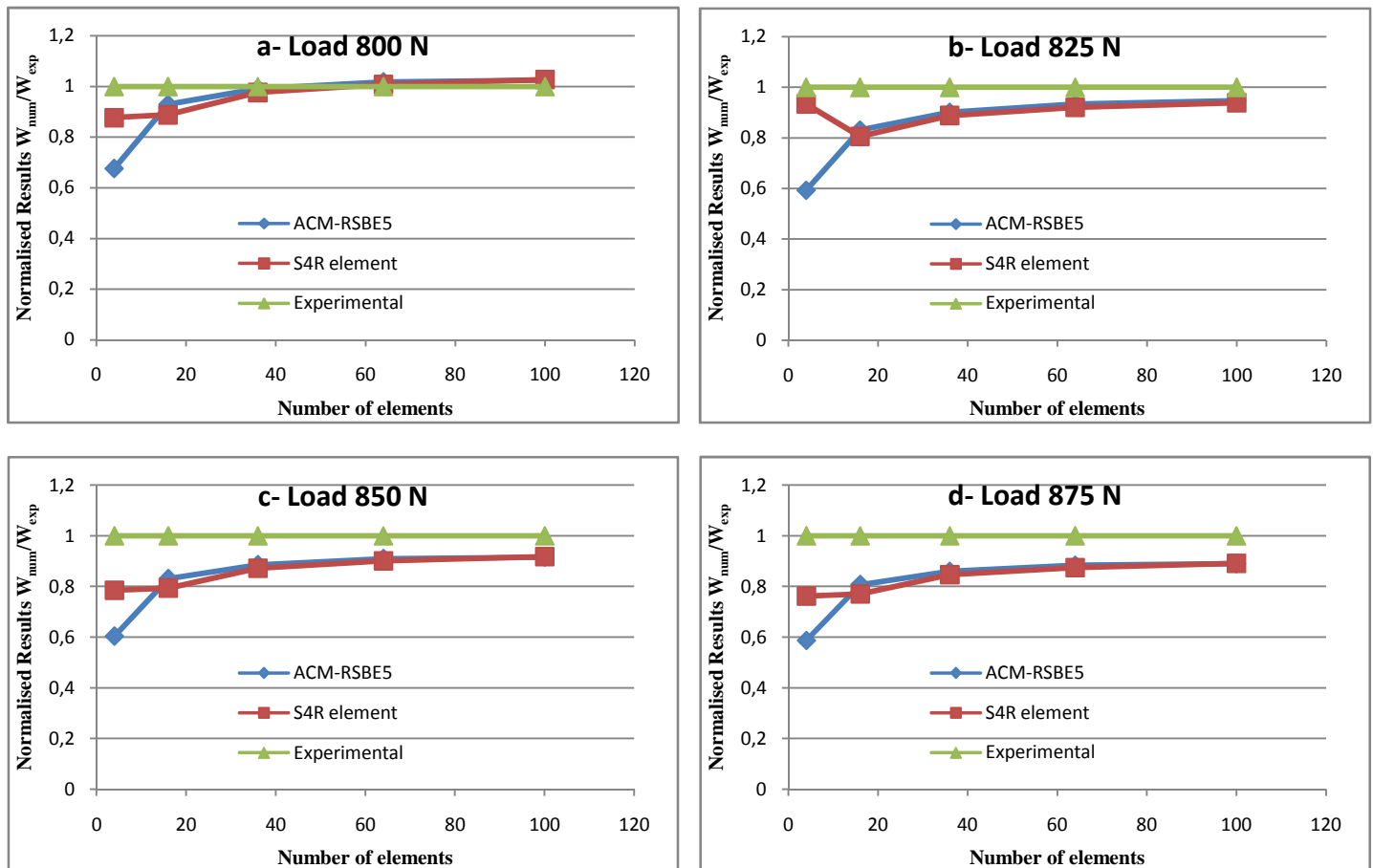
Fig. 4.9 Convergence curve for the deflection W_3 at point 3 under different loads

For test number 2 with another different thickness t = 1.2 mm, the ACM-RSBE5 element gives good results, Figure 4.9 shows that the present element has an excellent

convergence; up to 98% for the meshes 10 x10, and it converges faster than S4R element of ABAQUS.

4.3.2 Vertical Displacements W (mm) Under Different Applied Loadings with numerical analysis (10x10) meshes, deflection for point 3

Table 4.20 Vertical deflection W (mm) Under Different Applied Loads at point 3

Loads (N)	*800*	*825*	*850*	*875*	*900*
ACM-RSBE5	5.224	5.387	5.551	5.714	5.877
S4R Element	5.241	5.403	5.564	5.726	5.888
Exp.Work	**5.098**	**5.606**	**6.060**	**6.422**	**6.822**
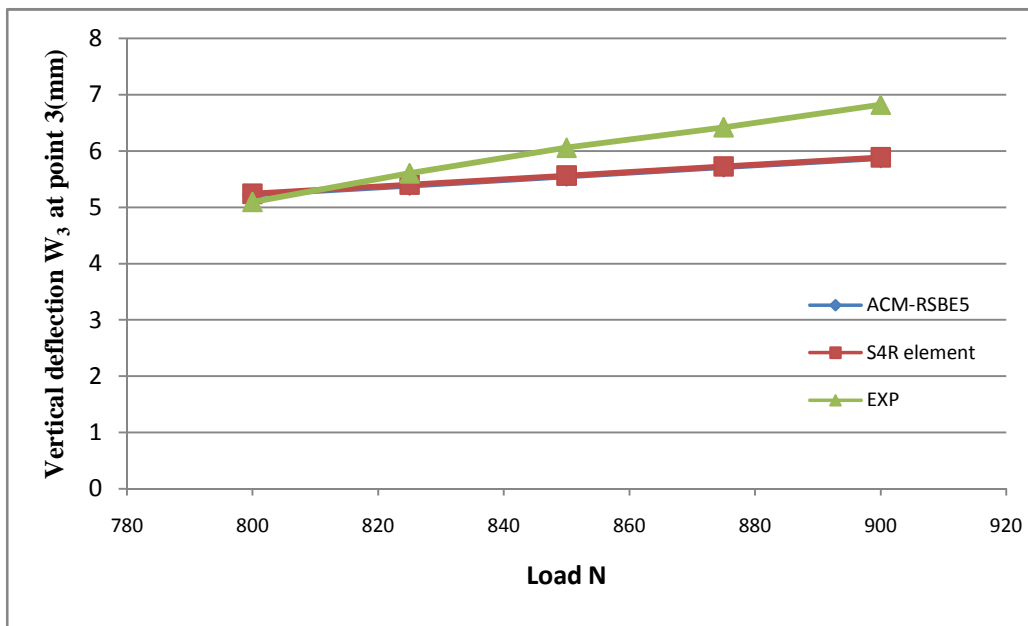
Fig. 4.10 Vertical dsplacement at point 3

Table 4.20 recapitulates the vertical deflections under different applied loads at point 3. Figure 4.10 shows that the results of **ACM-RSBE5** and **S4R** ABAQUS element very close to the experimental results, but when the applied load reach 850N the deflection start to diverge, which means the nonlinear stage behavior is beginning.

4.4 Cylindrical shell with end Rigid Diaphragms, t =1.2mm

4.4.1 Vertical Displacements at point 3

The same procedure as the previous one is used for this test. The applied loads are (575N, 600N, 625N, 650N, 675N and 700N) and the vertical displacements for the point 1 are record.

Table 4.21 The vertical Displacements at point 3 for the Load 575N

Meshes	Displacement W_3 at point 3		Normalised Results W_{num}/W_{exp}	
	ACM-RSBE5	S4R element	ACM-RSBE5	S4R element
2 x 2	0.112	1.927	0.16115108	2.77266187
4 x 4	0.455	0.379	0.65467626	0.54532374
6 x 6	0.560	0.485	0.8057554	0.69784173
8 x 8	0.614	0.557	0.88345324	0.80143885
10 x 10	0.649	0.597	0.93381295	0.85899281
Experimental solution	**0.695**		1	

Table 4.22 The vertical Displacements at point 3 for the Load 600N

Meshes	Displacement W_3 at point 3		Normalised Results W_{num}/W_{exp}	
	ACM-RSBE5	S4R element	ACM-RSBE5	S4R element
2 x 2	0.143	2.448	0.16666667	2.85314685
4 x 4	0.577	0.482	0.67249417	0.56177156
6 x 6	0.711	0.616	0.82867133	0.71794872
8 x 8	0.780	0.707	0.90909091	0.82400932
10 x 10	0.824	0.758	0.96037296	0.88344988
Experimental solution	**0.858**		1	

Table 4.23 The vertical Displacements at point 3 for the Load 625N

Meshes	Displacement W_3 at point 3		Normalised Results W_{num}/W_{exp}	
	ACM-RSBE5	S4R element	ACM-RSBE5	S4R element
2 x 2	0.149	2.552	0.1724537	2.9537037
4 x 4	0.601	0.502	0.69560185	0.58101852
6 x 6	0.741	0.642	0.85763889	0.74305556
8 x 8	0.812	0.737	0.93981481	0.85300926
10 x 10	0.858	0.790	0.99305556	0.91435185
Experimental solution	**0.864**		**1**	

Table 4.24 The vertical Displacements at point 3 for the Load 650N

Meshes	Displacement W_3 at point 3		Normalised Results W_{num}/W_{exp}	
	ACM-RSBE5	S4R element	ACM-RSBE5	S4R element
2 x 2	0.154	2.696	0.16923077	2.96263736
4 x 4	0.625	0.522	0.68681319	0.57362637
6 x 6	0.771	0.667	0.84725275	0.73296703
8 x 8	0.845	0.766	0.92857143	0.84175824
10 x 10	0.892	0.822	0.98021978	0.9032967
Experimental solution	**0.910**		**1**	
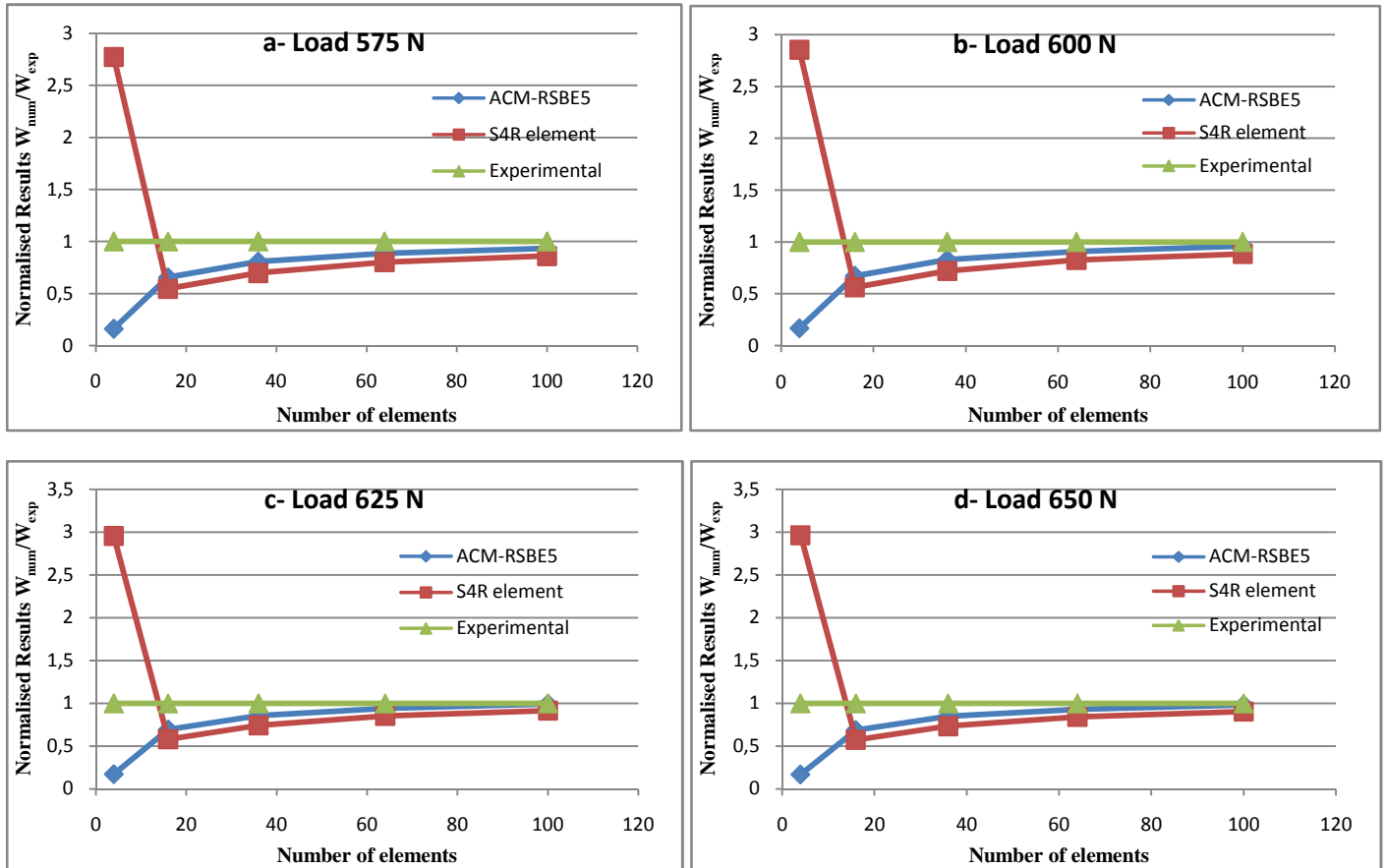
Fig. 4.11 Convergence curve for the deflection W_3 at point 3 under different loads

The deflections obtain with **ACM-RSBE5** element converges rapidly towards to the experimental results up to 99% with meshes 10x10 meshes Fig 4.11. Also, **ACM-RSBE5** element converges better than S4R ABAQUS element.

4.4.2 Vertical Displacements W (mm) Under Different Applied Loads with numerical analysis (10x10) meshes, deflections for point 3

Table 4.25 Vertical deflection W (mm) Under Different Applied Loadings at point 3

Loads (N)	600	625	650	675	700
ACM-RSBE5	0.8238	0.8581	0.8925	0.9268	0.9611
S4R Element	0.7585	0.7900	0.8216	0.8532	0.8848
Exp.Work	**0.858**	**0.864**	**0.910**	**0.958**	**1.231**
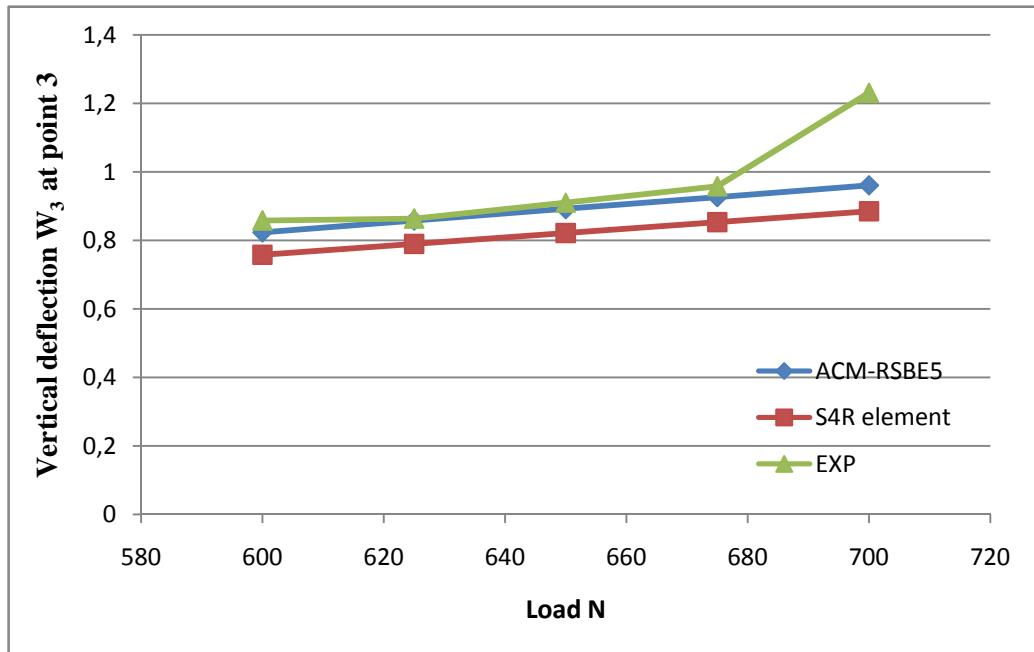
Fig. 4.12 Vertical displacement at point 3

Table 4.25 recapitulates the vertical deflections under different applied loads at point 3. Figures 4.12 shows that the results obtained with both elements ACM-RSBE5 and S4R ABAQUS element are close to the experimental results; but **ACM-RSBE5** much closer than ABAQUS element to the experimental results. Also, the same comments can be noticed when the applied loads attain 675N.
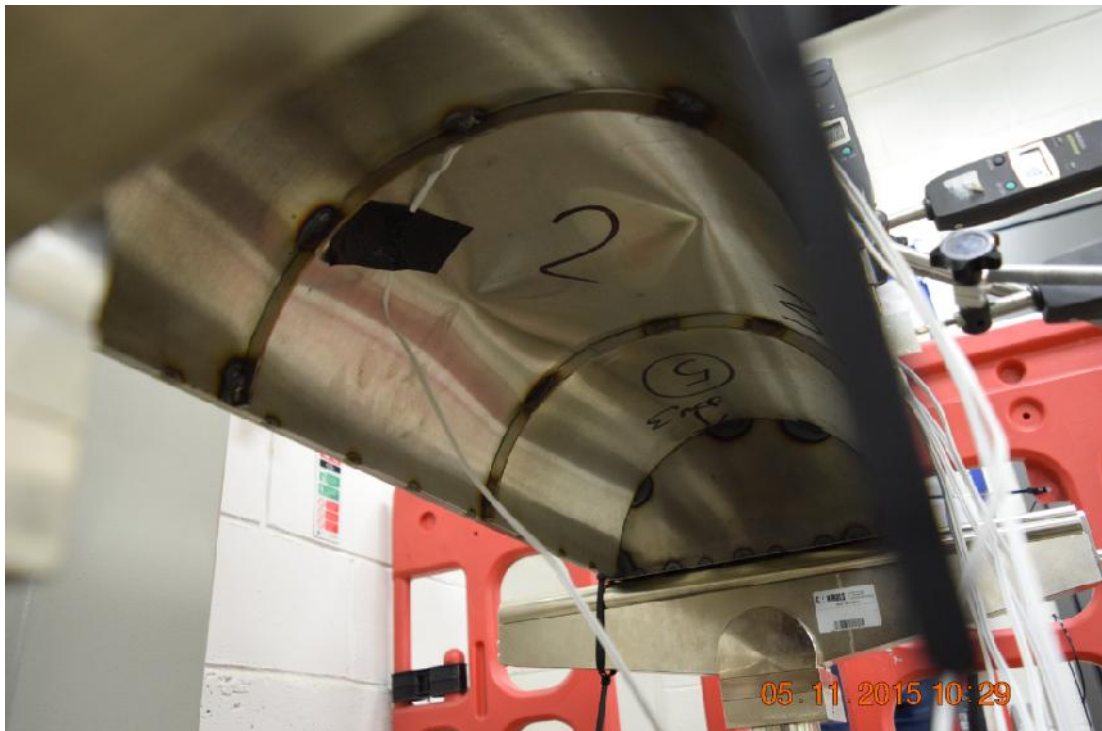
Fig. 4.13 The cylindrical shell with rigid diaphragm after the loading "deformed shape"

4.5 Conclusion

In this study, an experimental work was performed to examine the bending behaviour of cylindrical shells subjected to bending. Three cylindrical shell models with different boundary conditions were tested under concentrated loads. The loads are applied for each model. From the results obtained with this study, the following points can be summarized as follows:

- The ACM-RSBE5 element and S4R ABAQUS gave us good results and so nearly to those from the experimental tests, it converges to 99% for the meshes 10x10, and the ACM_RSBE5 results converges faster than S4R element of ABAQUS. The presented flat shell element 'ACM-RSBE5' has been demonstrated experimentally to be robust, effective and useful in analyzing thin shell structures. It also exhibits strong convergence, as can be seen from the numerical results presented. It did perform in general better than widely-used elements such as the S4R element currently adopted by the commercial software package ABAQUS.
- ACM-RSBE5 element can be used to analyze shell structures at the linear stage, and gives good results.

- After the three first tests, we saw that the displacement is very big especially in the cylinder of 1.2mm of thickness without stiffeners and reposed on 4 points, which means we have to add some stiffeners to decrease the deflection and minimize the deformation.

Chapter 5

Experimental and Numerical Investigation of The Behavior of The Cylindrical Shell Model With Stiffeners

Chapter 5

Experimental and Numerical Investigation of The Behavior of The Cylindrical Shell Model With Stiffeners

5.1 Introduction

The analysis of complex structures such as thin shells, where the structure covers a large area with a very complex geometry and sometimes supporting heavy loads, can cause very large displacements. This fact often requires the addition of stiffeners to increase the rigidity and minimize the deformation.

The proposed tasks to resolve this problem is through proper modeling of the stiffened shell structure along with validation using experimentally tested representative specimens.

In this chapter we will study and evaluate the structural performance of cylindrical shells under ultimate load conditions; and improve their behavior through the addition of appropriate stiffener members. A laboratory experiments on representative specimens will be conducted; and numerical simulation of several large shell structural systems will be performed accounting for different geometric and material parameters,

We will present the numerical and experimental results of many tests, and try to illustrate those results and discuss them. The tests that we will present are:

- *Cylindrical shell with No end Diaphragms and two Stiffeners, t=1.2mm,* **CNDS**
- *Cylindrical shell with two end Diaphragms and two Stiffeners, t=1.2mm,* **CDS**
- *Cylindrical shell with two end Diaphragms and two Stiffeners resting on longitudinal beams "Stringers", t=1.2mm,* **CDSS.**

5.2 Cylindrical shell with No end Diaphragms and two Stiffeners, t=1.2mm, CNDS

In this test we applied many loads, and take some results, the loads that we applied are [1200N,1250N, 1300N, 1350N, 1400N, 1450N, 1500N and 1550N]. The vertical displacements for point 3 for each load are recorded. The diagrams presented below show the convergence of displacement. In each diagram the number of elements used is presented with X-axis and the normalized results (W_{num}/W_{exp}) with Y-axis. The results obtained for vertical displacements are given in Figures 1 (a, b, c, d, e, f, g and h case loading) and compared with those obtained by the numerical analysis C3D8IH element of ABAQUS code.

Table 5.1 The vertical Displacements at point 3 for the Load 1200 N

Meshes	Displacement W_3 at point 3		Normalised Results W_{num}/W_{exp}
	Experimental	ABAQUS	
3x3		0.126	0.029563585
9x9	4.262	0.934	0.219145941
30x17		2.723	0.63890192
45x25		3.451	0.809713749

Table 5.2 The vertical Displacements at point 3 for the Load 1250 N

Meshes	Displacement W_3 at point 3		Normalised Results W_{num}/W_{exp}
	Experimental	ABAQUS	
3x3		0.132	0.029938762
9x9	4.409	0.972	0.220458154
30x17		2.835	0.64300295
45x25		3.593	0.814924019

Table 5.3 The vertical Displacements at point 3 for the Load 1300 N

Meshes	Displacement W_3 at point 3		Normalised Results
	Experimental	ABAQUS	W_{num}/W_{exp}
3x3		0.137	0.03022281
9x9	4.533	1.011	0.22303111
30x17		2.948	0.65034194
45x25		3.736	0.82417825

Table 5.4 The vertical Displacements at point 3 for the Load 1350 N

Meshes	Displacement W_3 at point 3		Normalised Results
	Experimental	ABAQUS	W_{num}/W_{exp}
3x3		0.142	0.03049173
9x9	4.657	1.049	0.22525231
30x17		3.061	0.6572901
45x25		3.879	0.83293966

Table 5.5 The vertical Displacements at point 3 for the Load 1400 N

Meshes	Displacement W_3 at point 3		Normalised Results
	Experimental	ABAQUS	W_{num}/W_{exp}
3x3		0.147	0.03071458
9x9	4.786	1.088	0.22732971
30x17		3.173	0.66297534
45x25		4.021	0.8401588

Table 5.6 The vertical Displacements at point 3 for the Load 1450 N

Meshes	Displacement W_3 at point 3		Normalised Results W_{num}/W_{exp}
	Experimental	**ABAQUS**	
3x3		0.152	0.03085668
9x9	4.926	1.127	0.22878603
30x17		3.286	0.66707268
45x25		4.164	0.8453106

Table 5.7 The vertical Displacements at point 3 for the Load 1500 N

Meshes	Displacement W_3 at point 3		Normalised Results W_{num}/W_{exp}
	Experimental	**ABAQUS**	
3x3		0.158	0.03040216
9x9	5.197	1.165	0.22416779
30x17		3.398	0.65383875
45x25		4.307	0.82874735

Table 5.8 The vertical Displacements at point 3 for the Load 1550 N

Meshes	Displacement W_3 at point 3		Normalised Results W_{num}/W_{exp}
	Experimental	**ABAQUS**	
3x3		0.163	0.02959332
9x9	5.508	1.204	0.21859114
30x17		3.511	0.63743646
45x25		4.449	0.8077342
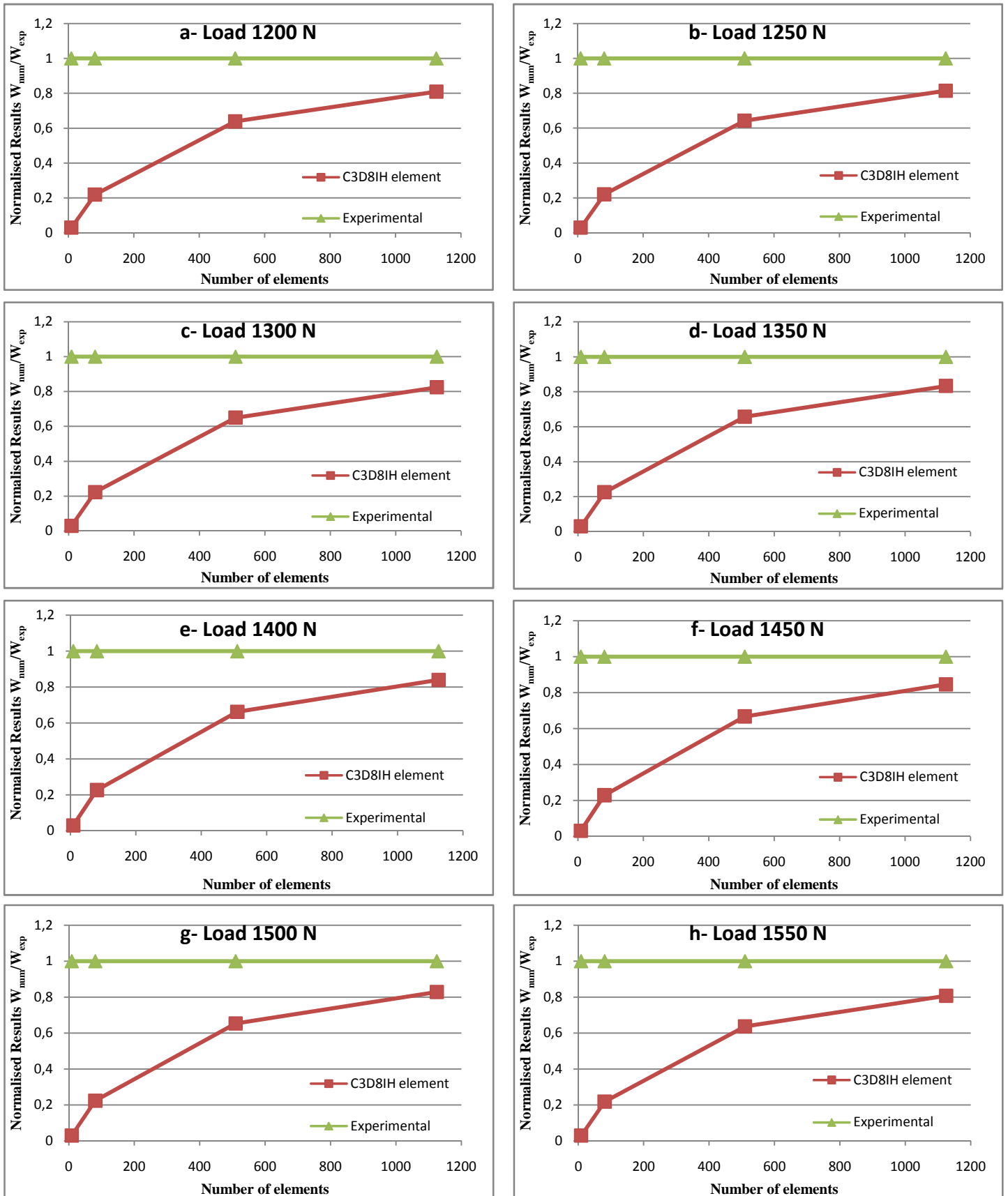
Fig. 5.1 Convergence curve for the deflections W_3 at point 3 under different loads

Figure 5.1 presents the convergence curve for the deflection at point 3 "point of applied the load".

For the cases (a) to (g) the displacement by C3D8IH ABAQUS element converge until 85%, all of this cases are in the elastic or linear range, but after the load reaches 1550N the behavior of the cylindrical shell change to the plastic range.

We observed that for a small number of meshes like 3x3 and 9x9, the displacement is so distant. But for a big number of elements, ABAQUS results converge to the experimental results.

5.2.1 Vertical Displacements W (mm) Under Different Applied Loadings with numerical analysis (45x25) meshes, deflection for point 3

Table 5.9 summarizes the vertical displacements W obtained by the experimental tests and the numerical analysis for the point 3 under different loads.

Table 5.9 Vertical deflection W (mm) Under Different Applied Loads at point 3

Loads (N)	1200	1250	1300	1350	1400	1450	1500	1550	1750
C3D8IH Element	3.451	3.593	3.736	3.879	4.021	4.164	4.307	4.449	5.020
Exp.Work	4.262	4.409	4.533	4.657	4.786	4.926	5.197	5.508	6.820
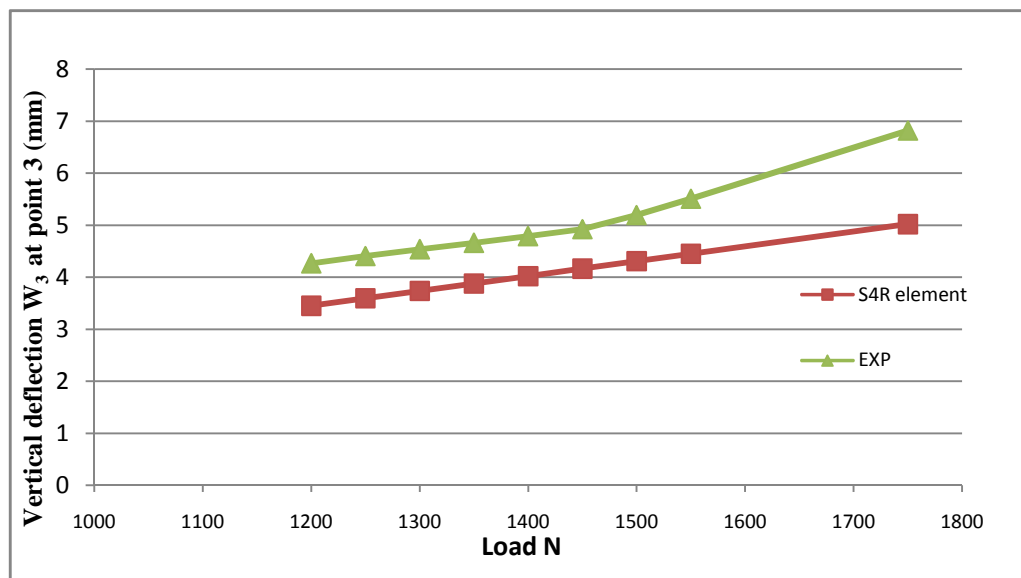
Fig. 5.2 Vertical displacement at point 3

Figure 5.2 shows that the results obtained with ABAQUS are very close to the experimental results, but when the load reach 1450N the deflection start to diverge, that may explain the beginning of the nonlinear stage, and the shell goes to the plastic behavior.

Figure 5.3 shows the shell model undergoing loading and the deformed shape of the shell, and figure 4 presents the cylindrical shell after the loading in the experimental test and ABAQUS simulation.
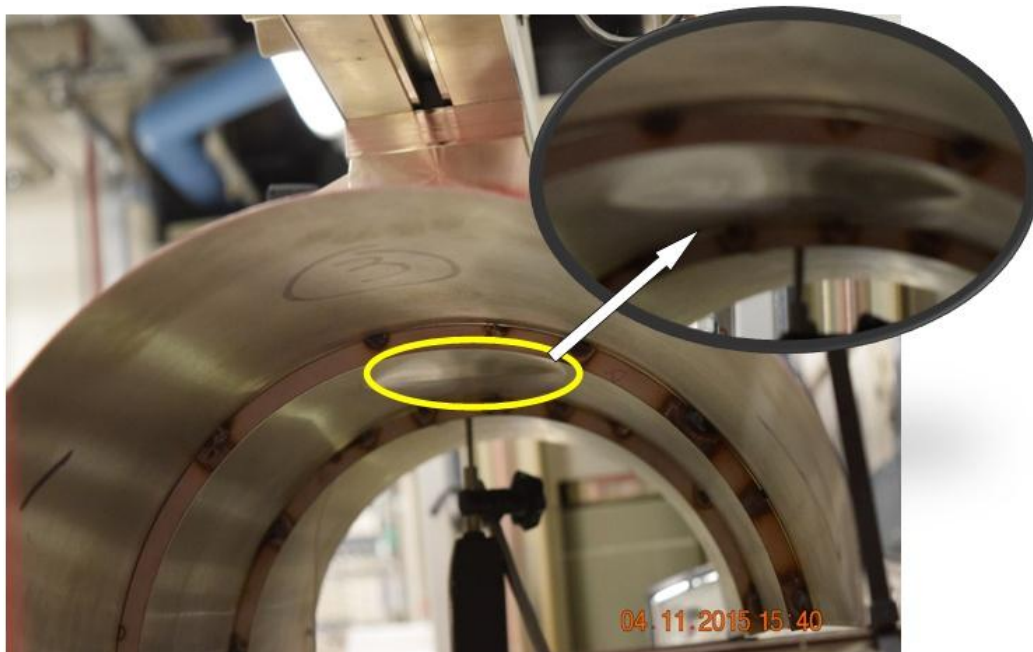
Fig. 5.3 Cylindrical shell model undergoing the loading
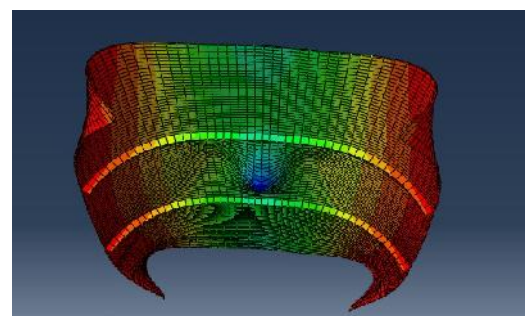
-a-   -b-

Fig. 5.4 Cylindrical shell model after the loading

-a- The deformation shell shape

-b- The simulation with ABAQUS code

5.3 Cylindrical shell with two end Diaphragms and two Stiffeners, t=1.2mm, CDS

The loads that we applied in these tests are [800N, 850N, 900N, 950N and 1000N]. The vertical displacements for point 3 for each load are recorded. The diagrams presented below show the convergence of displacement. The results obtained for vertical displacements are given in Figures 5 (a, b, c, d and e case loading) and compared with those obtained by the numerical analysis C3D8IH element of ABAQUS code.

Table 5.10 The vertical Displacements at point 3 for the Load 800 N

Meshes	Displacement W_3 at point 3		Normalised Results W_{num}/W_{exp}
	Experimental	**ABAQUS**	
3x3		0.070	0.05695688
9x9	1.229	0.283	0.23026851
30x17		0.943	0.76729048
45x25		1.286	1.04637917

Table 5.11 The vertical Displacements at point 3 for the Load 850 N

Meshes	Displacement W_3 at point 3		Normalised Results W_{num}/W_{exp}
	Experimental	**ABAQUS**	
3x3		0.075	0.05391804
9x9	1.391	0.301	0.21639109
30x17		1.002	0.72034508
45x25		1.366	0.98202732

Table 5.12 The vertical Displacements at point 3 for the Load 900 N

Meshes	Displacement W₃ at point 3		Normalised Results
	Experimental	**ABAQUS**	**W_{num}/W_{exp}**
3x3	1.591	0.079	0.04965431
9x9		0.318	0.19987429
30x17		1.061	0.66687618
45x25		1.447	0.90949089

Table 5.13 The vertical Displacements at point 3 for the Load 950 N

Meshes	Displacement W₃ at point 3		Normalised Results
	Experimental	**ABAQUS**	**W_{num}/W_{exp}**
3x3	1.755	0.083	0.04729345
9x9		0.336	0.19145299
30x17		1.120	0.63817664
45x25		1.527	0.87008547

Table 5.14 The vertical Displacements at point 3 for the Load 1000 N

Meshes	Displacement W₃ at point 3		Normalised Results
	Experimental	**ABAQUS**	**W_{num}/W_{exp}**
3x3	1.966	0.087	0.04425229
9x9		0.345	0.17548321
30x17		1.179	0.59969481
45x25		1.607	0.81739573
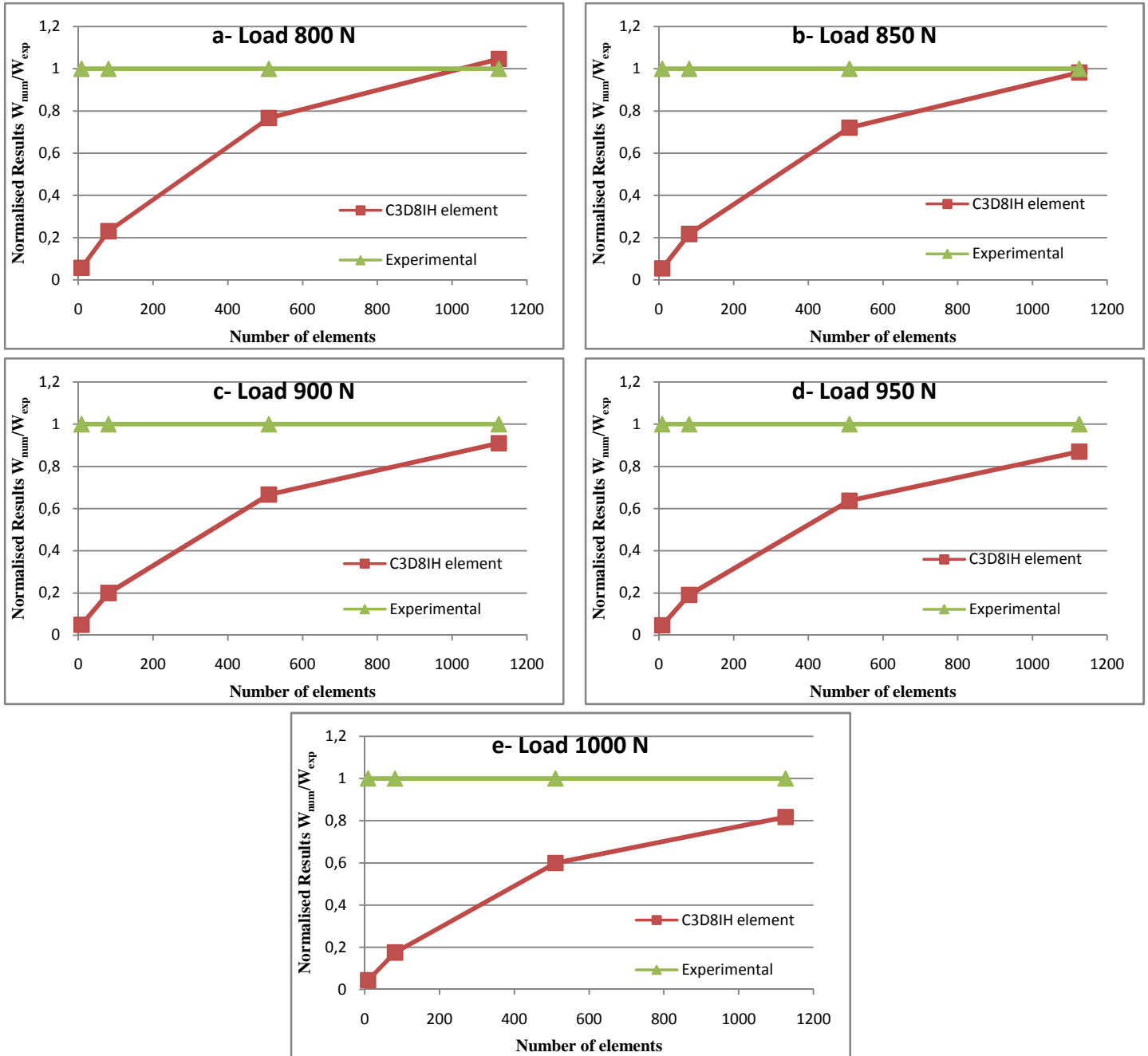
Fig. 5.5 Convergence curve for the deflections W_3 at point 3 under different loads

Figures 5.5 (a to c) until the load 900N presents that the ABAQUS results and the experimental results are very close to 98% in 45x25 meshes, after the load 900N we saw that the displacements diverge, it is conducted to the plastic range.

5.3.1 Vertical Displacements W (mm) Under Different Applied Loadings with numerical analysis (45x25) meshes, deflection for point 3

Table 5.15 summarizes the vertical displacements W obtained by the experimental tests and the numerical analysis for the point 3 under different loads.

Table 5.15 Vertical deflection W (mm) Under Different Applied Loads at point 3

Loads (N)	*800*	*850*	*900*	*950*	*1000*
C3D8IH Element	1.286	1.366	1.447	1.527	1.607
Exp.Work	1.229	1.391	1.591	1.755	1.966
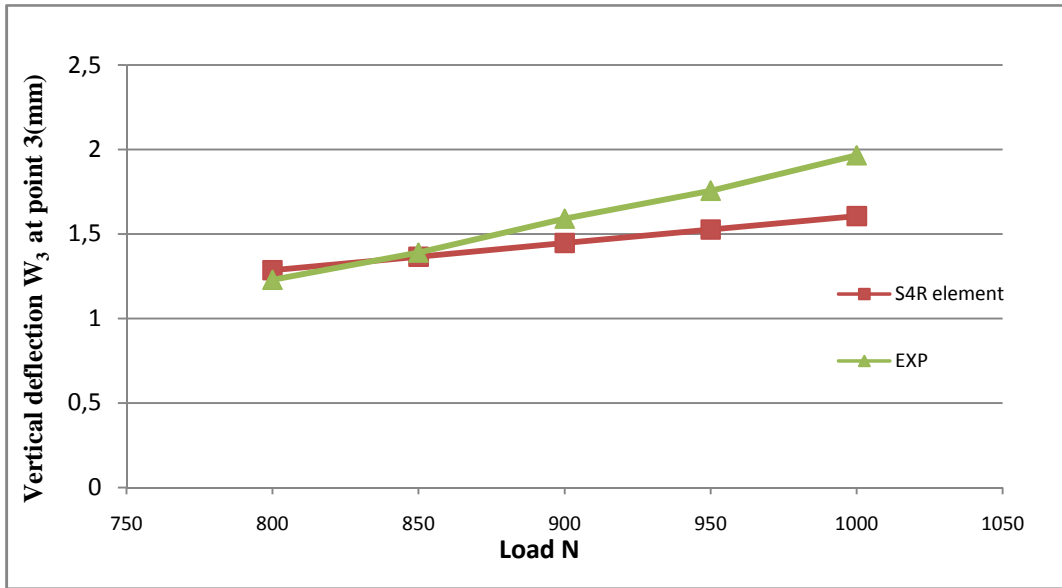
Fig. 5.6 Vertical displacement at point 3

Figure 5.6 shows that the results obtained with ABAQUS are very close to the experimental results, but when the load reach 900N the deflection start to diverge, which may be explained by the beginning of the nonlinear stage, and the shell goes to the plastic behavior.

Figure 5.7 shows the shell model undergoing loading and the deformed shape of the shell, and the figure 5.8 shows the deformation shape of the semi cylinder with rigid diaphragm and stiffeners and the simulation with ABAQUS code.

Fig. 5.7 Cylindrical shell model with rigid diaphragm and stiffeners undergoing the loading

-a-   -b-

Fig. 5.8 Cylindrical shell model with rigid diaphragm and stiffeners after the loading

-a- The deformation shell shape   -b- The simulation with ABAQUS code

5.4 Cylindrical shell with two end Diaphragms and two Stiffeners resting on longitudinal beams "Stringers", t=1.2mm, CDSS)

In this test we applied many loads, and take some results, the loads that we applied are [1100N,1150N, 1200N, 1250N and 1300N]. The displacements are recorded for many points. The diagrams presented below show the convergence of displacement. In each diagram the number of elements used is presented like the previous tests, the results obtained for vertical displacements are given in Figure 5.9 (a, b, c, d and e case loading) and compared with those obtained by the numerical analysis C3D8IH element of ABAQUS code.

Table 5.16 The vertical Displacements at point 3 for the Load 1100 N

Meshes	Displacement W_3 at point 3		Normalised Results
	experimental solution	ABAQUS	W_{num}/W_{exp}
3x3	1.686	0.072	0.04270463
30x17		1.252	0.742586
45x25		1.761	1.04448399

Table 5.17 The vertical Displacements at point 3 for the Load 1150 N

Meshes	Displacement W_3 at point 3		Normalised Results
	experimental solution	ABAQUS	W_{num}/W_{exp}
3x3	1.913	0.076	0.03972818
30x17		1.309	0.68426555
45x25		1.841	0.96236278

Table 5.18 The vertical Displacements at point 3 for the Load 1200 N

Meshes	Displacement W_3 at point 3		Normalised Results W_{num}/W_{exp}
	experimental solution	ABAQUS	
3x3		0.079	0.03654024
30x17	2.162	1.365	0.63135985
45x25		1.921	0.88852914

Table 5.19 The vertical Displacements at point 3 for the Load 1250 N

Meshes	Displacement W_3 at point 3		Normalised Results W_{num}/W_{exp}
	experimental solution	ABAQUS	
3x3		0.083	0.03361685
30x17	2.469	1.422	0.57594168
45x25		2.001	0.81044957

Table 5.20 The vertical Displacements at point 3 for the Load 1300 N

Meshes	Displacement W_3 at point 3		Normalised Results W_{num}/W_{exp}
	experimental solution	ABAQUS	
3x3		0.086	0.03159442
30x17	2.722	1.479	0.54335048
45x25		2.081	0.76451139
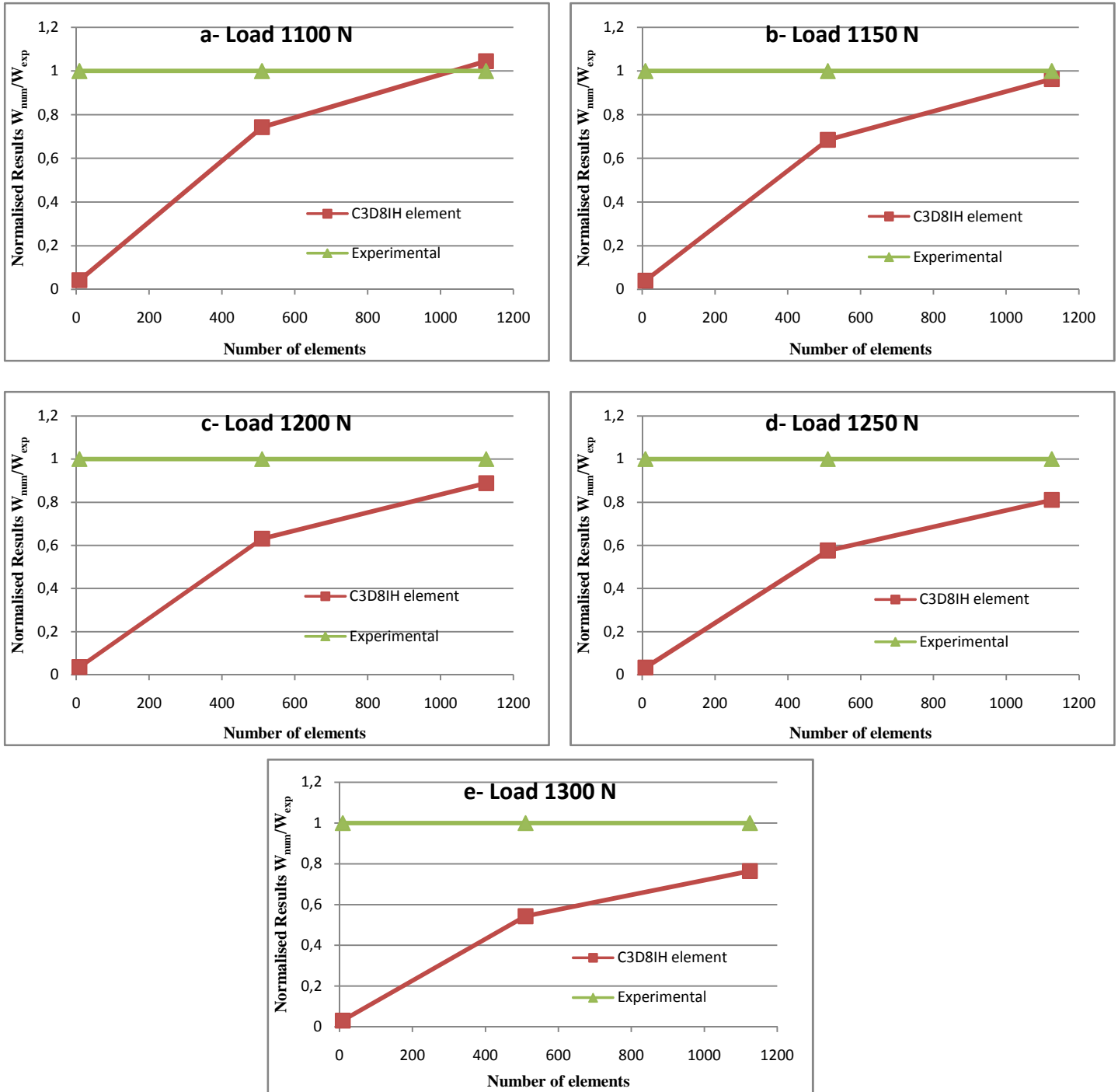
Fig. 5.9 Convergence curve for the deflections W_3 at point 3 under different loads

5.4.1 Vertical Displacements W (mm) Under Different Applied Loadings with numerical analysis (45x25) meshes, deflection for point 3

Table 5.21 summarizes the vertical displacements W obtained by the experimental tests and the numerical analysis for point 3 under different loads.

81

Table 5.21 Vertical deflection W (mm) Under Different Applied Loads at point 3

Loads (N)	1100	1150	1200	1250	1300
C3D8IH Element	1.761	1.841	1.921	2.001	2.081
Exp.Work	1.686	1.913	2.162	2.469	2.722
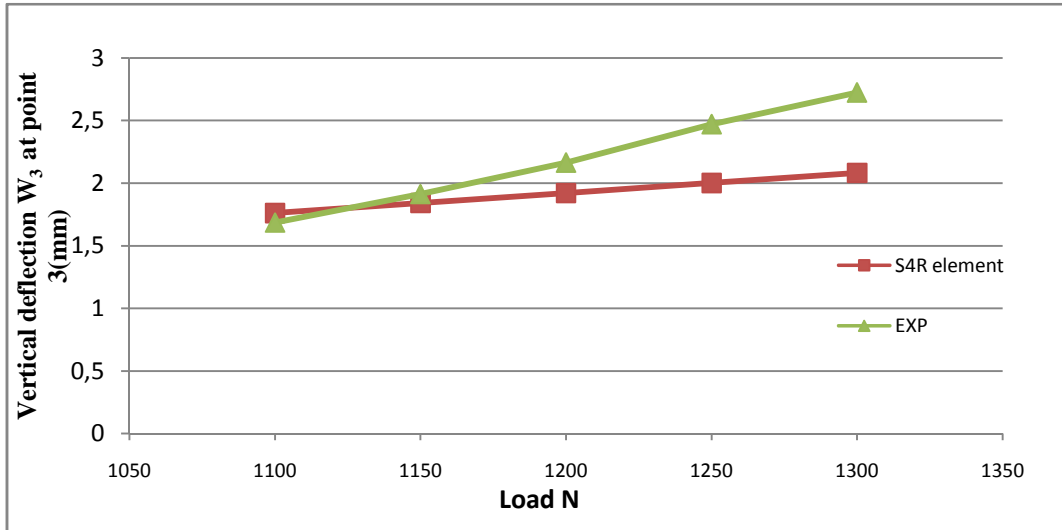
Fig. 5.10 Vertical displacement at point 3

Figure 5.10 shows that the results obtained with ABAQUS are very close to the experimental results, but when the load reach 1150N the deflection start to diverge, which may be explained by the beginning of the nonlinear stage, and the shell goes to the plastic behavior.

Figure 5.11 shows the shell model undergoing loading and the deformed shape of the shell, with presenting of the deformed shape of skin and the beam, also the deformation of the stiffeners, is presented clearly in the figures 5.12.
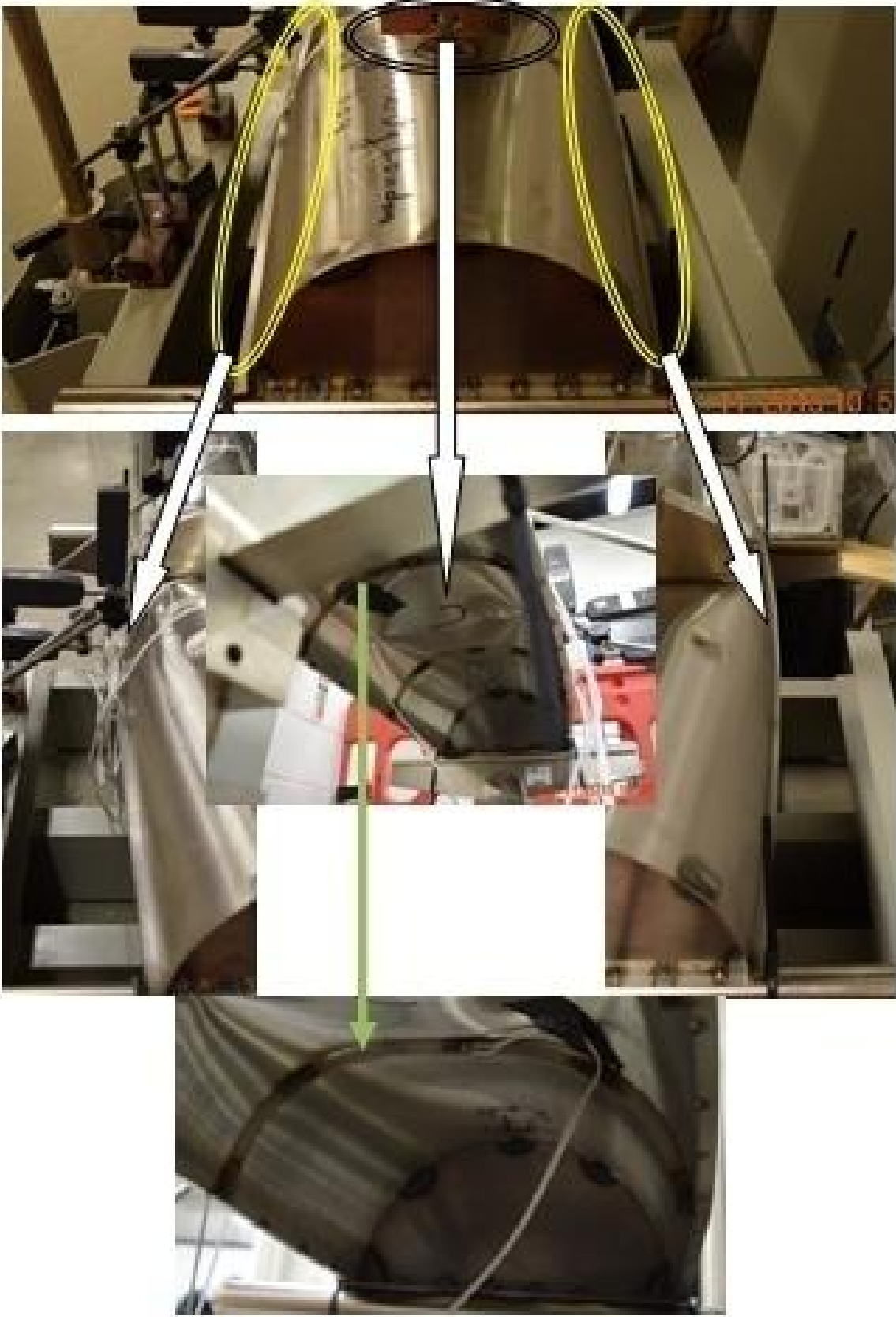
Fig. 5.11 Cylindrical shell model undergoing the loading
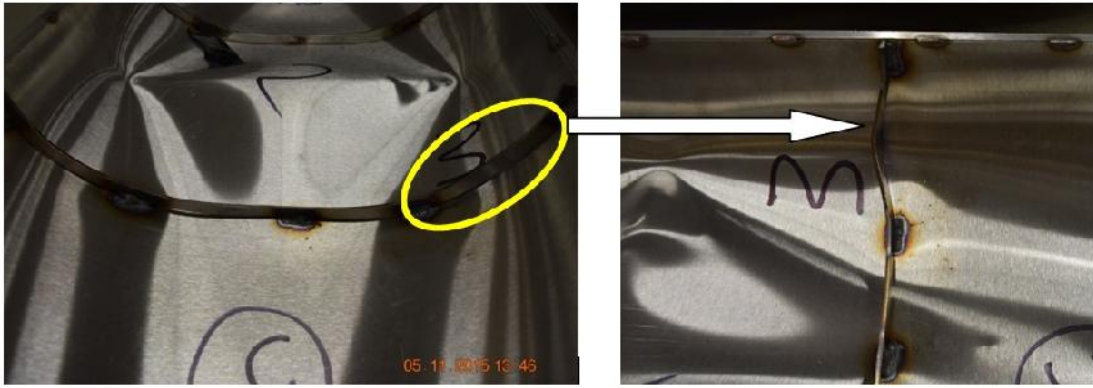
Fig. 5.12 A sample of stiffeners deformation

Figure 5.11 presents the deformation of shell, beams "stringers" and stiffeners, for the figure 5.12 , we saw the warping of stiffener that may be because the experimental test errors.

Figure 5.13 presents the simulation of the cylindrical shell with rigid diaphragm and stiffeners (the model and the deformation shape of the cylinder).
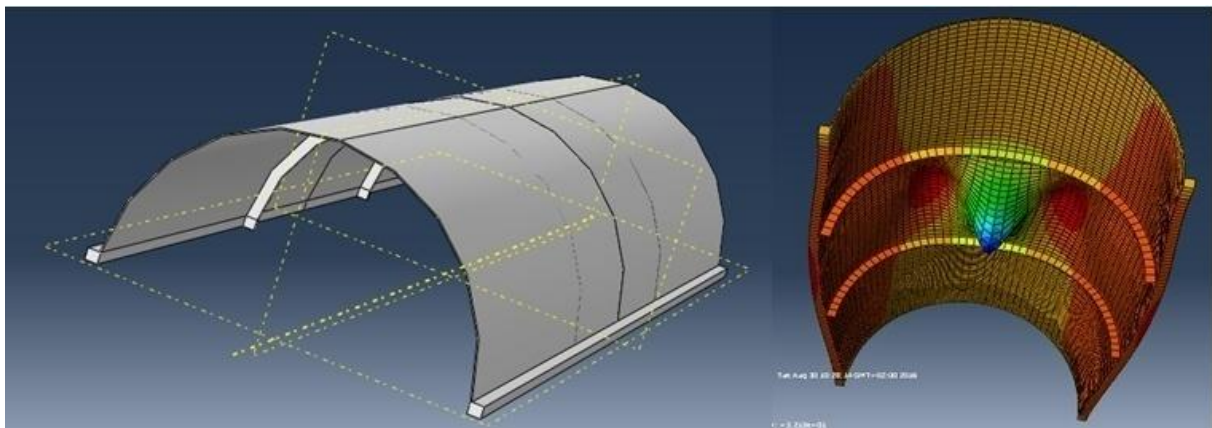
Fig. 5.13 Simulation with ABAQUS code

5.5 Conclusion

The using of circumferential stiffening and / or longitudinal stiffening increases the rigidity of structures and minimizes deformation. In the last studies and comparisons we saw that the adding of stiffeners decrease the vertical displacements, it means that the structure is more rigid, and we summarize many conclusions;

- For the cylindrical shell with two Stiffeners reposed on four points;

- ABAQUS results converge until 85% to the experimental results, and for a small number of meshes like 3x3 and 9x9, the displacements is so distant. But for a big number of elements, ABAQUS results converge to the experimental results.

- ABAQUS results are very close to the experimental results, but when the load reaches 1450N the deflection start to diverge.

- For the cylindrical shell with two end Diaphragms and two Stiffeners;

- ABAQUS results and the experimental results are very close until 98% for 45x25 meshes, after the load 900N we saw that the displacements diverge.

- For the cylindrical shell with two end Diaphragms and two Stiffeners resting on longitudinal beams "Stringers";

- ABAQUS results are very close to the experimental results, but when the load reaches 1150N the deflection start to diverge.

Chapter 6

Effect of Boundary Conditions and The Stiffeners on The Cylindrical Shells

Chapter 6

Effect of Boundary Conditions and the Stiffeners on The Cylindrical Shells

6.1 Introduction

The Effect of boundary conditions is so important in the analysis of cylindrical shells and is seldom studied in the literature probably because his hard experimental verification. Sometimes we need to change the boundary supports of the structures to minimize the stresses and the deflection, but in the other side we have to study the using of this important component of the structures. In this study an experimental and numerical investigation for the effect of different boundary supports for the stiffened and no stiffened cylindrical shells and the effect of stiffeners on the cylindrical shells was done. Two different comparison of the stiffened and no stiffened cylindrical shells in different boundary conditions "pinned and rigid diaphragm", and three different comparison of stiffened cylindrical shells:

- Effect of ring stiffeners on the vertical displacement at the top of the cylinder "point 3" for the cylindrical shell reposed on 4 points;

- Effect of ring stiffeners on the vertical displacement at the top of the cylinder "point 3" for the cylindrical shell with end Rigid Diaphragms;

- Effect of stringers on the vertical displacement at the "point3" and the horizontal displacement at the point 6 for the cylindrical shell with end diaphragms and stiffeners.

in the next paragraphs we present the results and the discussion.

6.2 Effectiveness of boundary conditions on the cylindrical shell

For the study of the effectiveness of boundary conditions especially the rigid diaphragms on a cylindrical shell structure, we choose some results from our tests and observe the decrease percentage of the vertical displacements. We chose tests 2 and 3:

- Cylindrical shell with No end Diaphragms and No Stiffeners **CNDNS**

- Cylindrical shell with two end rigid Diaphragms and No Stiffeners **CDNS**

In this comparison we took the loads (775N, 800N, 825N,850N, 875N and 900N) that we applied on the cylinders, for the cylindrical shell with no end Diaphragms and the cylindrical shell with end Rigid Diaphragms and compare the results.

6.2.1   Cylindrical shell with No end Diaphragms and No Stiffeners CNDNS

- **Vertical Displacements at point 3**

Table 6.1 presents the vertical displacement at point 3 for the loading (775N - 900N).

Table 6.1 The vertical Displacement W_3 at point 3 (Experimental, ACM-RSBE5 and ABAQUS results) with meshes 10x10

Loads (N)	Displacement W_3 at point 3 (mm)		
	ACM-RSBE5	S4R ABAQUS	Experimental solution
775	5.061	5.08	4.649
800	5.224	5.241	5.098
825	5.387	5.403	5.606
850	5.551	5.564	6.060
875	5.714	5.726	6.422
900	5.877	5.888	6.822

6.2.2   Cylindrical shell with two end rigid Diaphragms and No Stiffeners CDNS

- **Vertical Displacements at point 3**

Table 6.2 presents the vertical displacement at point 3 for the loading (775N - 900N)

Table 6.2 The vertical Displacement W_3 at point 3 (Experimental, ACM-RSBE5 and S4R - ABAQUS results) with meshes 10x10

Loads (N)	Displacement W_3 at point 3 (mm)		
	ACM-RSBE5	**S4R ABAQUS**	**Experimental solution**
775	1.064	0.9796	1.438
800	1.098	1.011	1.727
825	1.133	1.043	1.831
850	1.167	1.074	1.936
875	1.201	1.106	2.013
900	1.236	1.106	2.103

6.2.3   Comparison with the ACM-RSBE5 element results

The table 6.3 presents the vertical displacements at the top for the cylindrical shell with no end Diaphragms and the cylindrical shell with end Rigid Diaphragms with different loadings, and the percentage of diminution for the deflection, by using of ACM-RSBE5 element results.

Table 6.3 The deflection diminution percentage by using of ACM-RSBE5 element results.

Load N	775	800	825	850	875	900
Displacement **CNDNS (mm)**	5.061	5.224	5.387	5.551	5.714	5.877
Displacement **CDNS (mm)**	1.064	1.098	1.133	1.167	1.201	1.236
Percentage **(%)**	78.97649	78.981623	78.96789	78.976761	78.981449	78.968862

6.2.4   Comparison with ABAQUS results

The table 6.4 presents the vertical displacements at the top for the cylindrical shell with no end Diaphragms and the cylindrical shell with end Rigid Diaphragms with different loadings, and the percentage of diminution for the deflection, by using of ABAQUS element results.

Table 6.4 The deflection diminution percentage by using of ABAQUS element results.

Load (N)	775	800	825	850	875	900
Displacement **CNDNS (mm)**	5.08	5.241	5.403	5.564	5.726	5.888
Displacement **CDNS (mm)**	0.9796	1.011	1.043	1.074	1.106	1.106
Percentage **(%)**	80.716535	80.70979	80.69591	80.69734	80.684597	81.216033

6.2.5 Comparison with the experimental results

The table 6.5 presents the vertical displacements at the top for the cylindrical shell with no end Diaphragms and the cylindrical shell with end Rigid Diaphragms with different loadings, and the percentage of diminution for the deflection, by using of experimental results.

Table 6.5 The deflection diminution percentage by using of experimental results.

Load (N)	775	800	825	850	875	900
Displacement **CNDNS (mm)**	4.649	5.098	5.606	6.060	6.422	6.822
Displacement **CDNS (mm)**	1.438	1.727	1.831	1.936	2.013	2.103
Percentage **(%)**	69.06862	66.12397	67.338566	68.052805	68.654625	69.173263

Figure 6.1 presents the difference of deflection between the cylindrical shell on 4 points and the cylindrical shell reposed on two rigid diaphragms, for the numerical results and the experimental results.
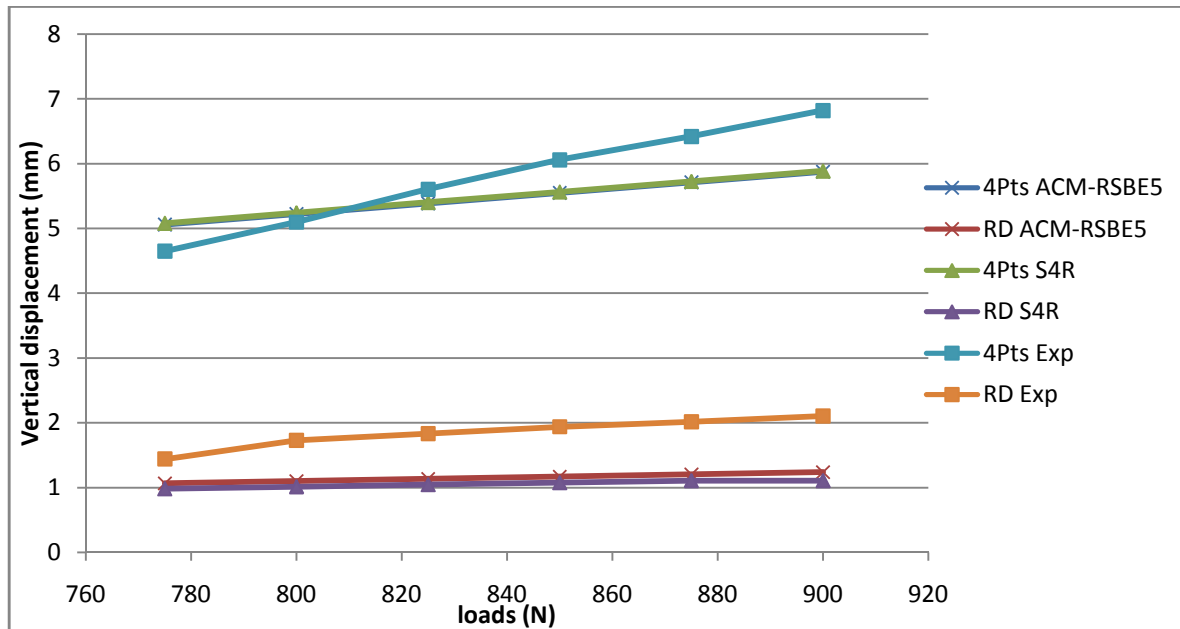
Fig. 6.1 The comparison of deflections for the cylindrical shell models with different boundary conditions (Experimental and numerical results)

In the comparison between cylindrical shell with no end Diaphragms and the cylindrical shell with end Rigid Diaphragms, good results and good work has been done by the rigid diaphragms, the percentage is closely to 80% with the ACM-RSBE5 element and for the ABAQUS element is 80%; it means that the vertical displacement at the top of cylinder "the point of applied the load" is minimized to 1/5 with using the rigid diaphragms.

But for the results giving by the experimental investigation, the percentage close to 69%, it is also a high percentage, it means that the rigid diaphragms minimized the deflection to 1/3 .

6.3 Effectiveness of boundary conditions on the "cylindrical shell with stiffeners"

For the study of the effectiveness of rigid diaphragms on a cylindrical shell structure with stiffeners, especially for deflection, we choose some results from our tests and observe the decrease percentage of the vertical displacements between the stiffened cylindrical shell reposed on four points and the stiffened cylindrical shell with end diaphragms.(Tests 4 and 5)

So we took the loads (900N, 950N, 1000N,1050N and 1100N) that we applied on the cylinders, for the stiffened cylindrical shell reposed on four points and the stiffened cylindrical shell with end diaphragms and compare the results, the loading is mentioned in last chapter, it is a concentrated static load acting on top of the cylinder.

Tables 6.6 and 6.7 presents the vertical displacement at point 3 (Experimental and ABAQUS results) for the stiffened cylindrical shell with no end Diaphragms **CNDS** and the stiffened cylindrical shell with end Rigid Diaphragms **CDS** with different loadings. Tables 6.8 and 6.9 presents the percentage of diminution for ABAQUS results and the experimental results.

6.3.1 Cylindrical shell with no end diaphragms and two stiffeners, t=1.2mm

Table 6.6 The vertical Displacement W_3 at point 3 (Experimental and ABAQUS results) with meshes 45x25 in ABAQUS

Loads (N)	Displacement W_3 at point 3 (mm)	
	Experimental solution	C3D8IH ABAQUS
900	3.453	2.595
950	3.529	2.737
1000	3.806	2.991
1050	3.829	3.023
1100	3.966	3.165

6.3.2 Cylindrical shell with two end diaphragms and two stiffeners, t=1.2mm

Table 6.7 The vertical Displacement W_3 at point 3 (Experimental and ABAQUS results) with meshes 45x25 with ABAQUS

Loads (N)	Displacement W_3 at point 3 (mm)	
	Experimental solution	C3D8IH ABAQUS
900	1.591	1.447
950	1.755	1.527
1000	1.966	1.607
1050	2.138	1.688
1100	2.355	1.768

6.3.3 Comparison with ABAQUS results

Table 6.8 Percentage of deflection diminution with ABAQUS results

Load (N)	900	950	1000	1050	1100
Displacement **CNDS (mm)**	2.595	2.737	2.991	3.023	3.165
Displacement **CDS (mm)**	1.447	1.527	1.607	1.688	1.768
Percentage **(%)**	44.238921	44.208988	46.27215	44.161429	44.139021

6.3.4 Comparison with the Experimental results

Table 6.9 Percentage of deflection diminution with experimental results for the CNDS and the CDS

Load (N)	900	950	1000	1050	1100
Displacement **CNDS (mm)**	3.453	3.529	3.806	3.829	3.966
Displacement **CDS (mm)**	1.591	1.755	1.607	2.138	2.355
Percentage **(%)**	53.924124	50.269198	57.777194	44.162967	40.620272

The figure 6.2 presents the difference of deflection between the stiffened cylindrical shell models reposed on 4 points and the stiffened cylindrical shell reposed on two rigid diaphragms, for the numerical results and the experimental results.

In the comparison between the stiffened cylindrical shell with no end Diaphragms and the stiffened cylindrical shell with end Rigid Diaphragms, good results and good work has been done by the rigid diaphragms, the percentage is closely to 45% with ABAQUS element; it means that the vertical displacement at the top of cylinder " the point of applied the load" is minimized by 45% with using of the rigid diaphragms.

But for the results giving by the experimental investigation, the percentage close to 50%, it means that the rigid diaphragms minimized the deflection to the half .
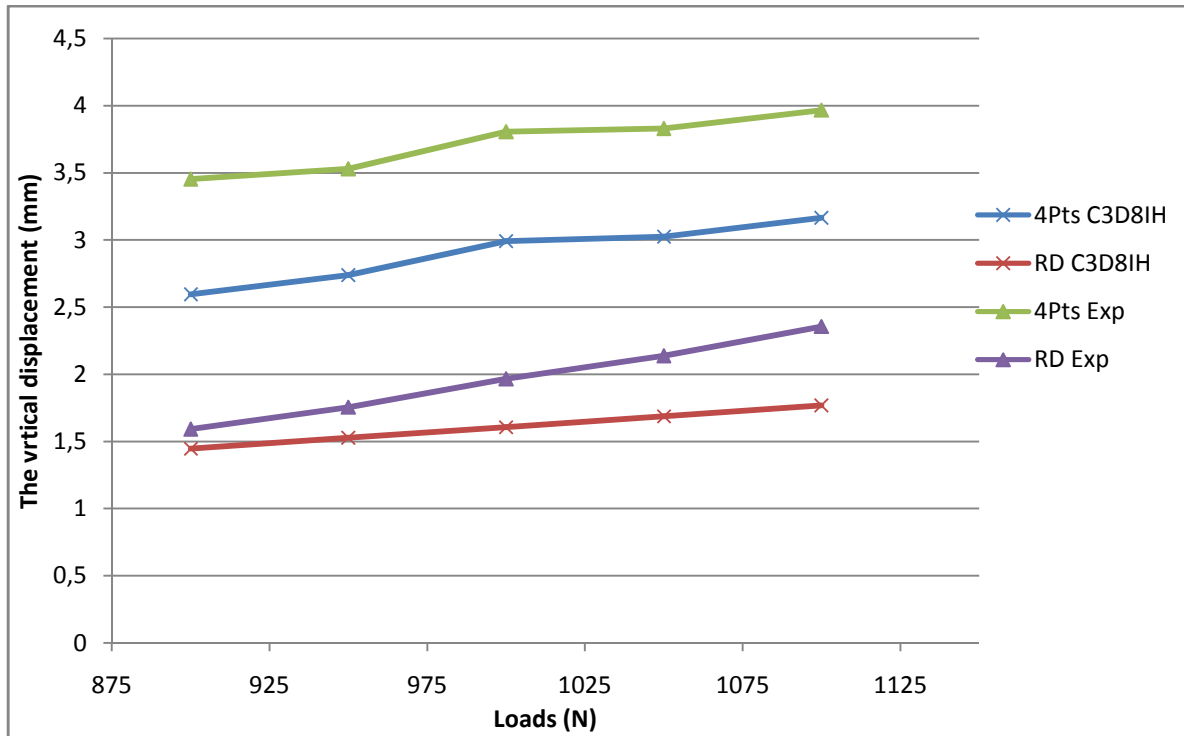
Fig. 6.2 The comparison of deflections for the stiffened cylindrical shell models with different boundary conditions (Experimental and numerical results)

6.4 Effectiveness of stiffeners on the cylindrical shell

The resistance of cylindrical shells in bending, buckling and any other possible deformation is often improved by the use of circumferential stiffening and / or longitudinal stiffening. The size, spacing and position of the stiffeners on the outer or inner surfaces of the cylinder wall are factors that influence the behavior instability of the shell. Thus stiffened shells are prominent in the field of engineering such as in aerospace structures, mechanical as well as in marine structures.

For our study of the effectiveness of stiffeners on the cylindrical shell we made many tests and took the vertical and the horizontal displacements:

- Cylindrical shell with No end diaphragms and No Stiffeners **CNDNS**

- Cylindrical shell with two end rigid Diaphragms and No Stiffeners **CDNS**

- Cylindrical shell with No end Diaphragms and two Stiffeners **CNDS**

- Cylindrical shell with two end Diaphragms and two Stiffeners **CDS**

- Cylindrical shell with two end Diaphragms and two Stiffeners resting on longitudinal beams "Stringers" **CDSS**

For the first comparison we took the second and the fourth tests, for the second comparison we took the third and the fifth test, and the last comparison between the fifth and sixth tests to seeing the effectiveness of two beams "stringers".

6.4.1   First Comparison: Effect of ring stiffeners on the vertical displacement at the top of the cylinder "point 3" for the cylindrical shell reposed on 4 points

This comparison is between the vertical displacements of **CNDNS** and the **CNDS,** we will present the displacements at each test for the same loading. Tables 6.10 and 6.11 presents the vertical displacements at point 3 of each test.

In the tables 6.12 and 6.13 we will see percentage of deflection diminution with ABAQUS results and the experimental results for the CNDNS and the CNDS.

6.4.1.1 Cylindrical shell with No end diaphragms and No Stiffeners, t=1.2mm

- **Vertical Displacements at point 3**

In this test many loads are applied (800N,825N,850N, 875N,900N,925N,950N,975N and 1000N). The Vertical displacements are recorded at point 3.

Table 6.10 The vertical Displacement W_3 at point 3 (Experimental and ABAQUS results) with meshes 45x25 with ABAQUS

Loads (N)	Displacement W_3 at point 3 (mm)	
	Experimental solution	S4R ABAQUS
800	5.098	5.420
825	5.606	5.587
850	6.060	5.755
875	6.422	5.922
900	6.822	6.089
925	7.3	6.256
950	7.568	6.423
975	7.804	6.590
1000	8.146	6.757

6.4.1.2 Cylindrical shell with No end Diaphragms and two Stiffens, t=1.2mm)

- **Vertical Displacements at point 3**

Table 6.11 The vertical Displacement W_3 at point 3 (Experimental and ABAQUS results) with meshes 45x25 with ABAQUS

Loads (N)	Displacement W_3 at point 3 (mm)	
	Experimental solution	**C3D8IH ABAQUS**
800	3.197	2.309
825	3.251	2.380
850	3.309	2.452
875	3.377	2.523
900	3.453	2.595
925	3.529	2.666
950	3.529	2.737
975	3.608	2.809
1000	3.806	2.991

The tables 6.10 and 6.11 present the vertical displacements at the top for the cylindrical shell with No end diaphragms and No Stiffeners and the cylindrical shell with No end Diaphragms and two Stiffeners, with different loadings, and the percentage of diminution for the deflection.

6.4.1.3 Comparison with the ABAQUS element results

Table 6.12 Percentage of deflection diminution with ABAQUS results for the CNDNS and the CNDS

Load (N)	Displacement for the CNDNS (mm)	Displacement for the CNDS (mm)	Percentage (%)
800	5.420	2.309	57.398524
825	5.587	2.380	57.40111
850	5.755	2.452	57.393571
875	5.922	2.523	57.39615
900	6.089	2.595	57.382165
925	6.256	2.666	57.38491
950	6.423	2.737	57.387514
975	6.590	2.809	57.37481
1000	6.757	2.991	55.734794

6.4.1.4   Comparison with the Experimental results

Table 6.13 Percentage of deflection diminution with the experimental results for the CNDNS and the CNDS

Load (N)	Displacement for the CNDNS (mm)	Displacement for the CNDS (mm)	Percentage (%)
800	5.098	3.197	37.289133
825	5.606	3.251	42.008562
850	6.060	3.309	45.39604
875	6.422	3.377	47.415135
900	6.822	3.453	49.384345
925	7.3	3.529	51.657534
950	7.568	3.529	53.36945
975	7.804	3.608	53.767299
1000	8.146	3.806	53.277682

In the first comparison between cylindrical shell with No end diaphragms and No Stiffeners and the cylindrical shell with No end Diaphragms and two Stiffeners, good results and good work has been done by the stiffeners, the percentage is closely to 58% with the ABAQUS element , it means that the vertical displacement at the top of cylinder " the point of application of the load" is minimized almost by 58% with using the ring stiffeners.

And the percentage is variable between 32% to 54% for the experimental tests, it means that the stiffeners minimized the deflection by 32% to 54% .

6.4.1.5   Diminution Percentage of the horizontal displacements at point 6 using the experimental results

The table 6.14 summarizes the horizontal displacements and the percentage of diminution of the horizontal displacements at point 6 for the two cylindrical shell models:

- Without stiffeners reposed on four points;

- With stiffeners reposed on four points.

Table 6.14 Percentage of diminution of Horizontal Displacements at point 6 using the experimental results

Load (N)	Displacement for the CNDNS (mm)	Displacement for the CNDS (mm)	Percentage (%)
1250	1.58	1.09	31.012659
1500	1.65	1.18	28.484848
1750	1.92	1.32	31.25
2000	2.23	1.58	29.147982
2250	2.8	1.88	32.857143
2500	3.78	2.5	33.862434

In this comparison we took the loads (1250N, 1500N, 1750N, 2000N, 2250N and 2500N). These loads passing from the elastic range to the plastic range, we looked that the percentage is almost the same, between 29% and 34%, it means that the diminution of displacement is between 29% and 34%, so the stiffeners decrease the displacement at the point 6h.

6.4.2 Second Comparison: Effect of ring stiffeners on the vertical displacement at the top of the cylinder "point 3" for the cylindrical shell with end Rigid Diaphragms

The same procedure as the previous one is used for this test. The applied loads are (800N, 825N, 850N, 875N and 900N) .

The tables 6.15 and 6.16 present the vertical displacements at the top for the cylindrical shell with two end rigid Diaphragms and No Stiffeners and the cylindrical shell with two end Diaphragms and two Stiffeners, with different loadings, and the percentage of diminution for the deflection. In the tables 6.17 and 6.18 we will observe the percentage of deflection diminution with ABAQUS results and the experimental results for the CDNS and the CDS.

6.4.2.1   Cylindrical shell with end Rigid Diaphragms, t =1.2mm

- **Vertical Displacements at point 3:**

The results of vertical displacement are presented in table 6.15.

Table 6.15 The vertical Displacement W_3 at point 3 (Experimental and ABAQUS results) with meshes 45x25 with ABAQUS

Loads (N)	Displacement W_3 at point 3 (mm)	
	Experimental solution	S4R ABAQUS
800	1.727	1.139
825	1.831	1.174
850	1.936	1.210
875	2.013	1.245
900	2.103	1.281

6.4.2.2 Cylindrical shell with two end diaphragms and two stiffeners, t=1.2mm

- **Vertical Displacements at point 3**

The results of vertical displacement are also presented in table 6.16.

Table 6.16 The vertical Displacement W_3 at point 3 (Experimental and ABAQUS results) with meshes 45x25 with ABAQUS

Loads (N)	Displacement W_3 at point 3 (mm)	
	Experimental solution	C3D8IH ABAQUS
800	1.229	1.286
825	1.306	1.326
850	1.391	1.366
875	1.476	1.406
900	1.591	1.447

6.4.2.3   Comparison with the ABAQUS element results

Table 6.17 Percentage of diminution of the vertical displacements at point 3 using ABAQUS results for the CDNS and CDS

Load (N)	Displacement for the CDNS (mm)	Displacement for the CDS (mm)	Percentage (%)
800	1.139	1.286	112.906058
825	1.174	1.326	112.947189
850	1.210	1.366	112.892562
875	1.245	1.406	112.931727
900	1.281	1.447	112.958626

6.4.2.4   Comparison with the Experimental results

Table 6.18 Percentage of diminution of the vertical displacements at point 3 using the experimental results for the CDNS and CDS

Load (N)	Displacement for the CDNS (mm)	Displacement for the CDS (mm)	Percentage (%)
800	1.727	1.229	28.836132
825	1.831	1.306	28.672856
850	1.936	1.391	28.150826
875	2.013	1.476	26.676602
900	2.103	1.591	24.346172

In the second comparison between cylindrical shell with two end rigid Diaphragms and No Stiffeners and the cylindrical shell with two end Diaphragms and two Stiffeners, the percentage is closely to 110% with the ABAQUS element , it means that the vertical displacement at the top of cylinder " the point of applied the load" is increased by 10% with adding of stiffeners. This is an unbelievable result; we must make a study about this problem, because after adding of the stiffeners the deflection is increased, but the logic says the opposite, may be the problem is in the ABAQUS analysis "because the elements are not the same; the first is S4R (shell element) and the second is C3D8IH (solid element)".

And the percentage is variable between 25% to 29% for the experimental tests, it means that the stiffeners minimized the deflection by 25% to 29%, these results is so logical.

6.4.3   Third Comparison: Effect of stringers on the vertical displacement at the "point3" and the horizontal displacement at the point 6 for the cylindrical shell with end diaphragms and stiffeners

In this comparison the same procedure as the previous one is followed. The vertical displacements are recorded at point 3; tables 6.19 and 6.20 presents the vertical displacements at the top by ABAQUS and experimental results for the Cylindrical shell with two end diaphragms and two stiffeners and Cylindrical shell with two end diaphragms and two stiffeners resting on longitudinal beams "stringers", with loadings (1000N, 1050N, 1100N, 1150N, 1200N, 1250N and 1300N) and the percentage of diminution for the deflection with ABAQUS results and the experimental results for the CDS and the CDSS. The tables 6.21 and 6.22 presents the percentage of diminution of the vertical displacements at point 3 using the experimental and ABAQUS results for the CDS and CDSS.

But for the horizontal displacements at point 6 we took the loads (1500N, 1750N, 2000N, 2250N and 2500N) and did the comparison with just the experimental results, the table 6.23 presents the percentage of diminution of the horizontal displacements at point 6 using the experimental and ABAQUS results for the CDS and CDSS.

6.4.3.1 Cylindrical shell with two end diaphragms and two stiffeners, t=1.2mm

- **Vertical Displacements at point 3**

Table 6.19 The vertical Displacement W_3 at point 3 (Experimental and ABAQUS results) with meshes 45x25 with ABAQUS

Loads (N)	Displacement W_3 at point 3 (mm)	
	Experimental solution	C3D8IH ABAQUS
1000	1.966	1.607
1050	2.138	1.688
1100	2.355	1.768
1150	2.575	1.849
1200	2.851	1.929
1250	3.146	2.009
1300	3.378	2.090

6.4.3.2   Cylindrical shell with two end diaphragms and two stiffeners resting on longitudinal beams "stringers", t=1.2mm

- **Vertical Displacements at point 3**

Table 6.20 The vertical Displacement W_3 at point 3 (Experimental and ABAQUS results) with meshes 45x25 with ABAQUS

Loads (N)	Displacement W_3 at point 3 (mm)	
	Experimental solution	**C3D8IH ABAQUS**
1000	1.229	1.600
1050	1.482	1.681
1100	1.686	1.761
1150	1.913	1.841
1200	2.162	1.921
1250	2.469	2.001
1300	2.722	2.081

6.4.3.3   Comparison with the ABAQUS element results

Table 6.21 Percentage of diminution of the vertical displacements at point 3 using ABAQUS results for the CDS and CDSS

Load (N)	Displacement for the CDS (mm)	Displacement for the CDSS (mm)	Percentage (%)
1000	1.607	1.600	0.435594
1050	1.688	1.681	0.414692
1100	1.768	1.761	0.395928
1150	1.849	1.841	0.432666
1200	1.929	1.921	0.414723
1250	2.009	2.001	0.398208
1300	2.090	2.081	0.430622

6.4.3.4   Comparison with the Experimental results

Table 6.22 Percentage of diminution of the vertical displacements at point 3 using the experimental results for the CDS and CDSS

Load (N)	Displacement for the CDS (mm)	Displacement for the CDSS (mm)	Percentage (%)
1000	1.966	1.229	37.487284
1050	2.138	1.482	30.682881
1100	2.355	1.686	28.407643
1150	2.575	1.913	25.708738
1200	2.851	2.162	24.166959
1250	3.146	2.469	21.51939
1300	3.378	2.722	19.419775

In the comparison between cylindrical shell with two end Diaphragms and two stiffeners, and cylindrical shell with two end diaphragms and two stiffeners resting on longitudinal beams "Stringers", it is almost the same for the ABAQUS results, with a decreasing of 0.4% of deflection, it means that the two beams don't do a good contribution for the vertical displacement at point 3, and it is not necessary to minimizing the deflections at this point.

But for the experimental comparison, the percentage of displacement shows another look, the vertical displacement minimized from 20% to 38%, it means that the two beams decreased the deflection by 20% to 38%; it is not a big contribution but it is acceptable .

6.4.3.5 Percentage of diminution of Horizontal Displacements at point 6 using the experimental results

The table 6.23 summarizes the horizontal displacements for the two models cylindrical shell with stiffeners and rigid diaphragm boundary conditions and the cylindrical shell with stiffeners and stringers and rigid diaphragm boundary conditions.

Table 6.23 Horizontal Displacements at point 6 for the CDS and CDSS

Load (N)	Displacement for the CDS (mm)	Displacement for the CDSS (mm)	Percentage (%)
1500	0.55	0.25	54.545455
1750	0.74	0.42	43.243243
2000	0.95	0.61	35.789474
2250	1.17	0.86	26.495726
2500	1.45	1.19	17.931034

In this comparison we took the loads (1500N, 1750N, 2000N, 2250N and 2500N). These loads passing from the elastic range to the plastic range, we saw the difference between the percentage of displacements diminution. The percentage is varied between 55% in the loading 1500N to 18% in the loading 2500N, it means that the diminution of displacement is getting smaller from 55% to 18%, so the beams has a good contribution in the elastic range and better than in the plastic range, especially in the horizontal displacements at the point 6.

6.5 Conclusion

In this chapter we studied the effectiveness of the boundary conditions on cylindrical shells, with and without stiffeners, and observe "the experimental results, the ACM-RSBE5 element results and S4R element results", we remark that:

- The using of rigid diaphragm on the cylindrical shell minimize the displacement to 1/5 with ACM-RSBE5 and S4R ABAQUS element, it is a good decreasing level. For the experimental results, the rigid diaphragm minimize the vertical displacement to 1/3 on the cylindrical shell, it is also an acceptable decreasing level.

- The rigid diaphragms minimized the vertical displacement at the top of the stiffened cylinder "the point of applied load" by 55% with using of ABAQUS results, but for the results giving by the experimental investigation, the percentage close to 50%; it means that the rigid diaphragms minimized the deflection to the half .

For the other study of the effectiveness of stiffeners, we showed that:

- The using of the ring stiffeners on the cylindrical shell reposed on four points minimized the vertical displacement at the top of cylinder "the point of applied load" by 58% with ABAQUS

results, and minimized the vertical displacement at the same point by 32% to 54% with experimental results, also we saw that the diminution percentage of the horizontal displacement at point 6 is between 29% and 34%, so the stiffeners decrease the displacement at point 6h.

- The using of two ring stiffeners on the cylindrical shell with rigid diaphragm minimized the vertical displacement by 25% to 29% with experimental results.

- The adding of two beams "stringers" on the stiffened cylindrical shell with rigid diaphragm decrease the vertical displacement at point 3 by 0.4% with ABAQUS results, it is not a good contribution, and decreased the vertical displacement by 20% to 38% with the experimental results, which is an acceptable contribution. But the using of two beams decreases the horizontal displacement at point 6 by 55%.

General Conclusion and Recommendations for Further Work

1. Conclusions

This thesis focuses on the modelling of complex structures. Numerical and experimental study of the cylindrical shells behaviour with and without stiffeners is carried out.

From the numerical analysis, the following points can be drawn:

- The ACM-RSBE5 and S4R ABAQUS element results are in close agreement with those from the experimental tests, they converge up to 99% for 10 x10 meshes.

- The flat shell element "ACM-RSBE5" has been demonstrated experimentally to be robust, effective and useful in analyzing thin shell structures.

- The ACM-RSBE5 exhibits strong convergence towards the experimental tests, as can be seen from the numerical results presented. Also, it presents, in general, better performance than the S4R element of ABAQUS code.

- By using the rigid diaphragms for the cylindrical shell model, the displacements decreased by about 80%, which is a significant value.

From the experimental tests, the following conclusions can be drawn:

- From all tests, the displacement obtained are very important (up to 50%), especially for the increasing loading and without stiffeners, i.e. it is very efficient to add some stiffeners to increase the rigidity and minimizing the deformations.

- For the experimental results, the rigid diaphragms minimize the vertical displacement up to 66%; which is very adequate decrease.

- From this study, using rigid diaphragm or stiffeners, the displacement are decreased, then we concluded that the using of them depends on the architectural design needed.

All of these results gave us some conclusions:

- From, the numerical and experimental results obtained for the stiffened cylindrical shell models; the ABAQUS element C3D8IH converges up to 98% to the experimental results

with 45x25 meshing. This proves its efficiency in modeling this type of structures instead of using 2 different elements.

- By using the *Rigid Diaphragms* on the Stiffened cylindrical shell model, the vertical displacement will be minimized on the top of the cylinder by 80% with ABAQUS and decreased to half in the experimental tests, which is a very significant value.

- With the addition of two Stiffeners on the cylindrical shell model reposed on 4 points, the vertical displacement at the top of cylinder "point of applied the load", the vertical displacement will be decreased by about 58% with ABAQUS results and up 32% to 54% with the experimental results.

- The adding of two stiffeners on the cylindrical shell reposed on rigid diaphragm increased the vertical deflection by 10% with ABAQUS results and decreased by 25% to 29% in the experimental tests; it is an unbelievable results for ABAQUS, we have to do further researches concerning this contradiction, may be the problem is in the ABAQUS analysis "because the elements used for the analysis are not the same; the first is S4R (shell element) and the second is C3D8IH (solid element)".

- For the cylindrical shell model with two end Diaphragms, two Stiffeners and two Edge beams "Stringers"; the vertical displacement is decreased at the top of the cylinder by up to 20% to 38%. Also the horizontal displacement at point 6 will be decreased by up 55% to 18%.

2. Recommendations for further work:

- The ACM_RSBE5 element has been proved to be efficient for the linear analysis of shell structures with great accuracy. Therefore; it is of importance to extend the presented element ACM-RSBE5 to take into account nonlinear behaviour, which will be recommended for future studies.

- For the small loads, the analysis of the cylindrical shell without stiffeners, ABAQUS results obtained for 2x2 meshes are unreasonable values, then; it is of importance to find out a response to this problem.

- In practice, the shell structures used generally cover very large areas, and sometimes having a complex geometrical shapes and supporting heavy loads; this can cause very large displacements. Therefore; the numerical non- linear analysis of shell structures is of great importance, worth to be studied and investigated by experimental work.

Using the solid element to model shell structures (thin shell + stiffeners), for some element (solid) it is not sufficient, so we should use 2 elements:

- Thin shell element ACM-RSBE4 for the cylindrical shell;

- The beam element as solid for the stiffeners.

References

[ABA2014]   ABAQUS, Version 6.14, 2014. Dassault Systemes Simulia Corp.

[Adi1961]   Adini, A., and Clough, R.W., Analysis of plate bending by the finite element method, Report to the Nat. Sci. Found., U.S.A., G 7337, 1961.

[Ahm1970]   Ahmad, S., Irons, B. M., and Zienkiewicz, O.C., Analysis of Thick and Thin Shell Structures by Curved Finite Elements, International Journal for Numerical Methods in Engineering, Vol. 2, 1970, pp. 419-451.

[Ami1992]   Aminpour, M.A., (1992), An assumed-stress hybrid 4-node shell element with drilling degrees of freedom, Int. J. Numer. Methods Eng., Vol. 33, pp 19-38.

[Arg1986]   Argyris, J.H., Mlejnek, H.P., (1986), Die methode der finite element, Band I, II, III, Viewg,Ed.

[Bar1965]   Baruch, M., Equilibrium and Stability Equations for Discretely Stiffened Shells, Israel Journal of Technology, Vol. 3, No. 2, pp. 138-146, June 1965.

[Bat1972]   Batoz J. L. and Dhatt G., Development of Two Simple Shell Elements, AIAAJ, Vol. 10, No. 2, 1972, pp. 237-238.

[Bat1980]   Batoz, J.L., Bathe, K.J., Ho, LW., (1980), A study of three-node triangular plate bending elements, lnt. J. Numer. Methods Eng., Vol. 15, pp 1771-1812.

[Bat1981]   Bathe, K. J., and Ho, L. W., A Simple and Effective Element for Analysis of General Shell Structures, Computers and Structures, Vol. 13, pp. 673.

[Bat1992]   Batoz, J.L., Dhatt, G., (1992), Modélisation des structures par éléments finis, volume 3, Coques, Hermès.

[Ber1985]   Bergan, P.G. and Fellipa, C.A., (1985), A triangular membrane element with rotational degrees of freedom, Comp. Methods. Appl. Mech., Vol. 50, pp 25.

[Ber1986]   Bernadou, M., (1986), Some finite element approximations of thin shell problems, in Finite Element Methods for Plate and Shell Structures, Vol. 1, Element Technology (Hughes et Hinton Eds), Pineridge Press, pp 62-84.

[Ber1986]   Bergan, P .G., Felippa, C.A., (1986), Efficient Implementation of a triangular membrane with drilling freedom, Chap. 5 : Finite element methods for plate and shell structures, Vol. 1, Hughes and Hinton Eds, pp 128

[Bil1982]   Billington, D.P. (1982), Thin Shell Concrete Structures. 2nd Ed. McGraw-Hill Book Company.

[Bis1999]   Bischoff. M., Theorie und Numerik einer dreidimensionalen Schalenformulierung. PhD thesis, Institut für Baustatik, Universität Stuttgart, 1999.

[Bis2004]   Bischoff, M., Wall, W.A., Bletzinger, K.-U. and Ramm, E., Encyclopedia of Computational Mechanics, chapter Models and finite elements for thin-walled structures. Wiley, 2004.

[Blo1964]   Block, D.L., Influence of Ring Stiffeners on Instability of Orthotropic Cylinders In Axial Compression, NASA TND-2482, October 1964.

[Bud1963]   Budiansky, B. and Sanders, J. L., On the 'Best' First Order Linear Shell Theory, Progress in Applied Mechanics (Prager Anniversary Volume), MacMillan, New York, 1963. pp 22-45.

[Car1969]   Carr, A. J., and Clough, R. W., Dynamic Earthquake Behavior of Shell Roofs, Fourth World Conference on Earthquake Engineering, Santiago, Chue, 1969.

[Car1985]   Carpenter, N., Stolarsky, M., Belytschko, T., (1985), A flat triangular shell element with improved membrane interpolation, Communications in Applied Numerical Methods, Vol. 1, pp 161-168.

[Cha1960]   Chao, C., New Developments in the Nonlinear Theories of the Buckling of Thin Cylindrical Shells, Proceedings of the Durand Centennial Conference, Hoff, N.J., and Vincenti, W.G., (Eds.), Pergamon Press, London, 1960, pp. 83.

[Che1963]   Cheng, S. and Ho, B.P.C., Stability of Heterogeneous Aeolotropic Cylindrical Shells Under Combined Loading, AIAA Journal, Vol. 1, 1963, pp. 892-898.

[Che1992]   Chen H. C., Evaluation of Allman Triangular Membrane Element used in general Shell Analysis, Computers and Structures, Vol. 43 (5), 1992, pp. 881-887.

[Coo1994]   Cook, R.D., Four-node 'flat' shell element: drilling degrees of freedom, membrane–bending coupling, warped geometry, and behavior, Computers & Structures Vol. 50, No. 4, pp. 549-555, (1994).

[Cos1965]   Cosserat, E., and Cosserat, F., Theorie Des Corps Deformables. Herman et fils, Paris, 1965.

[Cow1971]   Cowper, G.R., Lindberg, G.M., Oison, M.D., (1971), Comparison of two high precision triangular finite elements of arbitrary deep shells, Proc., Third Conf. on Matrix Methods in Struct. Mech., WPAFB, pp 277-344 .

[CSI2005]   CSI Analysis Reference Manual, (2005).

[Dat1970]   Dhatt, G., (1970), An efficient triangular shell element, AIAA, Vol. 8, N° 11, pp 2100.

[Daw1972]   Dawe, D.J., (1972), Shell analysis using a simple facet element, Journal for Strain Analysis, 7, 226-270.

[Dha1986]   Dhatt, G., Marcotte, L., and Matte, Y., A new triangular discrete Kirchhoff plate shell element, IJNME,23,(1986),453

[Djo1995]   Djoudi, M.S.and Sabir, A.B., Finite element analysis of singly and doubly curved dams of constant or variable thickness. Thin-walled structures (21): 279- 289, 1995.

[Djo2003]   Djoudi, M.S. and Bahai H., A shallow shell finite element for the linear and nonlinear analysis of cylindrical shells. Engineering structures (25): 769.

[Don1933]   Donnell, L.H., (1933), Stability of thin-walled tubes under torsion. NACA Report No 479.

[Far1992]   Farshad, M., (1992), Design and Analysis of Shell Structures, Dordrecht: Kluwer Academic Publishers.

[Fer1979]   Ferguson, G. H., and Clark, R. H., A Variable Thickness Curved Beam and Shell Stiffening Element with Shear Deformations, International Journal for Numerical Methods in Engineering, Vol. 14, 1979, pp. 581-592.

[Flü1932]   Flügge, W., Die Stabilitat der Kreiszy linderschale, Ingenieur Archive, Vol. 3, 1932, pp. 463-506.

[Gal1976]   Gallager, R.H., (1976) , Introduction aux éléments finis, Editions pluralis.

[Gir1968]   Girijavallabham, C. V., and Reese, L. C., Finite-Element Method for Problems in Soil Mechanics, Journal of the Structural Division, American Society of Civil Engineers, No. Sm2, pp. 473–497, Mar. 1968.

[Gre1965]   Green, A.E., Naghdi P.M., and Wainwright, W.L., A General Theory of a Cosserat Surface. Archive for Rational Mechanics and Analysis, 20(4): 287-308, 1965.

[Ham2006]   Hamadi, D., Analysis of structures by non-conforming finite elements, PhD Thesis, Civil engineering department, Biskra University, Algeria, 2006.

[Ham2014]   Hamadi, D., Temami, O., Zatar, A. and Abderrahmani, S., A Comparative Study between Displacement and Strain Based Formulated Finite Elements Applied to the Analysis of Thin Shell Structures, International Journal of Civil, Environmental, Structural, Construction and Architectural Engineering, Vol:8, No:8, 2014.

[Ham2015]   Hamadi, D., Ayoub, A. and Abdelhafid, O., (2015), A New Flat Shell Finite Element For The Linear Analysis Of Thin Shell Structures, European Journal of Computational Mechanics 24(6): 232-255.

[Haz1989]   Hazim F.E., Finite element analysis of shell structures, University of Wales College of Cardiff, Phd Thesis, 1989.

[Hec1993]   HECTOR, A. S., Flambage de coques raidies et non raidies sous chargements combines, PhD Thesis, Institut National des Sciences Appliquées de Lyon, 1993.

[Hed1965]   Hedgepeth, J.M., and Hall, D.B., Stability of Stiffened Cylinders, AIAA Journal, Vol. 3, No. 12, pp. 2275-2286, December 1965.

[Hes1988]   Hess, H., Large Deformation Effects in the Postbuckling Behavior of Composite with Thin Delaminarions, AIAA Journal, Vol. 27,1988, pp.624-631.

[HKS1995]   Habbit , Karlsson and Sorensen., Abaqus 5.4 theory manual and user's manual, providence: Habbit , Karlsson and Sorensen Inc 1995, 556p.

[Hoe2003]   Hoefakker, J.H. and Blaauwendraad, J., (2003), Theory of Shells, Delft: Delft University of Technology.

[Hoe2014]   Hoefakker, J.H. and Blaauwendraad, J., (2014), Solid Mechanics and Its Applications "Structural Shell Analysis: Understanding and Application". Volume 200. Department of Civil Engineering, University of Waterloo, Waterloo, Canada.

[Hug2000]   HUGHES, T.J.R., The Finite Element Method: Linear Static and Dynamic Finite Element Analysis. Dover Publications, Inc., Mineola, New York, 2000.

[Ibr1990]   lbrahimbegovic A., Taylor R.L., Wilson, E.L., (1990), A robust quadrilateral membrane finite element with drilling degrees of freedom, Int. j. numer. methods eng., 30, 445-457.

[Ibr1993]   lbrahimbegovic, A., Frey, F., Rebora, B., (1993), Une approche unifiée de la modélisation des structures complexes : les éléments finis avec degré de liberté de rotation, Revue Européenne des Eléments Finis, Vol. 2, pp 257-286.

[Iro1980]   Irons, B., Ahmad, S., (1980), Techniques of finite elements. Ellis Horwood, (John Wiley).

[Irw2015]   Irwan, K. , Batoz, J.L., Imam, J.M., Hamdouni, A., and Millet, O., The development of DKMQ plate bending element for thick to thin shell analysis based on the Naghdi/Reissner/Mindlin shell theory, Finite Elements in Analysis and Design 100(2015)1227.

[Jad1995]   Jadik, T., and Billington, D.P., (1995), Gabled Hyperbolic Paraboloid Roofs without Edge Beams. Journal of Structural Engineering, 121 (2), pp.328-335.

[Jon1967]   Jones, R. M., and Morgan, H. S., Buckling and Vibration of Cross-ply Laminated Circular Cylindrical Shells, AIAA Journal, Vol.5 , No.8 , 1967, pp. 1463.

[Jon1968]   Jones, R.M., Buckling of Circular Cylindrical Shells with Multiple Orthotropic Layers and Eccentric Stiffeners, AIAA Journal, Vol. 6, 1968, pp. 230 1-2305. Errata, Vol. 7, 1969, p. 2048.

[Kas1992]   Kassegne S,K., Layerwise theory for discretely stiffened laminated cylindrical shells, PhD Thesis,1992,Blacksburg, Virginia.

[Kim2011]   Kim, H.I. and Shin, S., (2011), A Study on Innovation in Technology and Design Variation for Super Tall Buildings. Journal of Asian Architecture and Building Engineering, 10(1), pp.61-68.

[Kim2012]   Kim, S.N., Yu, E.J. and Rha, C.S., (2012), Finite Element Analysis of Gabled Hyperbolic Paraboloid Shells. Journal of the Korean Association for Spatial Structures, 12 (1), pp.87-98.

[Kir1950]   Kirchhoff, G., Über das Gleichgewicht und die Bewegung einer elastischen Scheibe. Journal für reine angewandte Mathematik, 40:51–58, 1850.

[Kni1997]   Knight Jr. N. F., The Raasch Challenge for Shell Elements, AIAAJ, Vol. 35, 1997, pp.375-388.

[Koh1972]   Kohnke, P. C., and Schnobrich, W. C., Analysis of Eccentrically Stiffened Cylindrical Shells, Journal of the Structural Division, ASCE, Vol. 98, 1972, pp. 1493-1510.

[Koi1956]   Koiter, W.T., Buckling and Post-Buckling Behavior of a Cylindrical Panel under Axial Compression, Report S. 476, National Luchtvaartiaboratoriun, Amsterdam, Reports and Transactions, Vol. 20, 1956.

[Koi1960]   Koiter, W.T., The Theory of Thin Elastic Shells, chapter A: Consistent First Approximation in the General Theory of Thin Elastic Shells, pages 12–33. North- Holland, 1960.

[Koi1966]   Koiter, W.T., (1966), On the nonlinear theory of thin elastic shells, Proc. Konink. Ned. Akad Wentesch. Ser. B69 (1) pp 1-54.

[Koi1970]   Koiter, W. T., (1970), On the foundation of the linear theory of thin elastic shells, Proc. Konink. Ned. Akad Wentesch., B73, pp 169-197.

[Lai2009]   Lainez, J.M.C., Verdejo, J.R.J., Macias, B.S.M., and Calero, J.I.P. (2009), The Key-role of Eladio Dieste, Spain and the Americas in the Evolution from Brickwork to Architectural Form. Journal of Asian Architecture and Building Engineering, 8(2), pp.355-362.

[Lia1989]   Liao, C. L., An incremental Total Lagrangian Formulation for General Anisotropic Shell-Type Structures, AIAA Journal, Vol. 2, 1989 , pp. 453-435.

[Log 2007]   Logan,D.L., A First Course in the Finite Element Method, Fourth Edition, University of Wisconsin Platteville, 2007.

[Lov1888]   LOVE, A.E.H., On the Small Vibrations and Deformations of Thin Elastic Shells. Philosophical Transactions of the Royal Society, 179:491 ff., 1888.

[Man2000]   Manfred, A.H and Michel, C., Conception et dimensionnement des halles et bâtiments. Édition: Presses polytechniques et universitaires Romandes. Volume 11. 2000.

[Mar1961]   Martin, H. C., Plane Elasticity Problems and the Direct Stiffness Method, The Trend in Engineering, Vol. 13, pp. 5–19, Jan. 1961.

[Mar1989]   Martin, W., and Drew, D., The Effect of Delamination on the Fundamental anti Higher Order Buckling Loads of Laminated Beams, Journal of Composite Testing and Research, Vol. 11, 1989, pp. 87-93.

[McN1978]   McNeal R. H., A Simple Quadrilateral Shell Element, Computers and Structures, Vol. 8, 1978, pp. 175-183.

[McN1988]   McNeal R. H. and Harder R. L., Refined Four Node Membrane Element with Rotational Degrees of Freedom, Computers and Structures, Vol. 28, 1988, pp. 75-84.

[Mel1961]   Melosh, R. J., A Stiffness Matrix for the Analysis of Thin Plates in Bending, Journal of the Aerospace Sciences, Vol. 28, No. 1, pp. 34–42, Jan. 1961.

[Mil1966]   Milligan R., Gerard, G., Lakshmikantham, C., and Becker, H., General Instability of Orthotropic Stiffened Cylinders under Axial Compression, AIAA Journal, Vol. 4, No. II, pp. 1906-1913, November 1966, Also Report AFFDL-TR-65-161, Air Force Flight Dynamics Laboratory, USAF, Wright Patterson Air Force Base, Chio, July 1965.

[Moe1958]   Moe, J., Stability of Ring-Reinforced Cylindrical Shells Under Lateral Pressure, Publications, International Association for Bridge and Structural Engineering, Vol. 18, pp. 113-136, 1958.

[Nag1957]   Naghdi, P.M., (1957), On the theory of thin elastic shells, Q. Appl. Math., Vol. 14, pp 369-380.

[Nag1963]   Naghdi, P .M., (1963), Poundations of elastic shell theory, in progress in solid Mechanics, Vol. IV, Chapter 1 (ed. 1. N. Sneddon and R. Hill), North-Rolland.

[Nag1972]   Naghdi, P.M., (1972), The theory of shells and plates, Handbuch der Physik, Vol. VI, A2 (Flügge Ed.), Springer Verlag, Berlin.

[Nov1953]   Novozhilov, V. V., Foundations of the Nonlinear Theory of Elasticity , Greylock Press, Rochester, New York, 1953.

[Par2005]   Park, J.H., (2005), Early Shape Morphing: the Metamorphosis of Polygons in Antoni Gaudi's Sagrada Familia Cathedral and Le Corbusier's Firminy Chapel. Journal of Asian Architecture and Building Engineering, 4(1), pp.25-30.

[Pee2008]   Peerdeman B., Analysis of Thin Concrete Shells Revisited: Opportunities due to Innovations in Materials and Analysis Methods, Delft University of Technology. Delft, June 2008.

[Pou1996]   Poulsen, P.N and Damkilde, L., A flat triangular shell element with loof nodes, IJNME, 39, p.3867-3887, (1996).

[Rao1978]   Rao, K. P,. A Rectangular Laminated Anisotropic Shallow Thin Shell Finite Element, Computer Methods in Applied Mechanics and Engineering, Vol. 15, 1978, pp. 13-33.

[Red1984]   Reddy, J.N., A Simple Higher-order Theory for Laminated Composite Plates, Journal of Applied Mechanics, Vol. 51, 1984, pp. 745-752.

[Red1992]   Reddy, J. N., A Layerwise Shell Theory with Applications to Buckling and Vibration of Cross-Ply Laminated Stiffened Circular Cylindrical Shells, Virginia Polytechnic institute and State University, CCMS-92-01. January, 1992.

[Rei1952]   Reissner E., (1952), Stress-strain relations in the theory of thin elastic shells, J. Math. Phys., Vol. 31,pp 109-119.

[Rei1969]   Reissner E., (1969), On finite symmetrical deformations of thin shells of revolution, JAM, Vol. 36, pp 267-270.

[Rei1974]   Reissner E., (1974), Linear and nonlinear theory of shells, in Thin Shell Structures, (Fung and Sechler Eds.), Prentice Hall, pp 29-44.

[Rha2015]   Rha, C.S., Kim, S.N., and Yu, E., Behavior of Gabled Hyperbolic Paraboloid Shells, Journal of Asian Architecture and Building Engineering vol.14 no.1 January 2015.

[Sab1985]   Sabir, A.B. and Ramadhani, F., A shallow shell finite element for general shell analysis, Proc.2nd Int. Conf. on variational methods, Univ. of Southampton, 1985pp. 5-3 to 5-13.

[Sab1987]   Sabir, A.B., Strain-based shallow spherical shell element, Proc. Int. Conf. on the mathematics of finite elements and appl., Brunel Univ., 1987.

[Sab1996]   Sabir, A.B. and Moussa, A.I., Finite element analysis of cylindrical-conical storage tanks using strain-based elements. Structural Engineering Review (8) 4: 367-374. 1996.

[Sch1968]   Schmit, L. A., Developments in Discrete Element Finite Deflection Structural Analysis by Functional Minimization, Technical Report AFFDL-TR-68-126, Wright-Patterson Air Force Base, 0Mo, 1968.

[Sch1989]   Schnaell, W. and Bush, D., The Effect of Delamination on the Fundamental and Higher Order Buckling Loads of Laminated Beams, Journal of Composite Testing and Research, Vol. 11, 1989, pp. 87-93.

[Sha1976]   Shaaban, A. and Ketchum M.S., (1976), Design of Hipped Hypar Shells. Journal of the Structural Division, 102(ST11), pp.2151-2161.

[Sil1983]   Silvester, P. P., and Ferrari, R. L., Finite Elements for Electrical Engineers, Cambridge University Press, Cambridge, England, 1983.

[Sim1989]   Simmonds, S.H., (1989), Effect of Support Movement on Hyperbolic Paraboloid Shells. Journal of Structural Engineering, 115(1), pp.19-31.

[Sim1989a]   Simo, J.C., Fox, D.D. and Rifai, M.S., On a Stress Resultant Geometrically Exact Shell Model. Part I: Formulation and Optimal Parametrization. Computer Methods in Applied Mechanics and Engineering, 72(1):267–304, 1989.

[Sim1989b]   Simo, J.C., Fox, D.D. and Rifai, M.S., On a Stress Resultant Geometrically Exact Shell Model. Part II: the linear theory; computational aspects. Computer Methods in Applied Mechanics and Engineering, 73(1):53–92, 1989.

[Sin1967a]   Singer, J., The Influence of Stiffener Geometry and Spacing on the Buckling of Axially Compressed Cylindrical and Conical Shells, Paper Presented at the Second IUTAM Symposium on the Theory of Thin Shells, Copenhagen, September 8, 1967.

[Sin1967b]   Singer, J., Baruch, M. and Harari, O., On the Stability of Eccentrically Stiffened Cylindrical Shells under Axial Compression. international Journal of Solids and Structures, Vol. 3, No. 4, pp. 445-470, July 1967. Also TAE Report No. 44, Technion Research and Development Foundation, Haifa, Israel, December 1965.

[Sin1967c]   Singer, J. and Haftka, R., Buckling of Discretely Ring-Stiffened Cylindrical Shells, TAE Report 67, Technion Research and Development Foundation, Haifa, Israel, August 1967.

[Ste1951]   Stein, M., Sanders, S.L. and Crate, H., Critical Stress of Ring-Stiffened Cylinders, NACA Report 989, 1951.

[Tas1965]   Tasi, J., Feidman, A., and Starg, D. A., The Buckling Strength of Filament-Wound Cylinders Under Axial Compression, NASA TR-266, July 1965.

[Tem2016]   Temami, O., Hamadi, D., Zatar, A., and Ayoub, A. (2016). Experimental and numerical analyses of a thin cylindrical shell model. Journal of Applied Engineering Science & Technology, 2(2), 99-103.

[Thi1960]   Thielmann, W. F., New Developments in the Nonlinear Theories of the Buckling of Thin Cylindrical Shells, Proceedings of the Durand Centennial Conference, Hoff, N.J., and Vincenti, W.G., (Eds.), Pergamon Press, London, 1960, pp. 76.

[Tou2016]   Touzout, M. Chebili, R., Shape Optimization of Elliptical and Vaulted Reinforced Concrete Domes, International Journal of Engineering Research in Africa, Vol. 24, pp. 35-43, 2016.

[Ven1980]   Venkatesh, A., and Rao, K. P., A Doubly Curved Quadrilateral Finite Element for the Analysis of Laminated Anisotropic Thin Shells of Revolution, Computers and Structures, Vol. 12, 1980, pp. 825-832.

[Ven1982]   Venkatesh, A., and Rao, K. P., A Laminated Anisotropic Curved Beam and Shell Stiffening Finite Element, Computers and Structures, Vol. 15, 1982, pp. 197-201.

[Ven1983]   Venkatesh, A., and Rao, K. P., Analysis of Laminated Shells with Laminated Stiffeners Using Rectangular Finite Elements, Computers Methods in Applied Mechanics and Engineering, Vol. 38, 1983 pp. 255-272.

[Vla1958]   Vlasov (1958), General Theory of Shells and its Applications to Engineering. [Transl. from Russian, 1949; NASA Techn. Translation TTF-99, 1964 AIso, in German (Berlin: Akademic Verlag. 1958),]

[Wil1966]   Wilson, E. L., and Nickel, R. E., Application of the Finite Element Method to Heat Conduction Analysis, Nuclear Engineering and Design, Vol. 4, pp. 276–286, 1966.

[You1975]   Young, C., and Crocker, M., Transmission Loss by Finite-Element Method, Journal of the Acoustical Society of America, Vol. 57, No. 1, pp. 144–148, Jan. 1975.

[Zie1965]   Zienkiewicz, O. C., and Cheung, Y. K., Finite Elements in the Solution of Field Problems, The Engineer, pp. 507–510, Sept. 24, 1965.

[Zie1971]   Zienkiewicz O. C., The Finite Element Method in Engineering Science, 2nd ed., McGraw- Hill, 1971.

[Zie1977]   Zienkiewicz O. C., The Finite Element Method, Third Expanded and Revised Edition, McGraw

[Zie1991]   Zienkiewicz, O. C., and Taylor, R. L., The Finite Element Method — Solid and Fluid Mechanics, Dynamics and Non-Linearity, Fourth Edition, Vol. 2, McGraw-hill Book Company Europe, London, 1991.

[Zie2005a]   Zienkiewicz, O.C., Taylor, R.L. and Zhu, J.Z., The Finite Element Method: Its Basis & Fundamentals. Butterworth-Heinemann, 2005.

[Zie2005b]   Zienkiewicz, O.C. and Taylor, R.L., The Finite Element Method: Solid and Structural Mechanics. Butterworth-Heinemann, 2005.

Appendix A

A sample of results given by the ADVANTEST9 :

This sample is from the ADVANTEST's results, it is a table in excel form gives the vertical displacement at any time for each load, the below table summarizes some results.

Load ch 4 (kN)	Time (s)	Displacement ch 5 (μm)	Stress (MPa)
0.829	86.1	5731	3.32
0.829	86.3	5733	3.32
0.832	86.5	5737	3.33
0.832	86.7	5737	3.33
0.836	87	5737	3.35
0.832	87.1	5737	3.33
0.832	87.4	5740	3.33
0.832	87.6	5740	3.33
0.832	87.8	5737	3.33
0.829	88	5737	3.32
0.834	88.3	5738	3.34
0.832	88.5	5740	3.33
0.832	88.6	5742	3.33
0.832	88.9	5746	3.33
0.832	89.1	5753	3.33
0.832	89.3	5771	3.33
0.832	89.5	5786	3.33
0.839	89.8	5806	3.36
0.834	90	5818	3.34
0.834	90.2	5838	3.34
0.834	90.4	5851	3.34
0.844	90.7	5869	3.37
0.848	90.8	5884	3.39
0.851	91	5897	3.4
0.846	91.3	5911	3.38
0.846	91.5	5920	3.38
0.836	91.7	5926	3.35
0.834	91.9	5929	3.34
0.839	92.2	5937	3.36
0.841	92.3	5944	3.36
0.841	92.6	5949	3.36
0.839	92.8	5953	3.36
0.844	93.1	5957	3.37
0.846	93.2	5957	3.38
0.851	93.4	5960	3.4
0.856	93.7	5968	3.42

117

0.848	93.8	5978	3.39
0.848	94.1	5998	3.39
0.848	94.3	6009	3.39
0.856	94.6	6022	3.42
0.853	94.7	6031	3.41
0.851	94.9	6042	3.4
0.848	95.2	6060	3.39
0.851	95.4	6073	3.4
0.848	95.6	6089	3.39
0.848	95.8	6098	3.39
0.856	96.1	6108	3.42
0.858	96.2	6113	3.43
0.853	96.5	6117	3.41
0.856	96.7	6115	3.42
0.851	97	6115	3.4
0.853	97.1	6118	3.41
0.858	97.4	6135	3.43
0.858	97.6	6153	3.43
0.856	97.7	6171	3.42
0.856	98	6200	3.42
0.865	98.2	6218	3.46
0.87	98.5	6248	3.48
0.868	98.6	6269	3.47
0.865	98.9	6308	3.46
0.865	99.1	6344	3.46
0.875	99.3	6422	3.5
0.882	99.5	6486	3.53
0.889	99.8	6575	3.56
0.884	100	6635	3.54
0.884	100.1	6697	3.54
0.889	100.4	6782	3.56
0.899	100.6	6822	3.6
0.901	100.8	6873	3.61
0.899	101	6906	3.6
0.901	101.3	6951	3.61
0.904	101.5	6977	3.61
0.899	101.7	7006	3.6
0.901	101.9	7029	3.61
0.906	102.2	7060	3.62
0.911	102.3	7082	3.64
0.916	102.5	7100	3.66
0.913	102.8	7119	3.65
0.918	103	7120	3.67
0.918	103.2	7124	3.67

Appendix B

ABAQUS is a computer code using the finite element method, created in 1978 by Hibbit, Karlsson & Sorensen (HKS).

It simulates the physical response of structures and solid bodies of loads, temperatures, impacts and other external conditions, it contains many modules:

1. ABAQUS Standard

It is an implicit code of finite element analysis. it allows the resolution of a large number of different physical problems. ABAQUS / Standard is the possibility of static studies & forced displacement, linear or nonlinear dynamics, thermal and acoustic. Moreover, ABAQUS / Standard also addresses multi-physics problems such as thermo-structural-acoustics, thermoelectric or hydromechanical calculations. ABAQUS / Standard has optional internal modules to complete, for example, sensitivity studies or simulations offshore. ABAQUS / Standard also has an interface with MOLDFLOW to pursue a mechanical study, following a plastic injection.

2. ABAQUS Explicit

It is an explicit code of finite element analysis. Fully parallelized, ABAQUS / Explicit allows the resolution of studies like the fast dynamics problems of acoustic shock Crash1 or explosions. With its robust algorithms contacts, ABAQUS / Explicit is also a powerful tool for shaping simulations (dynamic and quasi-static). ABAQUS / Explicit has in addition to methods of using the adaptive mesh ALE techniques that provides a robust solution for highly nonlinear problems in large deformations.

3. ABAQUS/CAE (Complete ABAQUS Environment):

It is the perfect interactive graphical interface for modeling, management and postprocessing of ABAQUS models. Pre-post next-generation processor, ABAQUS / CAE allows the entire data layout, creating or importing parts, linkages to the advanced exploitation of results. Intuitive ABAQUS / CAE is fully adaptable to the specific needs of users with customization in Python.

4. ABAQUS FOR CATIA V5:

Is the fruit of close collaboration teams ABAQUS and CATIA. ABAQUS FOR CATIA V5 integrates the nonlinear capabilities of ABAQUS in the CATIA V5 design environment. The result is a complete package that will FEA simulation to the design process. The entire data layout and post-processing finite element models is fully integrated in CATIA

V5 CAD and transparent to the user. ABAQUS FOR CATIA V5 optimizes the steps of mechanical simulation in PLM cliaine for all CATIA V5 users.

Examples of use of ABAQUS are as diverse as engineering problems:

design, automotive crash simulation of manufacturing processes and formatting, validation, NVH, delamination of composite materials, fatigue analysis, damage, co-simulation.

5. Principle operations

The heart of Abaqus software is what might be called his "calculation engine". From a data file (characterized.inp suffix), which describes all of the mechanical problem, the software analyzes the data, performs the requested simulations, and provides the results in a file .odb.

Two tasks remain: to generate the data file (.inp), and use the results contained in the file .odb. The structure of the data file can be quickly complex: it must contain all the geometric definitions, descriptions of meshes, materials, loads, etc., following a precise syntax.

The common steps in ABAQUS are:

Step 1 - Create an input file: Works of ABAQUS next to read and respond to a set of commands (called KEYWORDS) in an input folder. Keyword contain information for defining the mesh, material properties, boundary conditions and to control the performance of the program.

Step 2 - Run the program: On Windows, ABAQUS is controlled by typing commands in a DOS window types.

Step 3 - Post Treatment: there are two ways to look at the results of a simulation of ABAQUS. You can ask the program to print the results to a folder, you can watch with a text editor.

Alternatively, you can use a program called ABAQUS / Post, which can be used to trace the various amounts that may be of interest.

ABAQUS offers Abaqus CAE module graphical interface to manage all operations related to modeling:

     - The generation of the data file.

     - The launch of the calculation.

     - Exploitation of results.

The CAE module is launched by entering the command: abaqus cae, and comes in the form of a graphical interface and offers ten sub-modules include:

120

1. Sketch

2. Part

3. Property

4. Assembly

5. Step

6. Interaction

7. Load

8. Mesh

9. Job

10. Visualization

The first eight sub-modules are used to define the mechanical problem to simulate. Job module is the one that manages the passage of the actual simulation calculation, that is to say the core code. The last module contains everything related to the exploitation of results in the form of various visualizations.

6. Modeling

This example shows the response of semi cylindrical shell model, undergoing a concentrated static load, with different thickness and boundary conditions.

6.1 Create a model

Use ABAQUS/CAE to create a three-dimensional model.

a- Defining the model geometry

- Start ABAQUS/CAE, and enter the Part module by clicking Part – Create. A dialog box of Create Part appears.

- In the dialog box, create a 3D, deformable part with an extruded shell base feature to represent the Model (See Figure 1). Use an approximate part size of 1000.

- Click the button Create Circle: Center and Perimeter tool to sketch a circle. Pick center point at (0, 0)and perimeter point at (0,160)or (160, 0)to define the circle geometry. The section sketch.

- When finish sketching the section, end the Create Circle: Center and Perimeter tool by clicking that button once again, and there appears a hint 'Sketch the section for the shell extrusion'. Click Done. Set the depth 900mm. After that, the sketch is extruded to a depth of 900 mm and a circular tube is therefore created. The final part is shown in Figure 1.
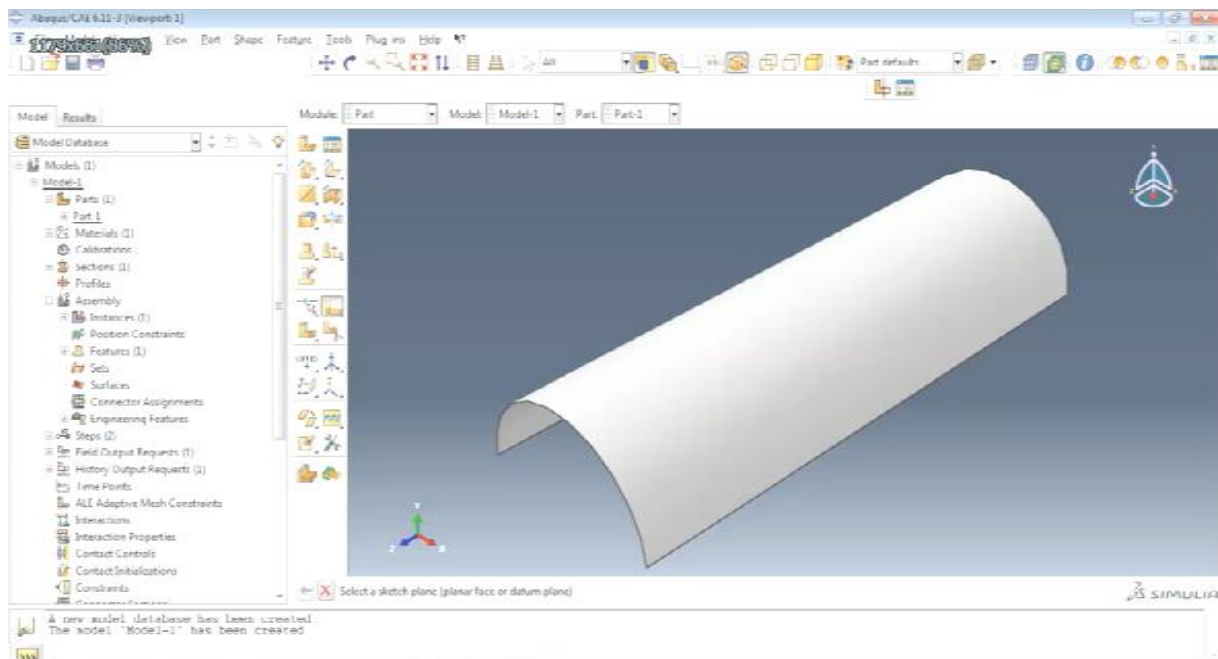
Fig. 1. The Final Part of the model

b- Defining the material properties

In the Module selection, select and click Property to define the material and section properties. Assume that the model is made of stainless steel, with a Young's modulus of 190 GPa, a Poisson's ratio of 0.265.

- ### Create material

To define an elastic-plastic material:

1) Click the button Create Material. The Edit Material dialog box turns up. Name the material Steel.

2) In the Edit Material dialog box, select Mechanical – Elasticity – Elastic to define the elastic material properties. Enter 190E9 Pa as the value for Young's modulus and 0.265 as the value for Poisson's ratio.

You should note that ABAQUS is numerical and hence it does not have default units. You need therefore to be consistent in using units when defining geometry, loads and material properties. In this example, we used mm as the unit of dimension in defining the geometry and presume the unit of load to be N, then the unit of stress and Young's modulus should be MPa.

- **Creating and assigning section properties**

To create homogeneous shell section properties and refer to the steel material definition and shell thickness:

1) Click Create Section. The Create Section dialog box appears. Name the shell section property Steel Section, select Shell Homogeneous and continue.

2) In the Edit Section dialog box, select Steel as the material, and specify 2 mm as the value for the Shell thickness. Then press OK.

To assign the Steel Section definition to the regions of the steel circular tube:

1) Click Assign Section.

2) Click the entire circular tube as the regions to be assigned a section, and press DONE.

3) Press Ok in the Edit Section Assignment dialog box.

You can click Section Assignment Manager to check or modify the section assignment in the dialog box.

b. **Creating an assembly**

Enter the Assembly module, and click Instance Part.

It is simple to create an assembly for an integrated structure such as this example. However, some models may be complicated if they are composed of several small parts which have different material properties. You should define the material properties for each part in the previous steps and assemble them in this step.

c. **Creating the mesh**

1) Enter the Mesh module to seed the part instance.

2) Select Seed – Edge By Number and specify that elements be created along the perimeter of the circular section. To do so, click the perimeter as the region to be assigned local seeds and press DONE. Then enter the number of elements along the edge.

3) Select Mesh – Controls, and use the default element shape and press OK.

4) Select Mesh – Element Type, and use the default quadrilateral shell elements (S4R) as the element type to be applied in this case.

5) Select Mesh – Part, and press OK to mesh the part.
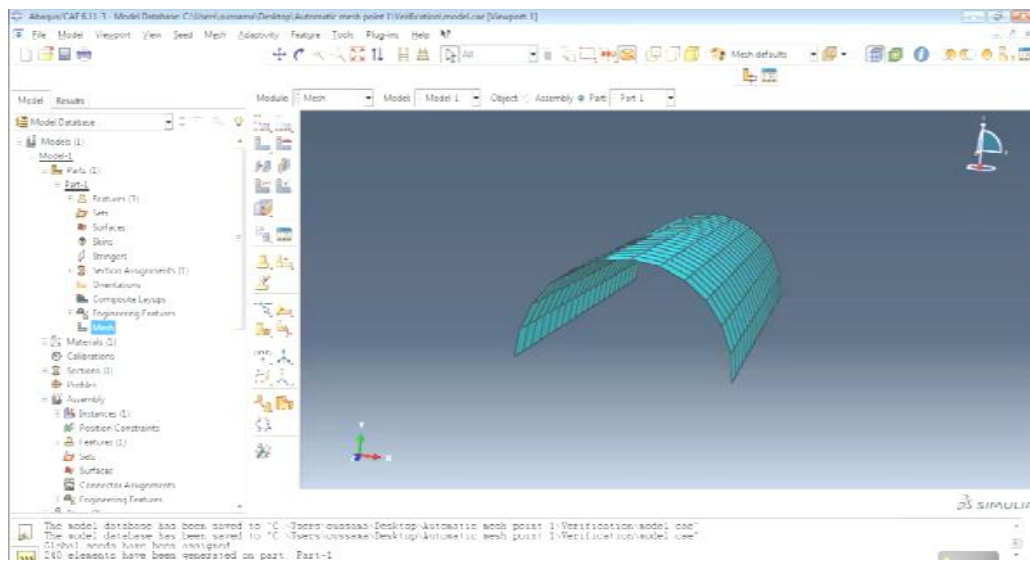
Figure. 2. Meshed model

The resulting mesh is shown in Figure 2. This relatively coarse mesh provides moderate accuracy while keeping the solution time to minimum. You can create finer mesh to get more accurate solution which however takes longer when running the job.

You should carefully consider what type of element should be used before meshing a model. Different element types may make significant difference. Check more details in relevant ABAQUS manuals.

### d. **Prescribing boundary conditions and loads**

1) Enter the Load module to define the boundary conditions used in this analysis.

2) Select Tool – Set – Create, and create a set named Fixed, select the perimeter edge of one end of the model as the geometry of the set, and press DONE. Similarly, create another set named Moving by selecting the other end of the model. Then, create a set named

Displacement, and click one node point of the moving end as the geometry. Enter Set Manager to check the three sets.

3) Select BC – Create, and create a boundary condition in the Initial step named Fixed Edge. Select Mechanical – Displacement/Rotation to be the type of step. Apply the boundary condition to the set of Fixed by clicking Set in the right corner and selecting Fixed. In the Edit Boundary Condition dialog box, tick U1, U2, U3, UR1, UR2, UR3 to fully constrain the set (U1 = U2 = U3 = UR1 = UR2 = UR3 = 0). Press OK.

The boundary conditions applied is shown in Figure 3.
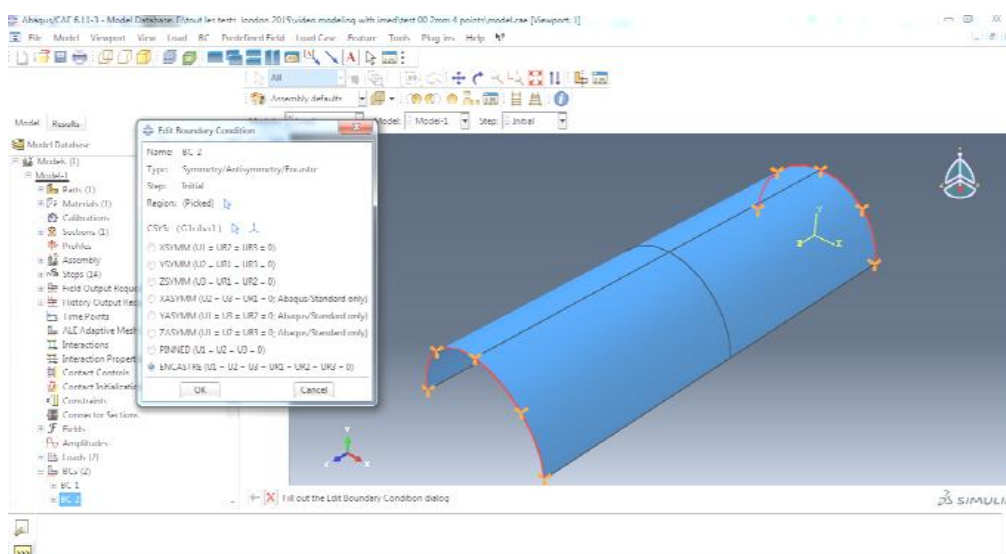
Fig. 3. Boundary Conditions

- e. **Analysis**
- f. **Defining and submitting a job**

Save your model in a model database file, and submit the job for analysis. Monitor the solution progress; correct any modeling errors that are detected, and investigate the cause of any warning messages.
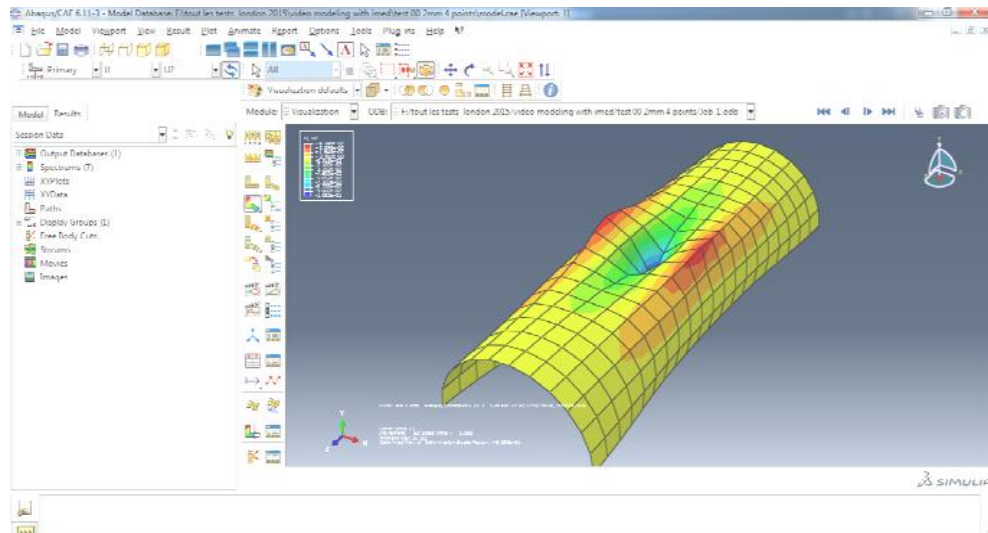
- g. **Postprocessing**
  - • **Visualization of results**

Enter the Visualization module, and open the .odb file created by this job .

You can view the following shapes or plots by clicking corresponding tool buttons:

- • Undeformed shape;

- Deformed shape;
- Animation of results;
- Contour plots;
- Eigenvalue.

Fig. 4. Deformed Shape

- **Data processing**

This section mainly introduces how to obtain a data plot of load-displacement in the movable end of the model. The principle is to collect the data of reaction force in the fixed end and the data of the displacement of the movable end. Both of them are in the z-coordinate direction.

1) Select Tool – XY Data – Manager – Create – OBD field output, there appears a dialog box.

2) Collect the data of reaction forces. In the catalogue of Variables, select Position as Unique Nodal. Then select RF3(Reaction force in the direction of z-coordinate). In catalogue of Elements/Nodes, click Node sets – Fixed. Then press Save – OK.

3) Collect the data of displacement. In the catalogue of Variables, select Position as Unique Nodal. Then select U3(Displacement in the direction of z-coordinate). In catalogue of Elements/Nodes, click Node sets – Displacement. Click Save – OK. Close the dialog box.

4) Select Tool – XY Data – Manager – Create – Operate on XY data, there appears a dialog box.

5) Row down the operation functions column on the right side, and click sum((A, A,…)). Multi-select all the RF3 data and click Add to Expression. Save as RF3.

6) Click Clear Expression. Row down the operation column to click combine (X, X). Select U3to Add to Expression and then RF3(which was saved in the above procedure) to add to expression. Give a negative sign to U3, as the displacement is in the negative direction of z-coordinate while we hope the see the plot which displacement is positive. Save as plot.

7) Click Plot Expression, the Load-Displacement diagram is shown as Figure 5.
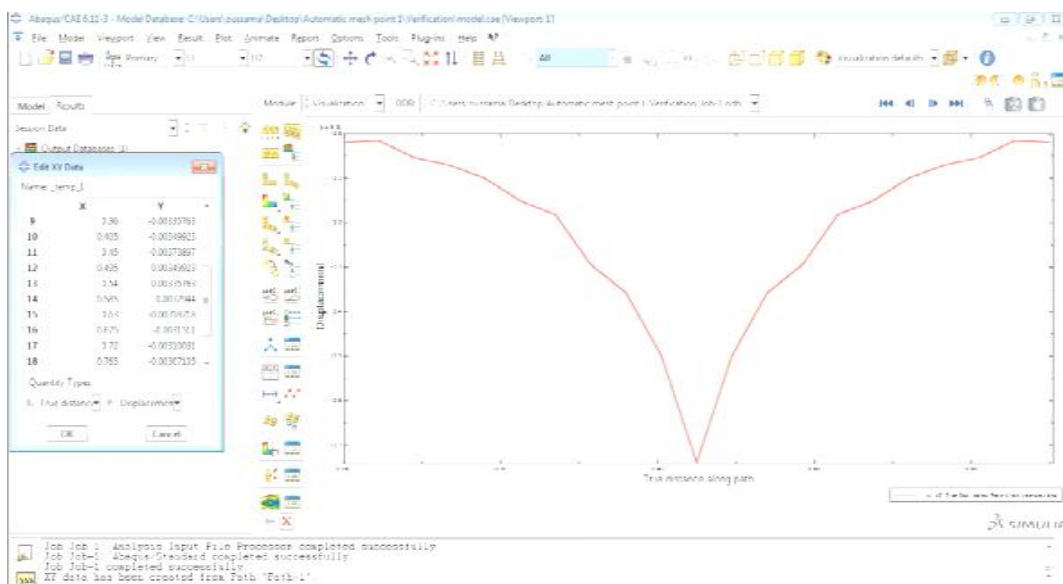
Fig. 5. Plot of displacement

Alternatively, you can do the following to save all the data of the plot as an Ms-Excel file.

1) Click Report – XY.

2) In the catalogue of XY Data, click plot.

3) In the catalogue of Setup, name a file xxx.xls and save in the hard drive.

4) Click OK.

Note: You must save it as an Excel file, otherwise it cannot be read. Check this file and you would find all the detailed data are included in. You can also make diagrams using these data.

Appendix C

ACM-RSBE5 Results with Fortran :

The data input

This the data file:

COQUE ** Cylindre **

2 2   NEx NEy

20 1   NTDI NTFI

19.E10 0.265 0.002   YOUNG POISSON EPAISSEUR

C 1.   TYPE DE CHARGEMENT   VALEUR DE LA CHARGE SI REPARTIE

COORDONNEES DES NOEUDS

0. 0.   0.16

0. 0.225 0.16

0. 0.450 0.16

0.113137085 0   0.113137085

0.113137085 0.225 0.113137085

0.113137085 0.450 0.113137085

0.16 0.   0.

0.16 0.225 0.

0.16 0.450 0.

DIPLECEMENTS IMPOSES

1 1 0

1 5 0

1 6 0

2 1 0

2 5 0

2 6 0

3 1 0

3 2 0

3 4 0

3 5 0

3 6 0

6 2 0

6 4 0

6 6 0

7 1 0

7 2 0

7 3 0

9 2 0

9 4 0

9 6 0

FORCES IMPOSEES

3 3 -875   Nø DIRECTION   VALEUR

*KRO

0 0 0 0 0 0 0 0 1 1

And this is the out put data for the displacement:

MAILLAGE: 2 x 2

    ****

    *   D I P L A C E M E N T S   *

    ****

****

*   *   *   *   *   *   *   *

* NODE*   U   * V * W   * 0x * 0y * 0z *

```
*      *      *      *      *      *      *      *
************************************************************************
*   1 * .4900E-22* .7440E-04*-.2723E-02* .5806E-02*-.1551E-23*-.4836E-30*
************************************************************************
*   2 * .7856E-22* .6051E-04*-.3226E-02*-.2570E-02*-.2942E-23* .3439E-30*
************************************************************************
*   3 *-.1779E-21* .4932E-21*-.3512E-02*-.1383E-24*-.1449E-23* .5730E-25*
************************************************************************
*   4 * .1359E-02*-.3519E-04* .5595E-03* .1278E-02*-.1967E-01* .5005E-02*
************************************************************************
*   5 * .1646E-02*-.3045E-04* .7388E-03*-.1451E-02*-.4874E-01*-.3963E-02*
************************************************************************
*   6 * .1795E-02*-.3511E-21* .8292E-03*-.6686E-25*-.5710E-01* .6464E-25*
************************************************************************
*   7 * .5036E-22*-.3380E-22*-.8750E-22* .1152E-01* .2749E-01*-.2800E-01*
************************************************************************
*   8 * .6616E-02* .1913E-05* .2798E-02* .7953E-02*-.4228E-01*-.2037E-01*
************************************************************************
*   9 * .8233E-02*-.1083E-21* .3499E-02* .2075E-25*-.5716E-01*-.5010E-25*
************************************************************************
```